Vapochromism in Coordination Complexes: Chemical Sensors for Volatile Organic Compounds

SCHOLARONE™
Manuscripts

1
2
3
4
5
6
7
8
9
10
11
12
13
14
15
16
17
18
19
20
21
22
23
24
25
26
27
28
29
30
31
32
33
34
35
36
37
38
39
40
41
42
43
44
45
46
47
48
49
50
51
52
53
54
55
56
57
58
59
60

Vapochromism in Organometallic and Coordination Complexes: Chemical Sensors for Volatile Organic Compounds

Oliver S. Wenger*

Universität Basel, Departement für Chemie, Spitalstrasse 51, CH-4056 Basel, Switzerland.

oliver.wenger@unibas.ch

Contents

1
2
3
4
5
6
7
8
9
10
11
12
13
14
15
16
17
18
19
20
21
22
23
24
25
26
27
28
29
30
31
32
33
34
35
36
37
38
39
40
41
42
43
44
45
46
47
48
49
50
51
52
53
54
55
56
57
58
59
60

1. Introduction

1.1 Scope of the review

The development of chemical sensors is a subject that continues to fascinate chemists in academic research. Aside from the purely academic interest there is of course the important issue of finding suitable sensors for harmful chemical substances that might be present in the environment or at our workplaces. Consequently, the detection of volatile organic compounds (VOCs) by simple means requiring only a low-cost technology is an attractive research target. In this context vapochromism is a promising phenomenon. A vapochromic substance changes color upon exposure to certain vapors,[1] and therefore the detection of analytes can often occur even by naked eye. In addition, there is the phenomenon of luminescence vapochromism, often called

vapoluminescence, which refers to changes in photoluminescence properties in the course of vapor exposure. The class of compounds in which these two closely related phenomena occur most frequently is undoubtedly the area of coordination complexes. This review therefore focusses on transition metal compounds that change color and/or their emission properties when exposed to VOCs. Where appropriate, information regarding the detection of other analytes (e. g., oxygen, humidity in air, acids or bases) will be included as well. Along the same lines, the related phenomena of mechanochromism or thermochromism will be discussed briefly where appropriate and were thematically fitting.

The article is written from the perspective of a coordination chemist with an emphasis on understanding the origin of the vapochromic / vapoluminescent responses of the individual sensor materials. In this sense the current review is less geared towards applications than much of what has been published under the broadly defined label "electronic noses".[2-6] Nevertheless the present review includes analytical details for the sensors for which such information is available, but many original studies do not report quantitative analytical results and focused themselves on understanding the vapochromism / vapoluminescence phenomenon on a molecular level rather aiming to develop actual sensing devices. A separate section with an comprehensive table summarizes the available analytical information in a compact manner.

Many of the coordination compounds discussed in the current article have been part of other reviews. For example, there exist several recent reviews on chemosensing with platinum(II) and gold(I) complexes.[7-17] Most recently, a "feature article" on the specific subject of recent advances in the field of vapo*luminescence* in metal complexes appeared,[18] but the scope of the current review is significantly broader, and it contains substantially more detailed information. The optical spectroscopic and photophysical properties of some of the metal complexes relevant

for the current article have been reviewed separately,[19-22] and reviews on the related phenomena of thermochromism and mechanochromism also exist.[23-27]

The two largest families of vapochromic / vapoluminescent substances are platinum(II) and gold(I) containing compounds which are treated in two separate dedicated sections of this review. Sensors devoid of these two elements are discussed in a subsequent section which is divided into subsections according to the transition metals they contain. Until now purely organic vapochromic / vapoluminescent substances are relatively rare and are not considered here. Pt(II) and Au(I) containing vapochromic substances are treated in separate sections not only because by mere number they represent the two most important classes of vapochromic substances, but also because a more or less common mode of operation can be identified for many of these particular substances (sections 1.3 and 6). Briefly, in many of the Pt(II) and Au(I) compounds the vapochromic response is the result of changes in intermolecular interactions (e. g., weak metal-metal interactions, π-stacking, hydrogen-bonding, C-H-π interactions) as a result of analyte uptake into the crystal lattice, while for many (but not all) of the substances presented in section 4 direct ligation of an analyte to a metal center is observed.

1.2 Metal-metal interactions in d^8 and d^{10} compounds

Because of the special importance of Pt(II) and Au(I) compounds in the field of vapochromism it is useful to recapitulate a few elementary aspects regarding weakly interacting metals with d^8 and d^{10} electron configurations. There exist numerous didactical articles on non-covalent Pt(II)-Pt(II) and aurophilic interactions,[7, 22, 28-31] hence only the most fundamental aspects needed to

comprehend the photophysical behavior of some of the vapochromic substances discussed in sections 2 and 3 will be briefly discussed here.

Square planar d^8 and linear d^{10} complexes tend to approach each other in such a way that their $5d_{z2}$ and $6p_z$ orbitals can interact with each other.[32] Figure 1 shows the relevant part of the molecular orbital diagram for d^8-d^8 dimers. The interaction of $5d_{z2}$ and $6p_z$ orbitals leads the formation of bonding and anti-bonding dimer orbitals, commonly designated as dσ / dσ* ($5d_{z2}$) and pσ / pσ* ($6p_z$).[31] In the electronic ground state of d^8-d^8 and d^{10}-d^{10} dimers the dσ and dσ* orbitals are filled whereas the pσ and pσ* orbitals are empty. In both cases there is the possibility of dσ* $\rightarrow$ pσ transitions leading to excited-states in which the metal-metal distance is shorter than in the ground state due to an increase in bond order. However, in many of the cases from sections 2 and 3 for which intermetallic interactions are relevant the LUMO is a ligand-based orbital, typically with π or π* character; π-π interactions between ligands may themselves lead to "dimer π orbitals". The HOMO-LUMO transition in these cases is a so-called metal/metal-to-ligand charge transfer (MMLCT) which distinguishes itself from ordinary metal-to-ligand charge transfer (MLCT) transitions in that the HOMO is a "dimer orbital" (or "oligomer" / "polymer" orbital) resulting from intermetallic interactions. Depending on the strength of the metal-metal interaction the dimer HOMO shifts in energy, and for many sensors this forms the basis for vapochromism or vapoluminescence. However, there are numerous other mechanisms that may lead to vapor-induced color and emission changes, and the full breadth of possibilities will become obvious from the following sections.
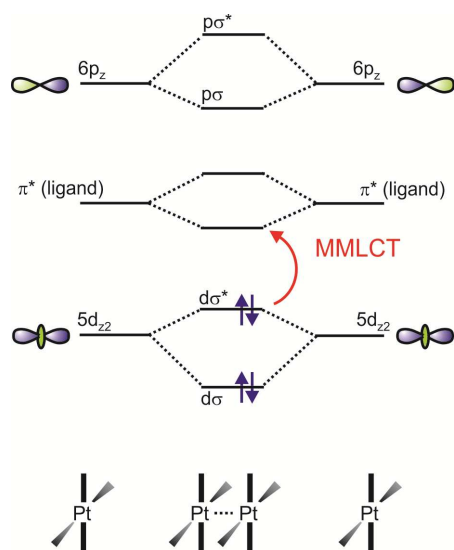
Figure 1. Simplified MO diagram illustrating metal-metal interactions between square planar Pt(II) complexes. MMLCT = metal/metal-to-ligand charge transfer. More elaborate diagrams can be found in the literature.[33, 34]

1.3 Unifying themes in research on vapochromic substances

The vapochromism of many of the Pt(II) and Au(I) containing substances discussed in sections 2 and 3 is more or less closely related to metallophilic interactions and/or π-stacking. A common theme for many (but not all) of the vapochromic substances presented in section 4 is the occurrence of changes in the first coordination sphere, including both alterations in coordination number and coordination geometry. This is particularly true for several of the vanadium, cobalt, nickel, copper, and metalloporphyrin-based vapochromic substances. One may therefore differentiate between two fundamentally different manners by which vapochromic substances respond to VOCs: Type I of vapochromic substances exhibits more or less subtle structural changes in crystal packing leading to alterations in intermolecular interactions such as for

example metal-metal interactions, π-stacking, hydrogen-bonding, and C-H-π interactions. In type II vapochromic substances direct ligation of an analyte to a solid-state material occurs. Type I is of key importance in sections 2 and 3, type II is prominent in section 4 (subsection 4.1) but several substances from section 4 are type I vapochromic systems (subsection 4.2).

A unifying theme for many vapochromic substances is an exceptionally high complexity of the solid-state structures. Aside from the intermolecular interactions mentioned above, the presence of voids plays an important role in many cases. In this context, the size and shape of counterions can have an important influence. In several cases the vapochromic property is strongly dependent on the polymorph or solvate which is formed; while one polymorph or solvate may exhibit spectacular vapochromism, a closely related polymorph or solvate may be completely insensitive to VOCs. The most important insights to vapochromism therefore come from solid-state investigations including X-ray crystallography, powder X-ray diffraction, thermogravimetry, and solid state absorption (or reflectance), and luminescence. Solution studies are usually considerably less insightful. However, as will be seen from this review, even the simplest structure-property relationships in many vapochromic materials have remained extremely elusive. Consequently, it is very difficult to "engineer" vapochromic materials. It is even difficult to optimize the VOC response behavior of known vapochromic substances because even the slightest changes can lead to complete disappearance of the vapochromic property. In short, many challenges are associated with research on vapochromism.

2. Platinum(II) compounds

2.1 Materials with charge-neutral Pt(II) complexes

2.1.1 [Pt(α-diimine)(CN)$_2$] complexes and their derivatives

One of the earliest reports of vapochromism in a platinum(II) coordination compound dates from 1974.[35] Gillard and coworkers found that [Pt(bpy)(CN)$_2$] (bpy = 2,2'-biypridine) (**1**) (Scheme 1) changes color from red to yellow when solid samples are exposed to HF, H$_2$O or H$_2$S vapors. Similarly, [Pt(phen)(CN)$_2$] (phen = 1,10-phenanthroline) (**2**) was observed to turn from yellow to red upon exposure to anhydrous organic solvent vapors. At that time the existence of a red and yellow form of [Pt(bpy)Cl$_2$] (**3**) was already known from the early work by Morgan and Burstall.[36] In the Gillard paper the vapor-induced color changes were discussed in terms of protonation of the CN ligands, and it was speculated that covalent addition of H$_2$O to one of the pyridine rings of bpy might also play a role.

Scheme 1. [Pt(α-diimine)(CN)$_2$] complexes, part I.
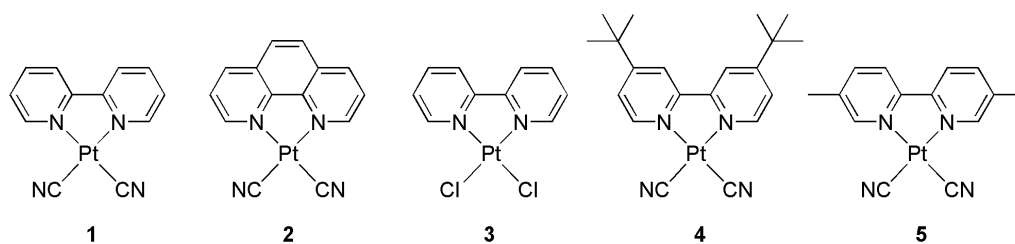
Nearly 20 years later Shih and Herber reported on water sorption by [Pt(^{t}Bu$_2$bpy)(CN)$_2$] (^{t}Bu$_2$bpy = 4,4'-di-*tert.*-butyl-2,2'-biypridine) (**4**).[37] At relative humidities above 40% this material reversibly uptakes 5 water molecules but no color changes occur because all relevant

absorptions are in the UV. The compound [Pt(5,5'-Me$_2$bpy)(CN)$_2$] (5,5'-Me$_2$bpy = 5,5'-dimethyl-2,2'-bipyridine) (**5**) was investigated in the same study and was found to change color from light yellow to deep orange on hydration.[37] Thus, by investigating a series of [Pt(bpy)(CN)$_2$] complexes with bpy ligands bearing substituents of variable steric bulk, Shih and Herber arrived at the conclusion that control over the metal-metal distance of neighboring complexes is desirable for obtaining materials which change color upon hydration. This important concept holds true for many vapochromic materials that are discovered only nowadays.

Nearly another 10 years later the Kato group began to publish an entire series of papers on vapochromic [Pt(α-diimine)(CN)$_2$] compounds.[13, 38-42] Initial studies focused on the [Pt(bpy)(CN)$_2$] material (**1**) investigated already by Gillard and coworkers.[38] Based on X-ray crystallographic investigations it was possible to elucidate the origin of the water-vapor induced color change. The anhydrous red form of [Pt(bpy)(CN)$_2$] was found to contain infinite stacks of complexes with regular intermolecular Pt(II)-Pt(II) distances of 3.34 Å, while in the yellow [Pt(bpy)(CN)$_2$]·H$_2$O (**1**·H$_2$O) material the sorbed water molecule causes a deformation of the stacking structure and an interruption of the infinite Pt(II)-Pt(II) chain. In the yellow form there are inclined stacks with alternating short (3.3289(3) Å) and long (4.6814(3) Å) Pt(II)-Pt(II) distances, and the crystal water connects individual stacks via hydrogen-bonding to the cyanide ligands. Thus it became clear that vapochromism of [Pt(bpy)(CN)$_2$] was due to changes in the Pt(II)-Pt(II) interaction brought about by a structural change upon water sorption. This conclusion was particularly obvious in light of prior vapochromism studies with platinum double salts by Mann and coworkers (see below), and the fundamental work on the electronic structures of d^8-d^8 dimers,[43, 44] stacked platinum(II) diimine complexes,[45-48] and tetracyanoplatinates.[22]

Kato and coworkers noted that the photoluminescence band maximum of [Pt(bpy)(CN)$_2$] (**1**)

shifts from 602 nm to 566 nm upon exposure to humid air while maintaining similar emission

intensity.[38] Thus, unlike the yellow form of [Pt(bpy)Cl$_2$] which is a much weaker emitter than its

red polymorph,[49] the yellow form of [Pt(bpy)(CN)$_2$] is strongly emissive. Presumably this is

because [Pt(bpy)(CN)$_2$]·H$_2$O (**1**·H$_2$O) contains dimers with short Pt(II)-Pt(II) distances which are

able to exhibit ^{3}MMLCT emission while yellow [Pt(bpy)Cl$_2$] (**3**) has no short contacts between

Pt(II) centers.[46]

Scheme 2. [Pt(α-diimine)(CN)$_2$] complexes, part II.
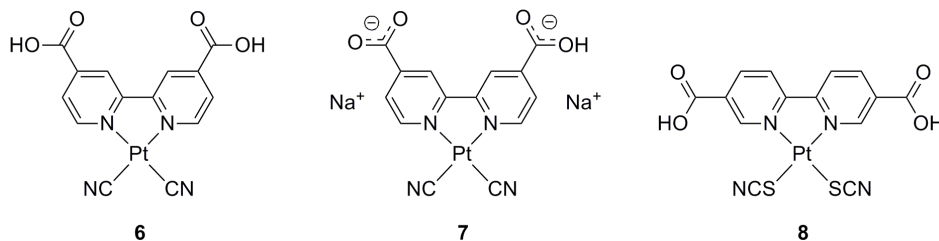
The complex [Pt(4,4'-H$_2$dcbpy)(CN)$_2$] (4,4'-H$_2$dcbpy = 4,4'-dicarboxyl-2,2'-bipyridine) (**6**)

(Scheme 2) represents a milestone discovery in the area of vapochromic platinum compounds.[13,]

[39] The color of this material is dependent on the pH at which it is recrystallized and can adopt a

range of colors from white to yellow, red, blue and purple. The different colors are a

manifestation of different polymorphs with variable Pt(II)-Pt(II) interactions and are unusually

diverse for linear-chain platinum(II) compounds. The red form was found to have short Pt(II)-

Pt(II) contacts of about 3.3 Å and a network structure with relatively large cavities in which

water molecules can be included. The cavities form as a result of molecular alignments dictated

by Pt(II)-Pt(II) interactions and hydrogen bonds between carboxylic acid and cyano groups.

Upon exposure of any of the polymorphs to volatile organic compounds, reversible color

changes can be induced. Because the differently colored forms of [Pt(4,4'-H$_2$dcbpy)(CN)$_2$] are all emissive, vapor exposure further induces changes in the luminescence properties (Figure 2).
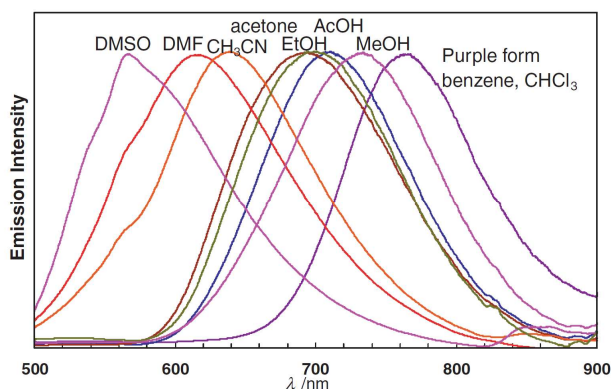
Figure 2. Photoluminescence of [Pt(4,4'-H$_2$dcbpy)(CN)$_2$] (**6**) after exposure to different VOCs.[13] Reproduced with permission from the Chemical Society of Japan.

In this system, there is a reasonably good correlation between the emission band maximum and the dielectric constant of the vapors to which the material is exposed; solvents such as DMSO and DMF cause significantly more blue-shifted emission than substances like benzene or chloroform. The emission originates from a ^{3}MMLCT state which shifts to lower energy with increasing metal-metal interaction; direct evidence for the correlation between the luminescence band maximum and the Pt(II)-Pt(II) distance comes from the observation of thermochromism in the red form of [Pt(dcbpy)(CN)$_2$] and from the observed shortening of the metal-metal distance from 3.28 Å at ambient temperature to 3.22 Å at 100 K.[39]

When [Pt(4,4'-H$_2$dcbpy)(CN)$_2$] (**6**) is exposed to sodium methoxide in CH$_3$OH solution the carboxylic acid groups of the bpy ligand are deprotonated and a material with the stoichiometry Na$_2$[Pt(4,4'-dcbpy)(CN)$_2$]·2H$_2$O (**7**·2H$_2$O) is obtained.[40] The coordination unit in this compound

is formally anionic, but since it contains the deprotonated form of the complex discussed in the preceding paragraph it appears meaningful to discuss this vapochromic material in the current section.

$Na_2[Pt(4,4'-dcbpy)(CN)_2]\cdot 2H_2O$ ($7\cdot 2H_2O$) was obtained as a red and amorphous substance which changes color to yellow in humid air or when exposed to hydrophilic organic vapors such as those from methanol, acetone or DMF. Powder X-ray experiments reveal that the color change is accompanied by a structural transformation from an amorphous to a crystalline state, but inclusion of organic vapors into the solid did not occur. According to single crystal X-ray studies the yellow form of $7\cdot 2H_2O$ has long (> 4.9 Å) intermolecular Pt(II)-Pt(II) distances while the red amorphous polymorph probably has short metal-metal contacts, hence the difference in color. The most interesting aspect of this material is certainly the fact that it exhibits structural changes upon exposure to hydrophilic VOCs without actually adsorbing anything. Unfortunately these structural transformations seem to be irreversible, limiting the application potential of the respective material severely. Both forms of $7\cdot 2H_2O$ are luminescent when irradiated with UV light, and thus vapor exposure can be monitored both in absorption and emission (Figure 3).
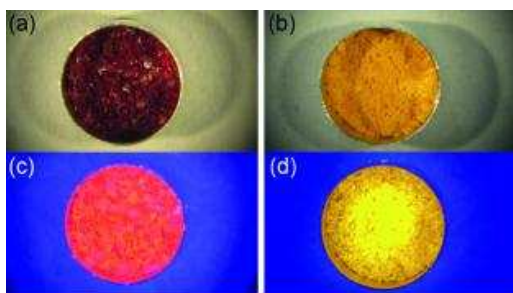
Figure 3. Photographs of $7\cdot H_2O$ before (a) and after (b) exposure to MeOH vapor. Panels (c) and (d) show the emission of the same compound before and after MeOH exposure. (A. Kobayashi, T. Yonemura, M. Kato: Vapor-Induced Amorphous-Crystalline Transformation of a

Luminescent Platinum(II)-Diimine Complex. Eur. J. Inorg. Chem., 2010, 2465-2470. Copyright

Wiley-VCH Verlag GmbH & Co. KGaA. Reproduced with permission.)

When the cyano ligands of [Pt(4,4'-H_2dcbpy)(CN)$_2$] are replaced by SCN$^-$ an unusual

vapochromic material results.[50] By synthesizing the [Pt(4,4'-H_2dcbpy)(SCN)$_2$] complex (**8**) at 0

°C it was possible to obtain the S-bound linkage isomer of this material, which, by analogy to the

thiocyanato complex [Pt(bpy)(SCN)$_2$] is presumably the kinetically (but not thermodynamically)

favored product. The [Pt(4,4'-H_2dcbpy)(SCN)$_2$] complex is an orange non-luminescent material

which crystallizes as a monohydrate (**8**·H_2O). Exposure to DMF vapor induces a change in color

to red, and the material becomes emissive (λ_{max} = 660 nm, τ = 16 ns), presumably from a

^{3}MMLCT excited state indicative of Pt(II)-Pt(II) interactions. The CN stretching frequency red-

shifts from 2128 cm^{-1} to 2115 cm^{-1} in the course of DMF uptake, and the three ^{1}H NMR

resonances from the bpy backbone undergo high-field shifts. These two observations are

consistent with a linkage isomerization reaction from S-bound thiocyanate to N-bound

isothiocyanate. According to thermogravimetric studies the DMF adduct contains 3 molecules of

DMF per formula unit (**8**·3DMF). By crystallization from DMF solution it was possible to obtain

single-crystals of the formulation **8**·4DMF in which the SCN$^-$ ligand is clearly nitrogen bound,

but there are no short intermetallic contacts in this specific material. Some of the DMF molecules

form hydrogen-bonds to the carboxyl groups and indeed, the CO stretching frequency of DMF in

8·3DMF is lowered by 22 cm^{-1} compared to liquid DMF, suggesting that in the material with

only 3 molecules of DMF, hydrogen-bonding between DMF and carboxyl groups of the H_2dcbpy

ligand occurs as well. Thus, hydrogen-bonding seems to play an important role in the vapor-

induced linkage isomerization. This interpretation is supported by the finding that solvents with a

Gutmann donor number above 26 induce the isomerization reaction for both SCN⁻ ligands of a given complex (DMSO, DMF, dimethylacetamide), whereas solvents with donor numbers between 10 and 26 (methanol, ethanol, acetone, acetonitrile) induce S-to-N isomerization of only one of the two ligands.[50] Presumably, the explanation for this behavior is that the initial S-bound form is stabilized by hydrogen-bonding between the terminal (more electronegative) N-atoms of the thiocyanato-ligands and the carboxyl-groups of neighboring complexes; upon sorption of a good hydrogen-bond donor these existing hydrogen-bonds are disrupted, making the thiocyanato-ligation thermodynamically unstable. Even though the crystal structure of **8**·4DMF fails to provide direct evidence for intermetallic interactions it is easy to see why such interactions are more likely to occur in **8**·3DMF than in **8**·H₂O: S-coordinated thiocyanate has a bent structure which can be directed up or down from the coordination plane, whereas N-coordinated isothiocyanate is expected to lead to essentially planar complexes, hence close Pt(II)-Pt(II) contacts become more readily possible.

Building on their own prior work Kato and Kobayashi recently reported on a series of coordination polymers containing [Pt(bpy)(CN)₂] units. Specifically, their work focused on [Pt(5,5'-dcbpy)(CN)₂]²⁻ complexes (5,5'-H₂dcbpy = 5,5'-dicarboxyl-2,2'-bipyridine) (**9**²⁻) bridged by Mg²⁺, Ca²⁺, Sr²⁺, Ba²⁺ or Zn²⁺ cations (Scheme 3).[41, 42] Respective systems with formally anionic platinum complexes are discussed in this chapter because of their chemical and functional kinship to the materials discussed above.

Scheme 3. [Pt(α-diimine)(CN)₂] complexes, part III.

9²⁻
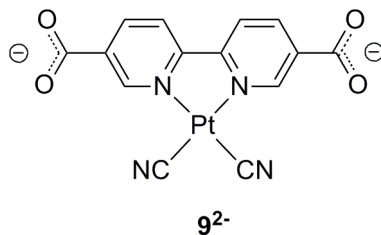
In the zinc compound the $[Pt(5,5'\text{-dcbpy})(CN)_2]^{2-}$ units act as bridges between individual Zn^{2+} ions to form an infinite chain.[41] The platinum complexes themselves are stacked perpendicularly to these chains with an intermetallic distance of 3.309(1) Å which is responsible for the orange color as well as the ^{3}MMLCT emission (at 614 nm) exhibited by the Zn[Pt(5,5'-dcbpy)(CN)_2]·4H_2O material at room temperature. Three of the four water molecules from this formula unit are coordinated to Zn(II) (along with two carboxylate oxygens), while the fourth water molecule is only hydrogen-bonded to a cyano group. When heating to 100°C all four water molecules can be driven off, thereby inducing a color change from orange to red and finally purple. The anhydrous purple form is vapochromic; when exposed to humid air at room temperature it readily re-converts to the initial orange tetrahydrate form. Thus, water adsorption/desorption occurs predominantly at the Zn(II) site, but this influences the stacking of the chromophoric and emitting platinum complexes (Figure 4).
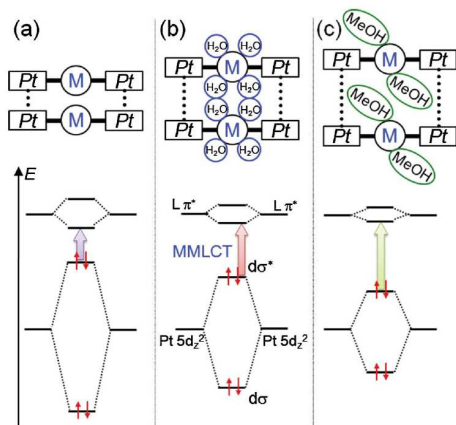
Figure 4. Illustration how solvent uptake at the Zn(II) sites in the M[Pt(5,5'-dcbpy)(CN)$_2$] coordination polymers affects the Pt(II)-Pt(II) distance (upper part) and the energy level structure (MO diagrams in lower part). Reprinted with permission from ref. [42]. Copyright 2011 The Royal Society of Chemistry.

When replacing Zn(II) by other dications it becomes possible to alter the intermolecular Pt(II)-Pt(II) distances in the M[Pt(5,5'-dcbpy)(CN)$_2$]·nH$_2$O coordination polymers;[42] in a way this is similar to cation exchange in tetracyanoplatinates although the accessible Pt(II)-Pt(II) distance range is more narrow for the newly explored coordination polymers.[22] Compounds with M^{2+} = Mg^{2+}, Ca^{2+}, Sr^{2+}, and Ba^{2+} are thought to be isomorphous with Zn[Pt(5,5'-dcbpy)(CN)$_2$]·4H$_2$O, and hence it appears plausible that the alkaline earth metals act as water adsorbing sites similar to the Zn(II) ion in the parent compound, but this is not known for sure. By analogy to the zinc compound discussed above, heating to 100°C drives off all four water molecules in all compounds, and the resulting anhydrous forms readily re-adsorb water vapor at ambient temperature. In the case of the compounds with Mg^{2+} and Ca^{2+} this is accompanied by significant chromic shifts both in absorption and emission, hence these two materials may be considered vapochromic substances. Contrary to the zinc compound, the alkaline earth metal based

coordination polymers can all adsorb methanol vapor, and this alters their luminescence with respect to the anhydrous forms. It is thought that the methanol molecules simply occupy the adsorption sites filled with water in the $M[Pt(5,5'-dcbpy)(CN)_2] \cdot nH_2O$ forms.

2.1.2 [Pt(α-diimine)(acetylide)₂] complexes

The search for phosphorescent metal complexes which can be used as triplet harvesters in organic light emitting diodes (OLEDs) has lead, inter alia, to platinum(II) complexes with acetylide ligands.[16, 51-55] When combining acetylide ligands with α-diimines or cyclometalating chelating agents very strong ligand fields can be exerted on coordinated Pt(II) centers,[56, 57] and this is beneficial for the luminescence properties due to suppression of multiphonon relaxation from metal-localized (d-d) excited states.[58] In the course of research on such complexes a few vapochromic materials have been discovered.

Scheme 4. [Pt(α-diimine)(acetylide)₂] complexes, part I.
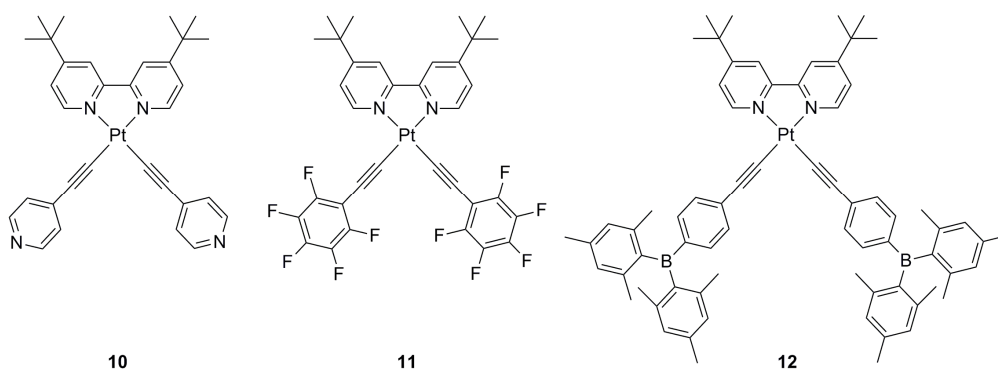
Che, Wong, and coworkers report on a series of [Pt(^{t}Bu$_2$bpy)(arylacetylide)$_2$] complexes two

of which are vapoluminescent (Scheme 4).[59] Thin films of the complex in which the

arylacetylide is 4-ethynylpyridine exhibit greatly enhanced green luminescence upon sorption of

CH$_2$Cl$_2$ or CHCl$_3$ vapor; the detection limits are around 25 and 450 ppm, respectively, while

polar VOCs such as methanol produce no response. In crystals of [Pt(^{t}Bu$_2$bpy)(4-

ethynylpyridine)$_2$]·CH$_2$Cl$_2$ (**10**·CH$_2$Cl$_2$) there are interactions between the relatively acidic

protons of CH$_2$Cl$_2$ and the 4-ethynylpyridine C≡C bonds.[59] As a consequence, an infinite chain

of CH$_2$Cl$_2$ molecules forms within a hydrophobic channel between the platinum complexes; C-

H–N interactions between the ^{t}Bu$_2$bpy ligands and the pyridyl N atoms complement the network

of noncovalent interactions. Presumably, the high selectivity for CH$_2$Cl$_2$ in the vapoluminescent

response of neat [Pt(^{t}Bu$_2$bpy)(4-ethynylpyridine)$_2$] (**10**) is at least partly due to the hydrogen

bonding interactions which have been observed in crystals of the CH$_2$Cl$_2$ adduct. Acetonitrile has

less acidic protons hence hydrogen bonding to the 4-ethynylpyridine C≡C bonds is weaker and

no vapoluminescence is observed; alcoholic vapors presumably cannot intrude into the

hydrophobic environment produced by the *tert.*-butyl substituents. The emission spectrum of the

crystalline CH$_2$Cl$_2$ adduct is similar to that obtained when dissolving the complex **10** in CH$_2$Cl$_2$

and has been interpreted in terms of ^{3}MLCT emission from discrete molecules; there are no short

Pt(II)-Pt(II) contacts in the crystalline form.

When the arylacetylide is ethynylpentafluorophenyl another vapoluminescent material is

obtained.[59] When crystallized from benzene solution [Pt(^{t}Bu$_2$bpy)(ethynylpentafluorophenyl)$_2$]

(**11**) forms orange crystals which exhibit an intense structureless emission with λ_{max} = 595 nm.

Upon exposure to CH$_2$Cl$_2$ vapor, the orange emission gradually changes to green (λ_{max} = 500

nm). While the orange photoluminescence is thought to be excimeric emission originating from

electronically interacting complexes the green luminescence was attributed to ^{3}MLCT emission from isolated complexes. The dichloromethane adduct of this material could not be crystallized but it was possible to investigate **11**·CH$_3$CN by X-ray crystallography. The shortest Pt(II)-Pt(II) contact in the acetonitrile adduct is at 9.957 Å, while in the solvent-free compound the shortest metal-metal distance is 5.172 Å. In the latter, the distances between neighboring luminophore layers are between 3.3 Å and 3.6 Å which is indicative of π-stacking between pentafluorophenyl-rings and ^{t}Bu$_2$bpy. The excimeric orange emission of solvent-free **11** may have its origin in these weak intermolecular interactions.

Wang and coworkers recently reported on a structurally related platinum(II) material exhibiting vapochromism that relies on an entirely different concept which has nothing to do with metal-metal distances or π-stacking.[60] Instead, the vapochromism of complex **12** appears to be due to changes in the excited-state structure resulting from direct interactions between the complex and adsorbed molecules. Complex **12** contains two triarylboron groups, similar to those investigated in the context of fluoride sensors or electron-deficient materials.[61-63] Neat **12** shows yellow ^{3}MLCT emission (λ_{max} = 559 nm) following UV irradiation (Figure 5). Exposure to *n*-hexane, toluene or methanol vapors quenches the luminescence, while exposure to benzene or cyclohexane induces a change in emission color from yellow to red (λ_{max} = 580 − 620 nm). By contrast, when the same complex is exposed to vapors of CH$_2$Cl$_2$, CHCl$_3$, CH$_3$CN, acetone, THF, or ethanol, the emission color shifts from yellow to green (λ_{max} = 490 − 500 nm). Thus, complex **12** exhibits unusual behavior in that different groups of solvent vapors induce emission color shifts to either shorter or longer wavelengths.
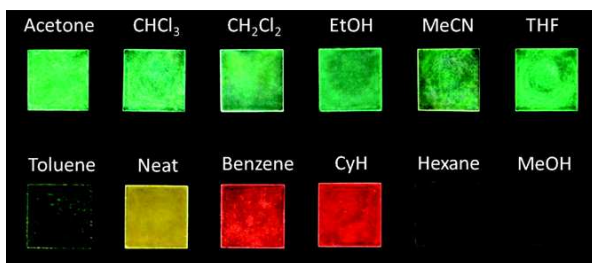
Figure 5. Photoluminescence of complex **12** after exposure to different VOCs. Reprinted with permission from ref. [60]. Copyright 2011 American Chemical Society.

This phenomenon has been explained in terms of solvent-induced switching in the nature of the emissive excited-states: While the yellow luminescence of neat **12** and the red emission after exposure to benzene or cyclohexane are assumed to originate from a ^{3}MLCT state, the green emission following adsorption of more polar vapors is attributed to ligand-centered emission (^{3}LC). This interpretation makes sense in view of the fact that many Pt(II) complexes exhibit negative solvatochromism, because of their large ground-state dipole moments which are opposite to the direction of the MLCT.[64, 65] In complex **12**, solvents of a certain threshold polarity shift the ^{3}MLCT state energetically above the ^{3}LC level which is then largely insensitive to further polarity changes (left part of Figure 6); this explains why solvents ranging in polarity from CH_2Cl_2 to CH_3CN all lead to essentially the same green emission.[60] Conversely, nonpolar solvents decrease the energy of the ^{3}MLCT state, resulting either in red luminescence (benzene, cyclohexane) or, in the extreme case (*n*-hexane), to emission quenching.

Single-crystal X-ray diffraction of **12**·4CH$_2$Cl$_2$ reveals that the shortest intermolecular Pt(II)-Pt(II) separation is above 12 Å and the shortest distance between aromatic planes is ~5.7 Å.[60] Powder X-ray studies show that CH_2Cl_2, benzene, and hexane adducts are structurally very similar to neat **12**. This finding is corroborated by solid state NMR studies monitoring the ^{1}H,

^{13}C, and ^{195}Pt nuclei. ^{11}B NMR spectroscopy shows that the boron center is unaltered by adsorption of CH_2Cl_2 or benzene. On the basis of these observations Wang and coworkers postulated that interactions between the bpy ligands and the adsorbed molecules are responsible for the energetic changes in the emissive ^{3}MLCT state.[60]
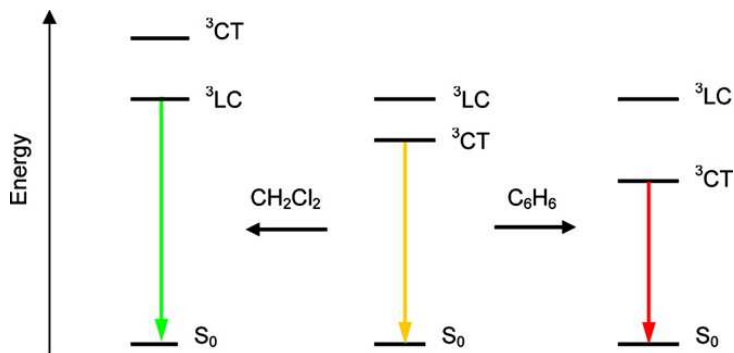
Figure 6. Changes of the excited-state structure in complex **12** as a function of VOC exposure. Reprinted with permission from ref. [60]. Copyright 2011 American Chemical Society.

Chen and coworkers report on a vapoluminescent platinum(II) bis(acetylide) complex (**13**) with a bpy ligand substituted at its 5- and 5'-positions with trimethylsilyl-protected ethynyl groups,[66] its acetylide ligands are two 5-ethynyl-2,2'-bipyridine molecules (Scheme 5). The luminescence of **13** is strongly sensitive to a variety of VOCs. When exposed to acetone, structured luminescence with a band maximum at 562 nm is observed while exposure to THF leads to unstructured emission with λ_{max} at 747 nm. For other solvent vapors, emission band maxima between these two extremes are detected. Structural investigations of different solvent adducts of **13** reveal that there is a correlation between the shortest Pt(II)-Pt(II) distance (d_{Pt-Pt}) with the solvent-induced shift of the emission band maximum: While for the acetone and *n*-hexane adducts d_{Pt-Pt} = 4.8406(15) Å and 4.3091(9) Å, respectively, chloroform and THF adducts

exhibit short Pt(II)-Pt(II) contacts of 3.2363(15) Å and 3.2195(5) Å. Thus, it appears plausible

that the emissive state changes from ^{3}MLCT to ^{3}MMLCT for VOCs such as acetone, CH_2Cl_2,

and *n*-hexane. In the CH_2Cl_2 adduct, intermolecular π-π stacking as well as C-H /π(C≡C)

interactions may play a role as well.[66]

Scheme 5. [Pt(α-diimine)(acetylide)$_2$] complexes, part II.
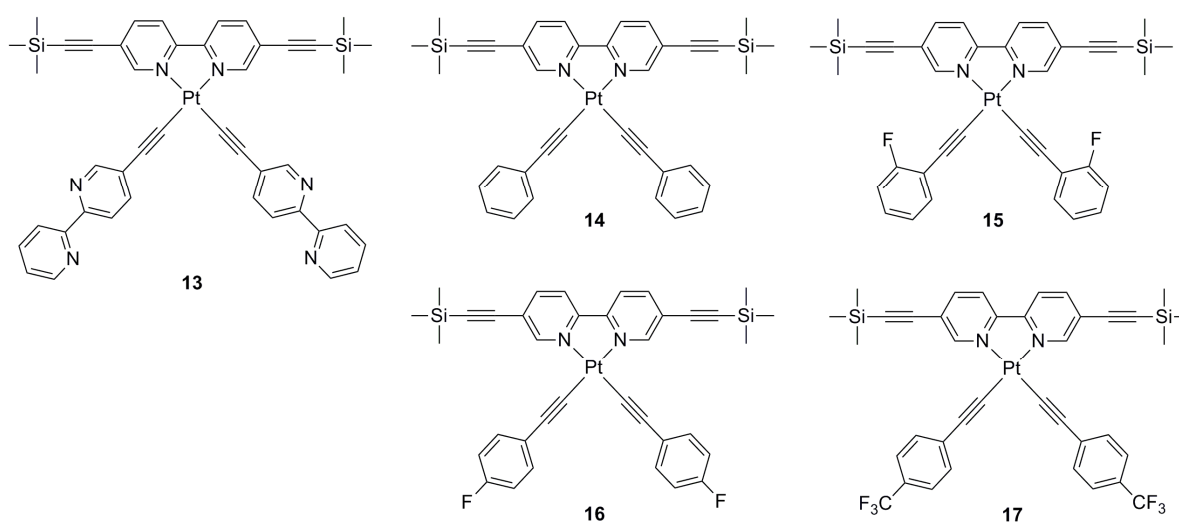
Chen and coworkers further reported on a Pt(II) complex with 5,5'-bis(trimethylsilylethynyl)-

2,2'-bipyridine and phenylacetylene ligands (**14**) exhibiting selective vapoluminescence response

to volatile halohydrocarbons with only one carbon atom and molecular masses below 150

g/mol.[67] The crystal structure of neat **14** as well as those of solvent adducts with 1,2-

dichloroethane and toluene exhibit no Pt(II)-Pt(II) distances shorter than 4.7 Å. By contrast, in

the structure of the CHCl$_3$ adduct there is a short intermetallic distance of 3.302(1) Å between

pairs of complexes. The structural changes following CHCl$_3$ uptake are accompanied by a

change from orange (λ_{max} = 561 nm and 603 nm) to red emission (λ_{max} = 761 nm), which has

been explained by a changeover from ^{3}MLCT emission with some admixed ^{3}LLCT character (τ = 2.12 μs) to ^{3}MMLCT emission. Computational studies support this interpretation and hint to an admixture of ^{3}LLCT character even to the ^{3}MMLCT luminescence. Neat **14** was exposed to a variety of different solvent vapors including those from diethyl ether, ethyl acetate, methyl acetate, acetone, methanol, ethanol, acetonitrile, pyridine, dibromomethane, bromoform, carbon tetrachloride, 1,2-dichloroethane, 1,2-dibromoethane, 1,1,2-trichloroethane, and toluene. However, a vapoluminescence response was only obtained with CH_2Cl_2, $CHCl_3$, and CH_3I. The vapochromic response to CH_2Cl_2 is illustrated by Figure 7.
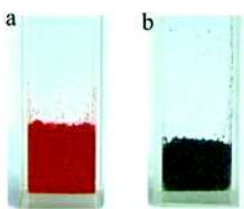
Figure 7. Photograph of crystalline samples of **14** (a) and **14**·CH_2Cl_2 (b). Reprinted with permission from ref. [66]. Copyright 2009 American Chemical Society.

Complexes **15** and **16** differ from **14** only by the fluoro-substituents at the phenylacetylene ligands yet exhibit substantially different vapoluminescence behavior.[68] Complex **15** is specifically selective to $CHCl_3$ vapors, while complex **16** responds to both $CHCl_3$ and CH_2Cl_2. Unlike **14**, neither **15** nor **16** are sensitive to CH_3I, but the effect of chloroform and/or dichloromethane exposure is the same in all three complexes, namely the change from orange ^{3}MLCT/^{3}LLCT to red ^{3}MMLCT/^{3}LLCT emission mentioned above for **14**. The structure of the adduct between **15** and 1,2-dichloroethane, as well as the structures of **16**·0.5CH_2Cl_2,

16·CH_2ClCH_2Cl, and **16**·CH_2BrCH_2Br were determined by single crystal X-ray diffraction (Figure 8). Individual complexes are either stacked in staggered or anti-parallel fashion in these structures. The staggered mode permits formation of Pt(II)-Pt(II) contacts shorter than 3.4 Å, whereas in the anti-parallel mode individual complexes are forced to slide away from each other so as to enforce intermetallic distances longer than 3.5 Å. Both stacking modes appear in the structure of **16**·0.5CH_2Cl_2 as there are pairs of complexes with short (3.315(9) Å) and long (4.853(10) Å) metal-metal distances (Figure 8). The structures of **15**·CH_2ClCH_2Cl and **15**·CH_2ClCH_2Cl exhibit relatively short intermetallic contacts (3.514(16) Å and 3.513(5) Å) as well, but there is no significant vapoluminescence response of **15** or **16** to 1,2-dichloroethane. A notable feature of several of the abovementioned crystal structures is the presence of C-H/π(C≡C) interactions between the halocarbon adsorbents and the fluorophenylacetylides. The reversible structural changes following the conversion of **16**·CH_2BrCH_2Br to **16**·CH_2Cl_2 were studied by monitoring X-ray diffraction (XRD) patterns after different times following exposure to CH_2Cl_2 or 1,2-dibromoethane vapors. Given the reversibility of the structural transformations the observation of fully reversible vapoluminescence responses by **15** and **16** is not particularly surprising. Several solvent adducts of **15** and **16** were found to exhibit mechanochromic luminescence.[23, 68]
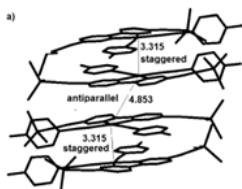
Figure 8. Molecular packing in single crystals of **16**·0.5CH$_2$Cl$_2$. (J. Ni, X. Zhang, Y.-H. Wu, L.-Y. Zhang, Z.-N. Chen. Chem. Eur. J., 2011, 17, 1171-1183. Copyright Wiley-VCH Verlag GmbH & Co. KGaA. Reproduced with permission.)

A closely related Pt(II) complex has two 4-trifluoromethylphenylacetylide ligands (**17**) and is selectively sensitive to vapors from cyclic ethers such as THF, dioxane, or tetrahydropyrane (THP) (Figure 9).[69] As in the case of **13** – **16**, the vapoluminescence response of **17** is triggered by changes in intermetallic distances causing a red-shift in luminescence due to the changeover from [3]MLCT/[3]LLCT to [3]MMLCT emission. In **17**·THF there is a short (3.255(8) Å) Pt(II)-Pt(II) distance between staggered complexes, and the overall crystal structure appears to be stabilized by host-guest interactions through hydrogen-bonding between C-H groups of the complex and the oxygen atom of THF, as well as between C-H groups of THF and the trifluoromethyl group of the phenylacetylide ligands. It is possible that this is the origin of the selective vapoluminescence response to certain O-heterocyclic compounds (Figure 9). XRD studies reveal that the structural conversion between **17**·CH$_2$ClCH$_2$Cl and **17**·THF is fully reversible. Exposure to vapors of methanol, ethanol, acetone, furan, diethyl ether, ethyl acetate, hexane, toluene, pyridine, and various halohydrocarbons produces no significant vapoluminescence changes. The initial motivation for introducing the electron-withdrawing trifluoromethyl group at the phenylacetylide ligands was to increase the HOMO-LUMO energy gap, and the expected emission blue-shift could indeed be observed (λ_{max} of **17** in CH$_2$Cl$_2$ solution: 568 nm; λ_{max} of **14** in CH$_2$Cl$_2$: 616 nm). However, the selective vapoluminescence response of **17** is most likely an accidental result.

Similar to **15** and **16**, neat **17** and some of its solvent adducts exhibit mechanochromic properties and luminescence thermochromism.[23, 69]
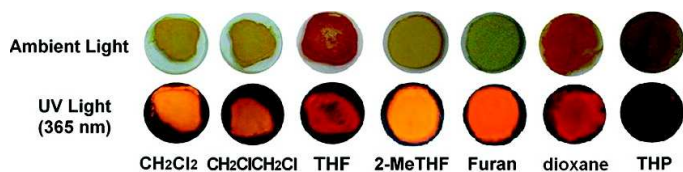
Figure 9. Vapochromic and vapoluminescent response of complex **17** to selected VOCs. Reprinted with permission from ref. [69]. Copyright 2012 American Chemical Society.

2.1.3 [Pt(isocyanide)$_2$(CN)$_2$] complexes

When heating double salt compounds of the stoichiometry [Pt(CNR)$_4$][Pt(CN)$_4$] (see next chapter) to their melting point in absence of solvent, ligand rearrangement occurs and isomeric charge-neutral [Pt(CNR)$_2$(CN)$_2$] complexes are formed.[70] Starting from the respective double salt, Mann and coworkers prepared [Pt(CN-C$_6$H$_4$-C$_2$H$_5$)$_2$(CN)$_2$] (**18**) at 201 °C (Scheme 6).

Scheme 6. Vapochromic [Pt(isocyanide)$_2$(CN)$_2$] complexes.
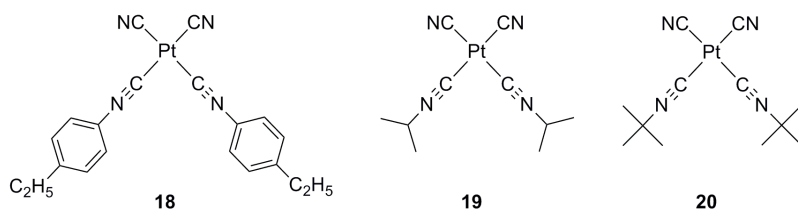
Subsequent re-crystallization of the raw product gives either an orange or a purple form of the same product: Slow crystallization from CH$_2$Cl$_2$ yields the orange form, while the purple isomer

is obtained via rapid addition of hexanes to the CH_2Cl_2 solution. Of specific interest here is the

orange form because it exhibits vapoluminescence, whereas the purple isomer does not appear to

respond to VOCs. Orange **18** is the *cis*-isomer of **18** (*cis*-**18**) and exhibits luminescence from a

$d\sigma^*\rightarrow p\sigma$ excited state similar to tetracyanoplatinates. When exposed to vapors of toluene,

benzene, chlorobenzene, *p*-xylene, mesitylene, or ethanol in an N_2 stream at 296 K, the

maximum of the broad emission band of *cis*-**18** shifts from 611 nm to shorter wavelengths by up

to 46 nm (Figure 10). In the case of toluene a VOC mole fraction of 0.0337 in the N_2 stream is

necessary to induce this blue-shift while in the case of mesitylene only a mole fraction of 0.0028

is required to induce the same effect. Analysis of the luminescence data suggests that toluene

sorption occurs in two steps, involving adducts with the stoichiometry *cis*-**18**·0.25$C_6H_5CH_3$ and

cis-**18**·0.5$C_6H_5CH_3$. Gravimetric studies, however, indicate that *cis*-**18** rapidly sorbs 0.5

equivalents of toluene while prolonged exposure produces an adduct with 0.9 equivalents of

toluene. Subsequent partial removal of toluene by continued purging with N_2 occurs readily, but

the last 0.25 equivalents are held with tenacity and neat *cis*-**18** can only be recovered with

simultaneous heating.
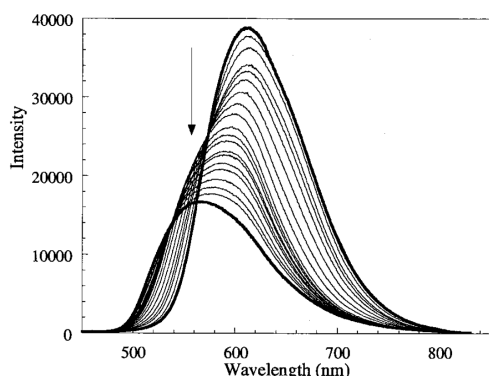
Figure 10. Emission spectral changes of *cis*-**18** in the course of toluene vapor uptake. Reprinted

with permission from ref. [70]. Copyright 2002 American Chemical Society.

The structures of *cis*-**18**·0.5C₆H₅CH₃ and *cis*-**18**·x(hexanes) were determined by X-ray analysis.[70] The packing arrangements in both structures are nearly identical, there are infinite stacks of *cis*-[Pt(CN-C₆H₄-C₂H₅)₂(CN)₂] molecules with chains of Pt(II) atoms along the c-axis. The in-chain Pt(II)-Pt(II) separation in the toluene adduct is alternating between 3.281 Å and 3.300 Å, but the chain is slightly zigzagged with Pt-Pt-Pt angles of 175.5°. The *cis*-**18**·0.5C₆H₅CH₃ adduct incorporates 4 toluene molecules per unit cell, thereby the volume of the latter increases by 160 Å³ or 43% of the estimated volume of 4 toluene molecules (372 Å³). Uptake of toluene vapor increases the packing efficiency by 10%, which is significantly greater to what is commonly observed for the vapochromic Pt(II) double salts discussed in the next section (6%). Toluene sorption increases the length of the unit cell along the c-axis by 0.35 Å, resulting in an increase of the Pt(II)-Pt(II) distance by about 0.09 Å. However, among the VOCs investigated, no obvious correlation between the magnitude of the vapochromic luminescence band shift and any one VOC molecular parameter was found, and it was cautiously suggested that the molecular shape of the VOC guest plays an important role.

When the [Pt(CNR)₄][Pt(CN)₄] double salt with R = C₆H₄-C₂H₅ is heated to reflux in chloroform, the purple *trans*-isomer of compound **18** is obtained.[71] Expectedly, *trans*-**18** differs from *cis*-**18** not only in color (purple vs. orange) but by an ensemble of physical properties, e. g., different cyanide stretching frequencies, different chemical shifts for the ¹⁹⁵Pt NMR signals, and molecular packing in single crystals. The Pt(II)-Pt(II) separation (3.1253(8) Å) in *trans*-**18** is one of the shortest in the entire class of Pt(II) double salts. Furthermore, there are intermolecular π-π interactions between isocyanide ligands of different stacks leading to a relatively close-packed structure in two of the three dimensions. As noted by Mann and coworkers, it is possible that the

compact two-dimensional packing motif is responsible for the absence of vapochromism or vapoluminescence of *trans*-**18**.[71]

This *cis*-isomer of [Pt(CN-^{i}C$_3$H$_7$)$_2$(CN)$_2$] (*cis*-**19**) was synthesized from the respective double salt like *cis*-**18**.[72] Individual Pt(II) complexes in *cis*-**19** are slip-stacked in staggered fashion along the c-axis with an intermetallic distance of 3.256 Å, the color of the material is yellow. When exposed to benzene vapors, the structure changes to an eclipsed orientation of Pt(II) complexes with an intermetallic separation that has increased to 3.485 Å, and the color of this compound (*cis*-**19**·0.5C$_6$H$_6$) is blue. The structural change including a 20% expansion in unit cell volume is further accompanied by a change in luminescence properties (Figure 11). Modeling of the spectral changes observed in the course of exposure to benzene leads to the conclusion that benzene uptake is a consecutive two-step reaction (A → B → C) with an intermediate B of unknown structure. Interestingly, *cis*-**19** does not respond to vapors of substituted derivates of benzene such as toluene, *p*-xylene, *m*-xylene, *o*-xylene, mesitylene, chloroform, and hexafluorobenzene. Presumably the selectivity of *cis*-**19** for benzene has its origin in the absence of a stable solvate phase for adducts such as *cis*-**19**·*n*(C$_6$H$_5$CH$_3$). Unfortunately, the reversibility of the benzene uptake is poor due to crystalline degradation. The slow kinetics for benzene sorption additionally limits the usefulness of *cis*-**19** as a benzene sensor for practical purposes.
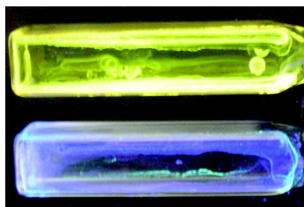
Figure 11. Photoluminescence of cuvettes filled with crystalline films of *cis*-**19** before (top) and after (bottom) exposure to benzene vapor. Reprinted with permission from ref. [72]. Copyright 2009 American Chemical Society.

Using the compound $[Pt(CN-^tBu)_2(CN)_2]$ (**20**) it has been possible to fabricate vapor-responsive microwires.[73] For this purpose, **20** was dissolved in methanol and deposited onto insulating SiO_2 substrates bearing two pre-installed small gold electrodes on the surface. The microwires were typically longer than 10 μm and hence they were able to cross over two neighboring electrodes. When slowly evaporating solvent over a time period of 6 days the diameter of the microwires was typically on the order of 1.2 μm. The electrical conductivity of an operating electrode-microwire-electrode device at a bias of 5 Volts was determined to be 6.86 μA. The conductivity is perturbed upon VOC exposure, but only toluene, acetonitrile, and methanol produce a significant response. Vapors of THF, acetone, ethyl acetate, diethyl ether, petroleum ether, hexane, nitromethane, ammonia, chlorobenzene, cyclohexane, dichloromethane, chloroform, and hydrazine lead to a comparatively small change in conductivity. It has been suggested that changes in the Pt(II)-Pt(II) interactions are responsible for the vapor-induced variations in conductivity.[73] X-ray diffraction indicates that upon acetonitrile uptake the Pt(II)-Pt(II) distance remains almost unchanged (3.354(1) Å vs. 3.3525(2) Å), but the coordination bond angles around the Pt(II) center are altered.[74] Consequently, CH_3CN exposure is associated with a relatively small change in luminescence properties and the $5d\sigma^*\leftarrow6p\sigma$ emission simply decreases in intensity but does not change color (λ_{max} stays at 534 nm).

2.2 Platinum(II) / palladium(II) double salts

When stirring an acetonitrile solution of $Pt(CH_3CN)_2Cl_2$ and $[(n\text{-}Bu)_4N]_2[M(CN)_4]$ (M = Pt, Pd) in presence of isopropylisocyanide one obtains two compounds which are reminiscent of the Magnus Green Salt (MGS, $[Pt(NH_3)_4][PtCl_4]$), namely $[Pt(CN\text{-}^iC_3H_7)_4][Pt(CN)_4]$ (**21**) and $[Pt(CN\text{-}^iC_3H_7)_4][Pd(CN)_4]$ (**22**) (Scheme 7).[75]

Scheme 7. Vapochromic d^8-d^8 double salts, part I.
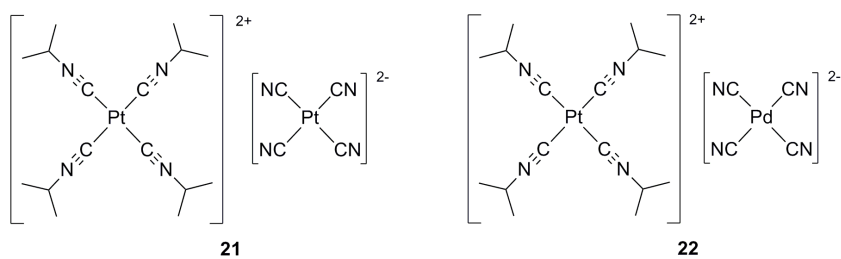
Bulk samples of **21** are red with a green metallic reflectance whereas **22** is yellow. From aqueous solution **21** crystallizes as a hexahydrate adduct with alternating cation-anion stacking similar to MGS (Figure 12), and the water molecules connect individual stacks through hydrogen-bonding to the cyanide ligands of the anion. Gravimetric investigations demonstrated that dry **21** readily uptakes either 12 molecules of H_2O, 8 molecules of methanol, 6 molecules of chloroform, or 4 molecules of trifluoroethanol when exposed to the corresponding vapors.
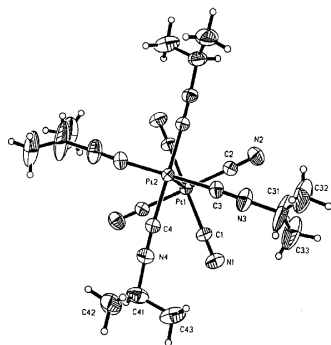
Figure 12. A cation-anion pair in compound **21**. Reprinted with permission from ref. [75].
Copyright 1998 American Chemical Society.

Interestingly, none of these sorption processes influences the Pt(II)-Pt(II) distance much, the
unit cell parameter in the stacking direction (*c*-axis) varies in the narrow range from 6.303(2) Å
to 6.337(2) Å. As a consequence, the absorption maximum of the lowest-energetic absorption
varies only from 573 nm to 603 nm and vapochromism is not particularly spectacular. However,
the vapor-sorption induced changes in the distance between individual Pt(II)-Pt(II) stacks in the
ab plane are all the more noteworthy; the respective distance varies between 10.416 Å(1) (in dry
21) to 18.271(4) Å (in **21**·12 H_2O). Large unit cell volume expansions reflecting the size of the
guest vapor are observed: For H_2O the cell volume expands by 54%, for methanol 60%, for
trifluoroethanol 73%, and for chloroform 94% relative to the volume of dry **21**. Thus, it is clearly
the size of the guest, and not the size of any preexisting pores in the host material which
determines the magnitude of the lattice expansion. Principally these changes in the plane
perpendicular to the Pt(II)-Pt(II) stacking direction are thought to be responsible for the weak
vapochromism of **21**, but how exactly this occurs is not known.[75]

Scheme 8. Vapochromic d^8-d^8 double salts, part II.

23

24a n=1
24b n=6
24c n=10
24d n=12
24e n=14
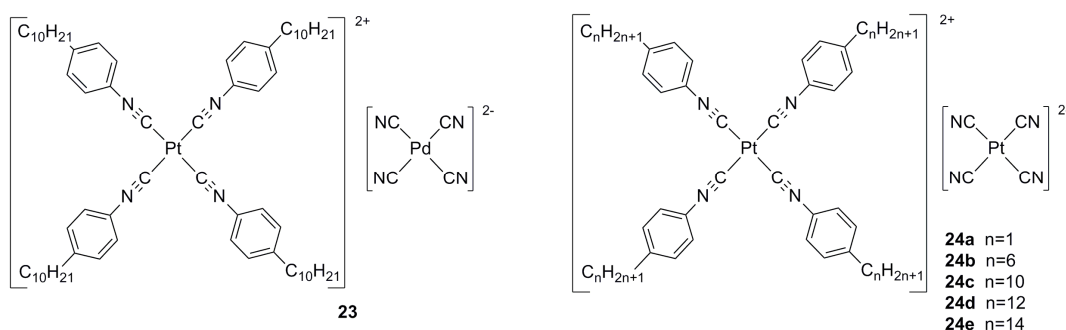
A variety of different isonitrile ligands can be used for obtaining vapochromic double salts similar to **21** or **22**, an early example is $[Pt(CN-C_6H_4-C_{10}H_{21})][Pd(CN)_4]$ (**23**) (Scheme 8).[76] Analogous compounds with isonitriles containing n C_6, C_{12}, and C_{14} chains were investigated as well, but the C_{10} compound has the highest responsivity to solvent vapors. Thin films of **23** change color from pink to blue with a response time ($t_{1/2}$) of ~350 ms when exposed to $CHCl_3$-saturated air at room temperature. The associated shift of the visible absorption band from 548 nm to 578 nm is reversible thanks to a minimal disruption of crystallinity upon vapor sorption. It has been suggested that this is possible due to the rather large size mismatch between Pt(II) dications and Pd(II) dianions, producing a relatively large free volume through which $CHCl_3$ can easily move in and out of the material. IR spectroscopy suggests that the $CHCl_3$ guest interacts predominantly with the $[Pd(CN)_4]^{2-}$ anion because the CN vibration in pure **23** exhibits a single band at 2125 cm^{-1} while in the $CHCl_3$ adduct a splitting into two bands (at 2127 and 2132 cm^{-1}) is observed; the CN stretching frequency of the isonitrile ligands of the cation are invariant to $CHCl_3$ uptake.

Bailey and Hupp reported on chemoresponsive diffraction gratings which make use of the vapochromic ($[Pt(CN-C_6H_4-C_{10}H_{21})_4][Pd(CN)_4]$ material (**23**).[77] A film of compound **23** was cast onto a patterned poly(dimethylsiloxane) stamp having 5×5 μm^2 wells arranged periodically, and

the stamp was subsequently brought into contact with a transparent microscope slide. The lattice periodicity of 10 μm is nicely observable by AFM and permits the diffraction of visible light. The uptake of chloroform vapor by the vapochromic layer results in an increase of the refractive index of the diffraction grating because voids (or initially present water molecules) in the vapochromic material are replaced by an organic substance. The increase in refractive index difference between grating and surrounding medium in turn causes an increase in diffraction efficiency. This effect is particularly strong when using light of a wavelength at which the diffraction lattice absorbs: Using 632.8 nm as an irradiation wavelength the loss-corrected diffraction efficiency is ~3000 times larger than when irradiating at a wavelength where the lattice does not absorb. Because the magnitude and the direction of the vapor-induced absorption band shifts in compound **23** depends on the VOC, the resonance effect observed in diffraction efficiency at a given irradiation wavelength is dependent on analyte, i. e., the effect shows certain solvent selectivity. Based on uptake isotherms a detection limit of a few mg/m^3 was estimated for $CHCl_3$ vapor.

Analogous double salts with tetracyanoplatinate(II) instead of tetracyanopalladate(II) anions exhibit vapochromism as well. On the cations, arylisocyanide ligands (p-CN-C_6H_4-C_nH_{2n+1}) with n = 1, 6, 10, 12, 14 were explored, and it was found that compounds with n = 1, 6 (**24a**, **24b**) respond better to polar VOCs whereas compounds with n > 6 are more sensitive to nonpolar VOCs (**24c**, **24d**, **24e**) with compound **24c** (n = 10) being the most responsive.[78] Despite the change from a 4d to a 5d metal in the dianion, there is still a significant size mismatch between counterions which is important for the reversible vapochromism of this family of compounds (Figure 13).
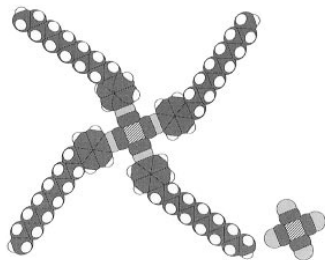
Figure 13. Space-filling model of double salt **24d**. Reprinted with permission from ref. [78]. Copyright 1998 American Chemical Society.

These Pt(II)-Pt(II) double salts are mostly insoluble solids with a blue color, caused by a dσ*→pσ transition arising from $5d_{z2}$-$5d_{z2}$ and $6p_z$ -$6p_z$ orbital overlaps between neighboring Pt(II) atoms in linear stacks of alternating cations and anions (Figure 2). In neat **24c** the maximum of the respective absorption is at 746 nm, and upon exposure of a thin film of **24c** to $CHCl_3$ λ_{max} shifts to 837 nm. Methanol, ethanol, 2-propanol, diethyl ether, acetonitrile, hexanes, acetone, benzene, and dichloromethane produce vapochromic shifts as well, but to a smaller extent than chloroform (11 – 65 nm). The luminescence of **24c** is affected by vapor sorption, too, but the emission band maximum of neat **24c** is already outside the visible spectral range (944 nm) and further moves into the NIR upon vapor sorption (e. g., to 1018 nm for $CHCl_3$). The timescale of the vapochromic response is ∼500 ms ($t_{1/2}$). IR spectroscopy monitoring the CN stretching vibrations of the cyanide and arylisonitrile ligands indicates that solvents capable of forming hydrogen bonds mostly interact with the $[Pt(CN)_4]^{2-}$ anion, whereas apolar VOCs (e. g., benzene) cause very small shifts in ν(CN) but produce a significant change in the NIR portion of the optical absorption spectrum. From these observations it was concluded that the vapochromic response of this family of compounds is governed by a complicated interplay of hydrogen-bonding, lypophilic, and dipole-dipole interactions.

In-depth IR studies of **24c** revealed a correlation between the cyanide stretching frequency and the hydrogen-bonding ability of the adsorbed VOC,[79] as expressed by Abraham's α parameter.[80] The vapor-induced $\nu(CN)$ shifts are between 1 and 17 cm^{-1}. The only solvent which does not at all fit into the correlation between $\nu(CN)$ and α is water, due to its inability to pass the hydrophobic barriers imposed by the long alkyl chains of the dications.

Scheme 9. Vapochromic d^8-d^8 double salts, part III.

25   26
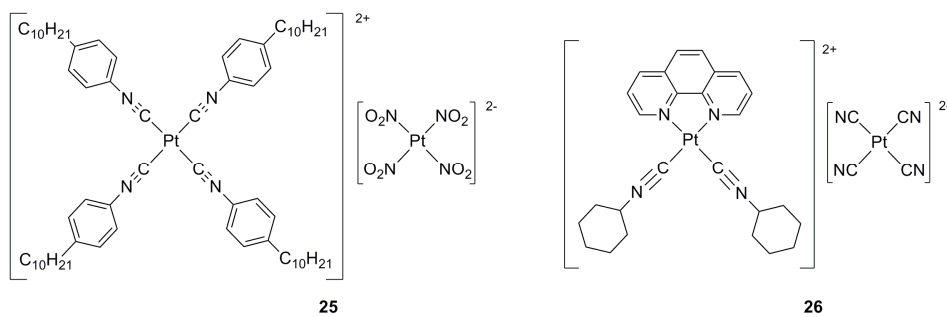
Based on the double salt family of vapochromic compounds several molecular devices were constructed. The first to be mentioned here is that of a vapochromic light-emitting diode (LED).[81] For this purpose, a 700-nm layer of tris-(4-(2-thienyl)phenylamine) was deposited on an ITO coated glass and oligomerized anodically to produce a hole transport layer. This was followed by casting a 200-nm film of compound **25** (Scheme 9) on top. Finally, vapor deposition was used to deposit a 700-nm film of aluminum on top of everything. Application of an external voltage then resulted in electron flow from aluminum through the two molecular layers to ITO, inducing electroluminescence with a photon/electron efficiency of about 0.01%. The electroluminescence was clearly due to compound **25** and exhibited a similar response to acetone vapor as the photoluminescence spectrum of **25**, namely a shift of λ_{max} from 540 to 575 nm. The

motivation for using **25** with its tetranitroplatinate(II) anion instead of the analogous tetracyanoplatinate(II) salt (**24c**) was mainly the experience that **25** forms better films.

A device containing the same components but with somewhat different film thicknesses was used as a vapochromic photodiode.[82] Rectification of the current favoring electron flow from aluminum through the two molecular layers was observed, the rectification ratio at 5 Volts was ~100. Under application of 2 Volts of reverse bias it is possible to induce a photocurrent using the visible light output of a 450 W Xenon lamp. When blowing acetone vapor into the device, the photocurrent increased more than 10 times within 2 minutes. It was noted that this photodiode acts like vapochromic absorption sensor without the need for a separate detector.

Scheme 10. Vapochromic d^8-d^8 double salts, part IV.
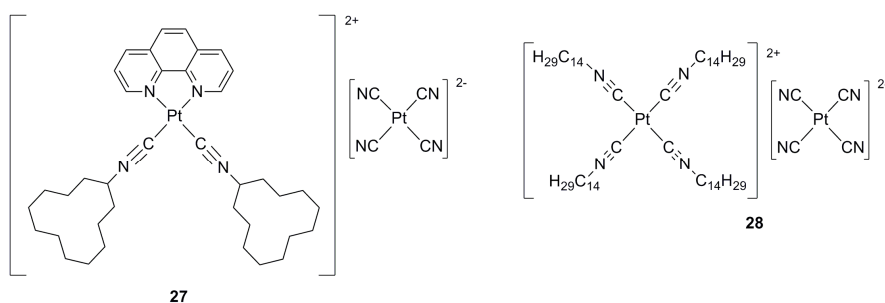
In addition to the vapochromic LED and the vapochromic photodiode Mann and coworkers reported on electronic nose devices based on vapoluminescent Pt(II)-Pt(II) double salts.[83, 84] The principle of electronic noses is to use an array of chemical substances which respond differently when exposed to different vapors such that one obtains a response pattern from which one is able to discriminate between various odors.[2, 85] Using a combination of compounds **27**, **28** and **26** (Scheme 10), deposited in submilligram quantities onto inert support disks made from platinum or carbon fibers, it was possible to construct a device which is able to differentiate chloroform,

water, methanol, and dichloromethane from a broad variety of other solvent vapors. Interestingly, the device is able to differentiate between two the isomeric forms of propanol, but *n*-hexane and cyclohexane are not well resolved from each other.[83] The discrimination ability of this device relies on the fact that compounds **27** and **26** give differently pronounced gradual vapor-induced luminescence shifts, whereas compound **28** acts essentially as a binary sensor with only two distinct responses. Principal component analysis of the overall luminescence spectra after vapor exposure then permits distinction between different vapors.

Scheme 11. Vapochromic d^8-d^8 double salts, part V.

29
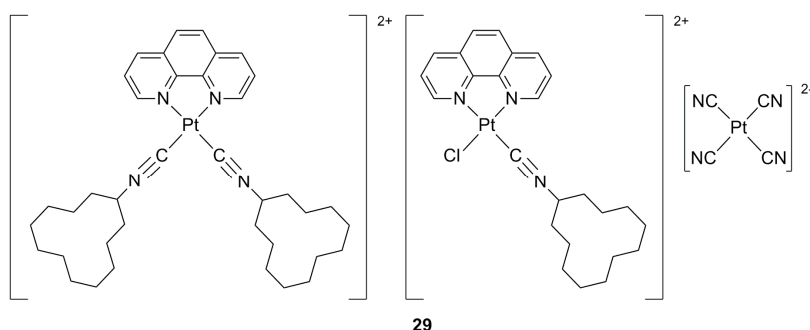
In subsequent electronic nose studies, compound **28** was replaced by the more temperature-resistant compound **29**, a mixed cation platinum(II) double salt which can be formulated as [dication]$_2$[monocation]$_2$[Pt(CN)$_4$]$_3$ (Scheme 11).[84] This was necessary because heating and cooling cycles of the array elements while purging with N$_2$ gas between solvent vapor exposures turned out to be the most effective way to increase the reversibility and reproducibility of the device response. In addition, elevated operating temperatures (typically 50°C) did at least partially eliminate the problem of undesired devices responses to air humidity. Using principal component analysis of vapor-induced luminescence changes the electronic nose constructed from

compounds **27**, **26** and **29** was able to differentiate between 10 different solvents. The detection

limit for acetone was at 12% saturation (75 g/m^3), for methanol an even lower detection limit of

3% (6 g/m^3) was determined.[84]

Scheme 12. Vapochromic d^8-d^8 double salts, part VI.
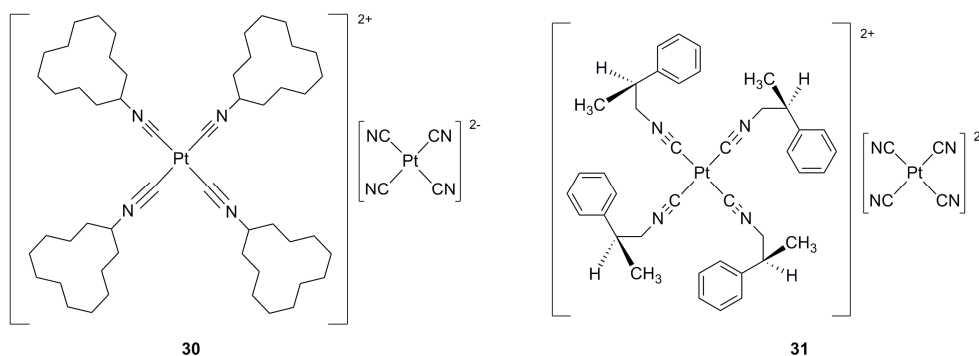
Unusually direct insight into the phenomenon of vapochromism in Pt(II)-Pt(II) double salts

was obtained from investigation of compound **30** using a quartz crystal microbalance on which

mass changes and spectral changes as a function of water uptake from air humidity could be

detected simultaneously (Scheme 12).[86] The employed experimental setup revealed a type of

behavior which was not previously known for this class of compounds, namely a strongly

nonlinear response behavior to varying concentrations of water vapor. At low water vapor

concentrations compound **30** sorbs 0.5 water molecules per formula unit, followed by a sudden

uptake of 2.5 water molecules per formula unit when the water vapor concentration increases to

~25% relative humidity. This phenomenon is accompanied by a stepwise change of the

reflectance spectrum of compound **30** on the quartz crystal microbalance, i. e., optical

spectroscopic and sorptive properties of thin films of **30** changed in a correlated fashion. CH_2Cl_2

and $CHCl_3$ vapors produce reflectance changes as well, but as their concentrations are increased

the step-like response behavior is much less pronounced than for water vapor. Benzene, toluene, and *p*-xylene induce a gradual vapochromic response. It thus appears that vapors capable of hydrogen-bonding produce fundamentally different optical species in **30** than non-hydrogen-bonding VOCs.

Starting from enantiomerically pure isocyanide ligands, Drew, Mann and coworkers recently synthesized and explored a double salt which is capable of enantiomerically selective vapoluminescence sensing.[87] Compound **31** with chiral β-methylphenethylisocyanide ligands on the cation can be obtained in pure *R*- and *S*-forms, and the two enantiomers are able to differentiate between vapors of *R*-2-butanol and *S*-2-butanol. The enantiomeric selectivity cannot be pinned down to one specific effect but was rather considered as resulting from a combination of three possible effects: (i) differential selective hydrogen-bonding between the chiral 2-butanol guest and the cyanide ligands, (ii) selective solvation at the chiral host sites, and (iii) selective permeation of the chiral guest into the interstitial voids of the chiral host. Compound **31** suffers from water sensitivity and stability issues which need to be resolved before efficient vapochromic devices with enantiomeric selectivity can be envisaged; however, the proof of concept has clearly been provided.

2.3 Cationic Pt(II) complexes with tridentate N^N^N ligands

2.3.1 Terpyridine complexes

Electrostatic repulsion is a significant obstacle to obtaining stacks of cationic Pt(II) complexes with short metallophilic contacts. In view of this problem, many researchers have turned their

attention to 2,2':6',2''-terpyridine ligands because they have strong σ-donating and π-accepting

character, because these properties are beneficial for Pt(II)-Pt(II) stacking.

Scheme 13. Pt(II) terpyridine complexes, part I.

32a⁺ R=H
32b⁺ R=OC₄H₉
32c⁺ R=OC₆H₁₃
32d⁺ R=OC₈H₁₇
32e⁺ R=OC₁₂H₂₅

33⁺

Cl⁻, PF₆⁻, ClO₄⁻
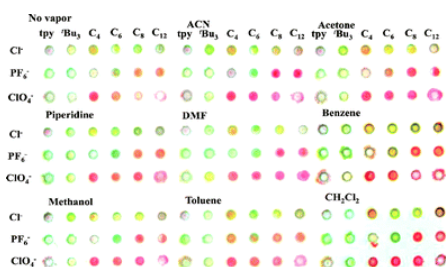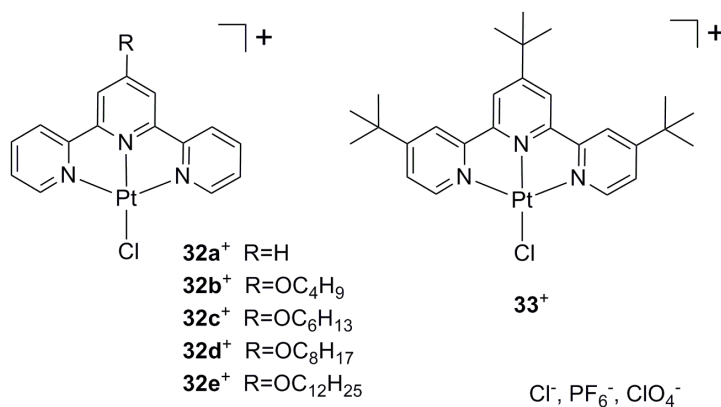
Figure 14. Vapochromic response of microarrays with complexes **32a-e⁺ – 33⁺**. Reprinted with permission from ref. [88]. Copyright 2008 The Royal Society of Chemistry.

Among the structurally most simple Pt(II) terpyridine complexes that have been investigated in

the context of vapochromism and vapoluminescence are the cations **32a-e⁺ – 33⁺** which were

each isolated as a chloride, hexafluorophosphate, and perchlorate salt, resulting in a total of 18

compounds (Scheme 13).[88] 4 nmol portions of these substances were put into 6 × 3 microarrays

from which the vapor-induced color and luminescence changes could be detected using a flatbed

scanner (Figure 14). Alkoxy-substitutents on terpyridine were used because they have previously been demonstrated to favor π-stacking,[89] whereas the *tert.*-butyl groups are likely to lead to longer metal-metal contacts. Variation of the counterion affects packing of the Pt(II) terpyridine cations in the crystals.[48] Making these simple chemical variations on the chloro(terpyridine)platinum(II) backbone, it was hoped that exposure to different VOCs would produce distinct colorimetric / luminometric patterns and that the microarrays would be able to qualitatively mimic the olfactory system.[88] Indeed, the individual Pt(II) salts respond distinctively to different analytes, but research on microarrays with these salts did not go far beyond providing the proof of concept. Anyhow, it was demonstrated that VOCs with lone pairs such as acetonitrile, piperidine and DMF produce the greatest vapochromic and vapoluminescent changes in the salts of complexes **32a-e$^+$ – 33$^+$**.

Scheme 14. Pt(II) terpyridine complexes, part II.
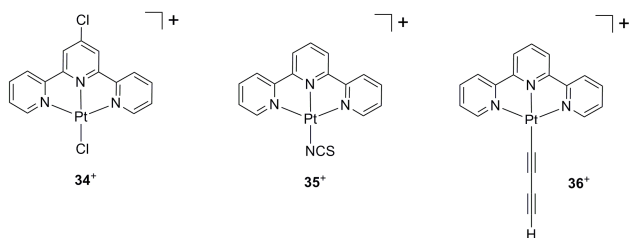
Despite its chemical simplicity the chloride salt of the (4-chloroterpyridine)platinum(II) complex **34$^+$** is a highly selective vapoluminescent sensing material (Scheme 14).[90] It responds only to methanol vapor whereas all other tested VOCs, including halogenated solvents (CH_2Cl_2, $CHCl_3$, CCl_4), aromatic substances (benzene, toluene, *p*-xylene, pyridine), amines (triethylamine, diethylamine, diisopropyl amine), other alcohols (ethanol, isopropanol, *n*-butanol, *t*-butanol),

THF, diethyl ether, acetone, ethyl acetate and alkanes elicit no response. Methanol uptake is accompanied by a color change from red to yellow, and the emission band maximum undergoes a blue-shift from 665 nm to 615 nm. Even though no crystallographic data is available it is reasonable to assume that the red form contains short Pt(II)-Pt(II) contacts which make a ^{3}MMLCT state the energetically lowest and emissive excited state, whereas the yellow color of the methanol-exposed material signals the absence of significant metallophilic interactions. Consequently, the vapoluminescence response most likely relies on the disruption metal-metal contacts and changeover from ^{3}MMLCT to ^{3}MLCT emission. In addition to the unusual selectivity, the high reversibility of the vapoluminescence response is an attractive feature of **34**Cl.
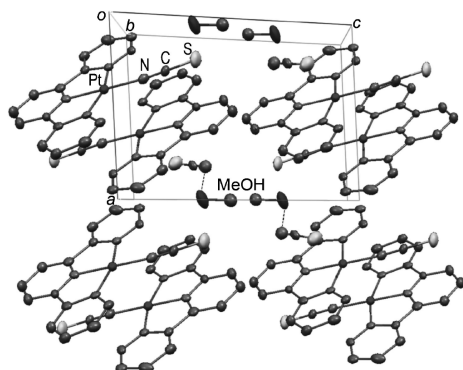
Figure 15. Packing diagram for **35**SCN·MeOH. Reprinted with permission from ref. [91]. Copyright 2009 The Chemical Society of Japan.

After the chloro(terpyridine)platinum(II) complexes the chemically next simple Pt(II) terpyridine exhibiting vapochromism is the thiocyanato complex **35**[+]. When exposing the rhodanide salt of this complex (**35**SCN) to methanol vapor, an unusual stepwise vapochromism

1
2
3
4
5
6
7
8
9
10
11
12
13
14
15
16
17
18
19
20
21
22
23
24
25
26
27
28
29
30
31
32
33
34
35
36
37
38
39
40
41
42
43
44
45
46
47
48
49
50
51
52
53
54
55
56
57
58
59
60

response is detected.[91] Initially, the **35**SCN compound is red but upon methanol exposure there is first a color change to dark red before the material turns yellow. The structure of the yellow compound was determined by X-ray diffraction on single crystals grown from methanol solution and was found to consist of dimers of cations with an intermetallic distance of 3.4567(3) Å (Figure 15). Between individual dimers there are no metal-metal contacts shorter than 6 Å. Methanol solvate molecules are hydrogen-bonded to the N atoms of the NCS⁻ anions, forming one-dimensional channels along the crystallographic b-axis. In air, the yellow crystals rapidly change to red due to facile methanol loss. On the basis of combined diffuse reflectance and powder X-ray diffraction studies, a two-step structural transformation from the initial red methanol-free form to an intermediate dark red form containing some methanol to finally a yellow fully adsorbed form was postulated. The color changes were explained by an increase of π-π stacking and/or Pt(II)-Pt(II) interactions when the first methanol molecules enter the structure of neat **35**SCN, followed by a decrease of the respective interactions in the course of further methanol uptake. In other words, methanol sorption is accompanied by shrinking and elongation processes resembling a breathing motion of the crystalline lattice.[91]

The hexafluoroantimonate salt of **35**⁺ was found to exhibit vapochromic behavior which is selective and reversible for vapors of acetonitrile, DMF, and pyridine.[92] Using ^{15}N NMR spectroscopy it was demonstrated that in solution 95% of the complexes have nitrogen-bound NCS ligands while only 5% are sulfur-bound, and this was explained by the electron-withdrawing nature of the terpyridine ligand making the Pt(II) center relatively hard. The crystal structure of the acetonitrile solvate **35**SbF₆·CH₃CN contains dimers of cations with Pt(II)-Pt(II) distances of 3.293(1) Å, the shortest intermetallic distance between individual dimers is 4.246(1) Å. The crystal structure of **35**SbF₆ without CH₃CN is not known, but it is assumed that the Pt(II)-

Pt(II) interactions within dimers are retained when acetonitrile is removed and that intact cation dimers can slide into new positions such that an infinite linear chain structure with extensive Pt(II)- Pt(II) interactions is adopted. This structural transformation would explain the maroon color and the observation of ^{3}MMLCT emission of neat **35**SbF$_6$. Upon exposure to acetonitrile, DMF or pyridine the maroon color rapidly changes to yellow, and thermogravimetric studies demonstrated that 1 equivalent of CH$_3$CN or 0.5 equivalents of DMF or pyridine are adsorbed. The solvates can be converted back to the neat material upon gentle heating.
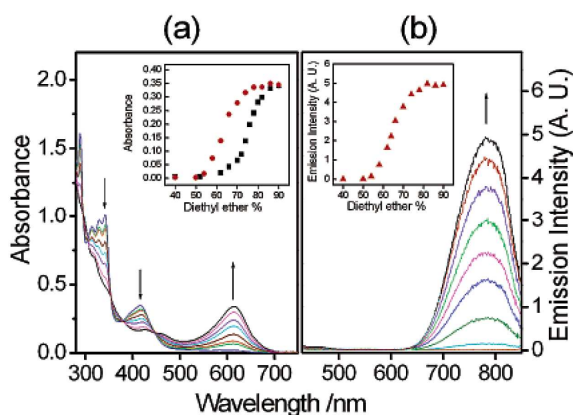
Figure 16. (a) Absorption and (b) emission changes as a function of diethyl ether addition to acetonitrile solutions of compound **36**. Reprinted with permission from ref. [64]. Copyright 2002 American Chemical Society.

A Pt(II) terpyridine diynyl complex was found to exhibit strong solvatochromism but no vapochromism and will therefore be treated only very briefly here.[64] [Pt(tpy)(C≡C–C≡CH)]OTf (**36**) crystallizes in a dark green form with platinum atoms arranged in a linear chain with intermetallic contacts of 3.388 Å, and a red form exhibiting a dimeric structure with zigzag arrangement and alternating short (3.394 Å) and long (3.648 Å) Pt(II)-Pt(II) distances. When

dissolved at ~10^{-4} M concentration in CH_3CN the color of the resulting solution is yellow but upon addition of increasing amounts of diethyl ether the color changes first to green and finally to blue (Figure 16). This phenomenon has been explained by solvent-induced aggregation of individual Pt complexes to dimer, trimer, or even oligomer structures. Moreover, ether addition induces a dramatic enhancement of the luminescence emitted by these solutions; the emission has been assigned to a ^{3}MMLCT state.

Scheme 15. Pt(II) terpyridine complexes, part III.
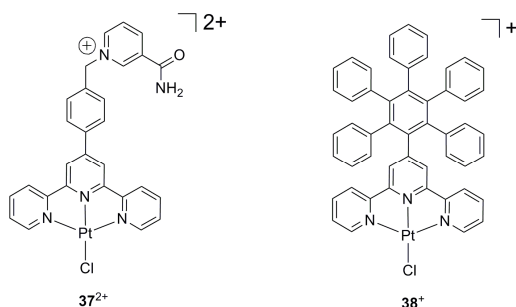
A study of a Pt(II) terpyridine-nicotinamide complex (37^{2+}) (Scheme 15) provided unusually direct insight into the phenomenon of vapochromism because it was possible to structurally characterize both the neat form of $37(PF_6)_2$ as well as its CH_3OH adduct using *the same* single crystal before and after methanol vapor exposure.[93] This is remarkable because such single-crystal transformations involving the loss or gain of solvent molecules while at the same time retaining the integrity of the crystal lattice are rare. Both the red solvent-free form and the orange methanol adduct contain dimers of cations which are doubly hydrogen-bonded through their nicotinamide groups.[93] There are three important differences in cation packing between the two forms: (i) the Pt-Pt-Pt arrangement is significantly more linear in the red form (Pt-Pt-Pt angle of

171.9°) than in the orange form (126.7°) (Figure 17); (ii) the separation between the planes of individual tpy ligands alternates between 3.453 Å and 3.660 Å in the red form (distance between N-atoms of central pyridine ring), but increases to alternating distances of 3.692 Å and 3.763 Å in the orange form; (iii) the Pt(II)-Pt(II) distances increase from 3.301 Å / 3.336 Å in the red form to 3.622 Å / 3.964 Å in the orange form. These structural changes clearly help to promote π-π stacking and Pt(II)-Pt(II) interactions between neighboring complexes in the solvent-free red form, while such interactions are essentially absent in the orange methanol adduct. Accordingly, the emission of red **37**(PF$_6$)$_2$ is assigned to a ^{3}MMLCT state (λ_{max} = 660 nm) while the luminescence of **37**(PF$_6$)$_2$·CH$_3$OH (λ_{max} = 630 nm) is attributed to ^{3}MLCT emission of isolated chromophores. Thus, compound **37**(PF$_6$)$_2$ is not only vapochromic but also vapoluminescent. It exhibits a selective and reversible vapochromic response when exposed to methanol, acetonitrile, or pyridine.[93]
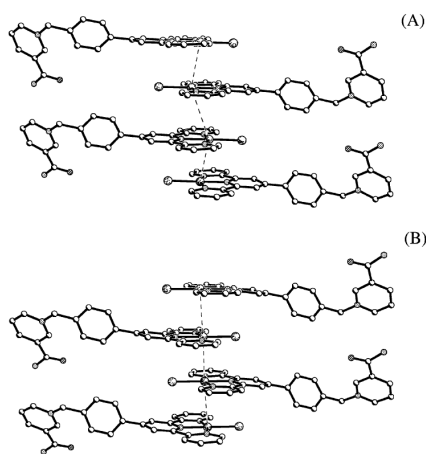
Figure 17. Stacking of complexes in (a) **37**(PF$_6$)$_2$·CH$_3$OH (orange form) and (b) **37**(PF$_6$)$_2$ (red form). Reprinted with permission from ref. [93]. Copyright 2004 American Chemical Society.

A platinum(II) complex with a pentaphenyl-benzene moiety linked to a terpyridine chelating agent (**38**Cl) has been reported to exhibit unusually large vapor-induced luminescence band shifts from the red to the green spectral range upon exposure to VOCs (Figure 18).[94] This vapoluminescence response is relatively selective and occurs only for CH_2Cl_2, ethanol, CH_3CN, and ethyl acetate although the response time is by far the shortest for CH_2Cl_2. The initial red form of **38**Cl is a methanol adduct and contains Pt(II) cations which are stacked in a spiral fashion with each complex rotated by ca. 120° along the stacking direction. There are four independent nearest-neighbor Pt(II)-Pt(II) distances in this helix, two of which (3.30 Å and 3.34 Å) are indicative of metallophilic interactions. Therefore it has been concluded that the red emission (λ_{max} = 654 nm) of this form originates from a ^{3}MMLCT state. Crystals of the green form of **38**Cl were grown from dichloromethane solution and contain one molecule of CH_2Cl_2 (instead of CH_3OH) per formula unit. This entails a dramatic change in cation packing and leads to a zigzag arrangement of neighboring Pt(II) complexes which are now found to be in head-to-tail orientation with Pt(II)-Pt(II) distances (3.9092(9) Å and 4.5483(11) Å). Both of these distances are both significantly beyond what can be considered a metallophilic contact. Consequently, the green emission (λ_{max} = 514 nm) of this form was attributed to ^{3}MLCT luminescence from isolated Pt(II) terpyridine chromphores. Clearly the disruption of Pt(II)-Pt(II) interactions is responsible for the strong vapochromic and vapoluminescence response of compound **38**Cl.
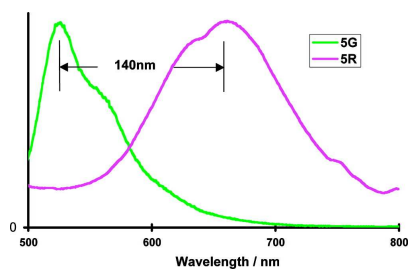
Figure 18. Photoluminescence of the green (5G) and red (5R) form of **38**Cl. Reprinted with permission from ref. [94]. Copyright 2008 American Chemical Society.

An interesting aspect is the absence of thermochromism of the red form of **38**Cl.[94] This is noteworthy because linear-chain compounds with stacked Pt(II) complexes exhibiting ^{3}MMLCT luminescence often show a pronounced red-shift of the emission with decreasing temperature due to contraction of the crystal lattice and a shortening of Pt(II)-Pt(II) distances, resulting in a smaller HOMO/LUMO energy gap.[13, 46] The absence of thermochromism in red **38**Cl is presumably due to the bulky nature of the pentaphenyl-benzene unit and its propeller-shaped nature which impedes tighter stacking of individual Pt(II) complexes at lower temperatures.

2.3.2 Complexes with 2,6-bis(*N*-alkylbenzimidazol-2'-yl)pyridine

Scheme 16. Vapochromic 2,6-bis(*N*-alkylbenzimidazol-2'-yl)pyridine complexes.

39$^+$

40a$^+$ R = C$_8$H$_{17}$
40b$^+$ R = C$_{12}$H$_{25}$
40c$^+$ R = C$_{16}$H$_{33}$
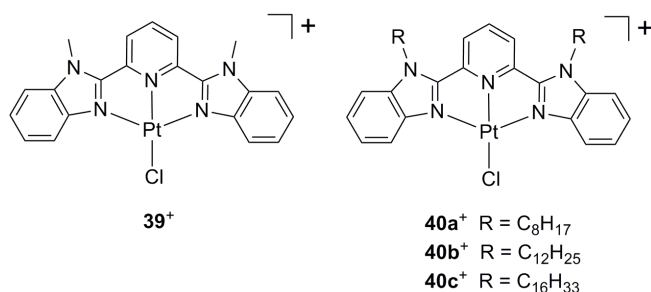
Complex **39**$^{+}$ (Scheme 16) forms vapochromic salts with chloride and hexafluorophosphate anions.[95] **39**Cl changes color from yellow-orange to red when exposed to methanol, ethanol, chloroform, or acetonitrile (Figure 19). A color change from yellow to violet is detected upon exposure of **39**PF$_6$ to acetonitrile, but many other solvents (including water, methanol, ethanol, 2-propanol, diethyl ether, CH$_2$Cl$_2$, CHCl$_3$, CCl$_4$, acetone, hexanes, and benzene) produce no response. Gravimetric studies indicate that **39**Cl sorbs up to two molecules of CH$_3$OH per formula unit whereas **39**PF$_6$ can only sorb one equivalent of CH$_3$CN. Unlike for some of the Pt(II) terpyridine materials from the prior section in which VOC uptake results in the disruption of metallophilic contacts, the yellow-to-red color change observed for **39**Cl and **39**PF$_6$ rather suggests that Pt(II)-Pt(II) interactions strengthen in the course of methanol and acetonitrile sorption. Indeed, 2,6-bis(*N*-alkylbenzimidazol-2'-yl)pyridine complexes of Pt(II) are known to have a strong tendency to aggregate in solution.[47, 96]
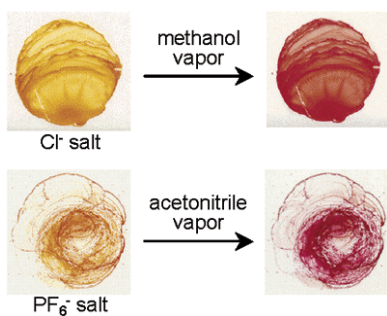

Figure 19. Vapochromic response of **39**Cl and **39**PF$_6$. Reprinted with permission from ref. [95]. Copyright 2004 American Chemical Society.

In the crystal structure of **39**PF$_6$·DMF Pt(II) complexes are oriented in zigzag head-to-tail arrangement with long intermolecular contacts (4.336(2) Å and 4.565(2) Å) but comparatively short distances between the ligand planes (3.35 Å and 3.39 Å).[97] Chloride anions and DMF solvent molecules fill the voids between the columns of cations. Exposure of single crystals of **39**PF$_6$·DMF to acetonitrile vapor induced a color change from orange to violet as noted above for powder samples of solvent-free **39**PF$_6$, but subsequent X-ray diffraction yielded only powder rings. Thus, the precise structure of the acetonitrile adduct remains unknown, but an interesting hypothesis has been put forward: The slippage of Pt(II) complexes by 1.35 Å along vectors lying parallel to the plane of each complex to give cation dimers with Pt(II)-Pt(II) distances of ~3.39 Å is conceivable since this represents the simplest imaginable deformation upon CH$_3$CN uptake. This structural rearrangement would be in line the yellow-to-violet color change and the high reversibility of the vapochromism.

An unrelated but noteworthy observation is that orange powder samples of **39**PF$_6$ quickly sorb 1 equivalent of DMF and turn violet, but the **39**PF$_6$·DMF single crystals grown from mixed CH$_3$CN/DMF solution are orange and unresponsive to DMF vapor. These observations suggest that there is both an orange and a violet polymorph of the DMF adduct.

When complex **39**Cl is incorporated into a zirconium phosphate (ZrP) framework, a different type of vapochromic behavior is observed.[98] First of all, different colors than in neat **39**Cl are obtained with certain VOCs. Secondly, despite the lower concentration of the platinum(II) complexes in ZrP compared to neat **39**Cl, the color response is equally strong or even stronger in the inorganic framework. The Pt:ZrP ratio was typically between 1:5 and 1:30, yet the vapochromic response upon exposure to water, MeOH, CH$_3$CN, CH$_2$Cl$_2$, THF, benzene, and *n*-hexane occurs within minutes. Interestingly, the vapochromic response patterns of the ZrP-

incorporated complex are different than those of neat **39**Cl or **39**PF$_6$. Fast and reversible

(^{3}MMLCT) vapoluminescence responses were detected.

An entire series of 2,6-bis(*N*-alkylbenzimidazol-2'-yl)pyridine complexes of Pt(II) with

various alkyl-substituents (R) and counterions was found to exhibit vapochromic behavior

similar to that of **39**Cl and **39**PF$_6$.[99] This includes the chloride salts of complexes with R = C$_8$H$_{17}$

(**40a**), C$_{12}$H$_{25}$ (**40b**), C$_{16}$H$_{33}$ (**40c**), as well as the hexafluorophosphate, perchlorate,

tetrafluoroborate, triflate, and acetate salts of the complex with R = C$_{16}$H$_{33}$ (**40c**). Both the alkyl

chain length and the size of the anion affect the vapochromic response because these factors

influence the molecular stacking pattern. However, no clear systematic trends could be

recognized. When constructing an array from all these vapochromic substances it becomes

possible to distinguish between different VOCs, i. e., to some extent the array can function as an

electronic nose. The solvents to which these arrays were exposed are acetone, acetonitrile,

methanol, ethanol, dichloromethane, chloroform, ethyl acetate and benzene. The majority of the

vapochromic responses involve a transition from lighter to darker color (typically from yellow-

orange to red or violet), similar to what has been observed for **39**Cl and **39**PF$_6$, suggesting that

Pt(II)-Pt(II) interactions are strengthened upon VOC uptake. Two notable exceptions are the

chloride and triflate salts of **40c** which change from deep orange to yellow. In these two salts

solvent uptake seems to reduce Pt(II)-Pt(II) and/or π-π interactions.

2.3.3 Complexes with 2,6-*bis*-(1*H*-imidazol-2-yl)pyridine

Scheme 17. A vapochromic Pt(II) 2,6-*bis*-(1*H*-imidazol-2-yl)pyridine complex.

41⁺
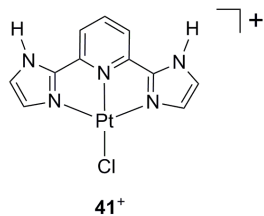
Complex **41⁺** was synthesized along with a few other related complexes with a view to obtaining a quasi-2D framework made of planar Pt(II) complexes.[100] The idea was to exploit Pt(II)-Pt(II) interactions and π-π stacking to induce ordering of individual complexes along one direction while at the same time making use of hydrogen-bonding interactions to induce ordering along a second direction. In the course of these studies it was discovered that **41**Cl is a vapoluminescent substance. Solvent-free **41**Cl exhibits emission with λ_{max} at 525 nm, the occurrence of vibrational fine structure with ~1500 cm^{-1} intervals between individual progression members suggests that the emission contains significant intraligand π-π* character. When brought in contact with vapors from CH_2Cl_2, CH_3CN, CH_3OH or acetone, the emission red-shifts to $\lambda_{max} = 630$ nm and becomes broad and unstructured. The red emission has been tentatively attributed to the presence of close Pt(II)-Pt(II) contacts or π-π interactions between ligands. Support for this hypothesis comes from the X-ray crystal structure of **41**Cl ·DMSO·2H$_2$O which exhibits intermolecular π-π distances of 3.370 Å and 3.395 Å, but in this specific solvate structure the shortest Pt(II)-Pt(II) distance is 4.33 Å.

An electron mobility value of 0.4 cm^{2}V^{-1}s^{-1} has been determined for solvent-free **41**Cl which is a low value compared to that measured for a related 2,6-bis(1*H*-pyrazol-3-yl)pyridine complex of Pt(II) (20 cm^{2}V^{-1}s^{-1}).[100] Cofacial π-π and Pt(II)-Pt(II) interactions are thought to be responsible for the high electron mobility in the pyrazolyl-complex. It has been noted that if such

interactions could be induced by vapor (e. g., in **41**Cl or related other materials), transistor-based

sensors and other multi-functionalized optoelectronic devices could be created based on Pt(II)

complexes.

2.4 Cyclometalated Pt(II) complexes

2.4.1 Complexes with 2,6-diphenylpyridine (N^C^N) ligands

Scheme 18. Vapochromic cyclometalated Pt(II) complexes, part I.
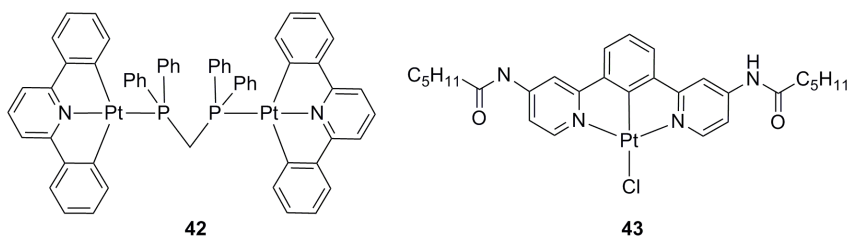
The bis(diphenylphosphino)methane (dppm) bridged dinuclear Pt(II) complex **42** (Scheme 18)

is a vapochromic substance functioning on the basis of intramolecular π-π stacking rather than

inter- or intramolecular Pt(II)-Pt(II) interactions.[101] Both a solvent-free yellow form and an

orange chloroform adduct of this charge-neutral complex were characterized

crystallographically, and it was found that the yellow form exhibits weak π-π interactions

between one of the Pt(N^C^N) planes and a phenyl ring of the dppm ligand with interplanar

separations ranging from 3.38 Å to 3.67 Å. In the orange chloroform adduct each Pt(N^C^N)

plane makes a π-π interaction with a phenyl ring from different P-atoms of the dppm ligand, and

the interplanar distances are in the range of 3.12 Å to 3.29 Å (Figure 20), i. e., noticeably shorter

than in the yellow form. A variety of different VOCs (CH_2Cl_2, CH_3OH, acetone, benzene,

pentane) induce a change in color from yellow to orange, and given the structural information

from above it appears plausible to conclude that each of these solvents induces a strengthening of

intramolecular π-π interactions when sorbed by the yellow form of **42**.
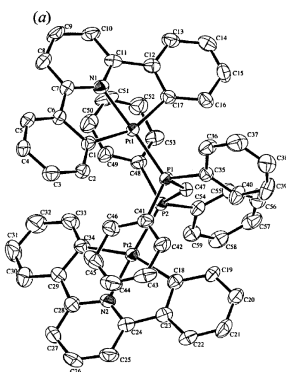
Figure 20. Crystal structure of **42**. Reprinted with permission from ref. [101]. Copyright 2001

American Chemical Society.

The amide-decorated [Pt(2,6-diphenylpyridine)Cl] complex **43** exhibits an interesting

combination of mechanochromism and vapochromism.[102] When crystallizing from DMF, one

obtains green emitting **43**·DMF. This material exhibits sharp diffraction peaks in powder X-ray

analysis. When **43**·DMF is ground in a ceramic mortar one obtains an orange luminescent

powder which does not give clear X-ray diffraction. Subsequent exposure of this amorphous

substance to methanol vapors leads to **43**·CH_3OH, a yellow emitter which exhibits sharp X-ray

diffraction peaks again. This two-step conversion from crystalline **43**·DMF to amorphous **43** and

finally crystalline **43**·CH_3OH is a highly unusual phenomenon. X-ray diffraction studies on

single crystals reveal long Pt(II)-Pt(II) contacts of 4.854 Å between nearest neighbors in the

DMF adduct, whereas in **43**·CH_3OH the shortest intermetallic separation is only 3.385 Å. The

observation of metal-metal distance shrinking may explain the change from green to red

luminescence accompanying the two-step transformation from **43**·DMF to **43**·CH₃OH. The hydrogen-bonding ability of the dangling amide groups is suspected to play an important role for the mechano- and vapochromism of **43** because the hexanoylamide groups form hydrogen-bonds to the DMF and methanol guest molecules in crystals of **43**·DMF and **43**·CH₃OH. Heating crystals of **43**·DMF to 150 °C induces release of the DMF molecule and produces the same luminescence change as grinding, suggesting that the amorphous orange-luminescent powder is a solvent-free form of **43**. Along with complex **43** two closely related Pt(II) complexes with shorter alkanoylamide groups were investigated, but these substances did not show any mechano- or vapoluminescence properties, demonstrating once again how subtle the search for materials with such properties has to be.[102]
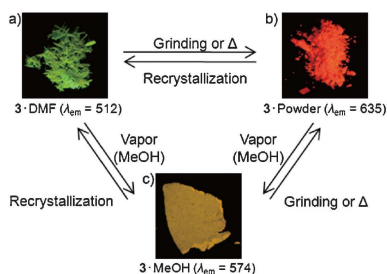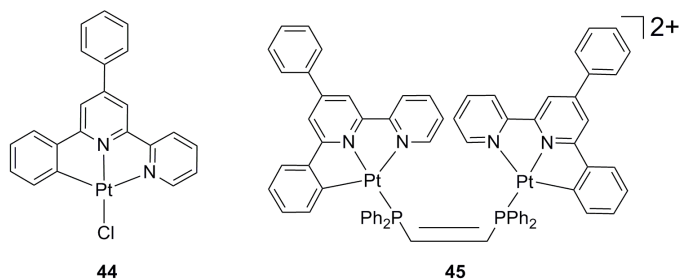

Figure 21. Mechano- and vapoluminescent properties of **43**. Copyright 2012 The Chemical Society of Japan.

2.4.2 Complexes with 6-phenyl-2,2'-bipyridine (C^N^N) ligands

Scheme 19. Vapochromic Pt(II) complexes with C^N^N ligands.

44　　　　　　　**45**

The luminescent complex **44** (Scheme 19) was reacted with amino-decorated silica gel in order to immobilize a luminescent probe on the surface of a supporting matrix.[103] It was envisioned that host-guest interactions between the surface-bound complexes and VOC analytes would affect metal-metal and/or ligand-ligand interactions to the extent that a vapochromic or vapoluminescent response would result. Indeed this turned out to be possible when using MCM-41 and MCM-48 silica gel supports which were first reacted with (3-aminopropyl)triethoxysilane and then loaded with 2.8 wt% of platinum in the form of complex **44**. The resulting material displays red emission at 662 nm (λ_{max}) at room temperature. When placing the Pt-decorated silica gel samples into an air-tight tank containing a saturated atmosphere of pentane, benzene, chloroform, or dichloromethane for ~10 minutes, the emission shifted to substantially shorter wavelength (λ_{max} = 548 nm). Drying in air for 3 days then restores the initial red luminescence. Presumably the red emission is due to ^{3}MMLCT states resulting from tightly interacting Pt(II) complexes whereas the yellow luminescence comes from ^{3}MLCT excited states of isolated complexes. The disruption of metal-metal and/or π-π interactions following the uptake of nonpolar solvents may potentially be explained by the high sorption capacity of silica for such substances.

Complex **45**$^{2+}$ contains two Pt(C^N^N) units which are linked by a rigid *cis*-1,2-bis(diphenylphosphino)ethylene ligand. This dinuclear complex responds to vapors of

heteroatom-containing VOCs such as acetonitrile, ethanol, diethyl ether, THF, ethyl acetate, CH_2Cl_2, $CHCl_3$ by a change in color from yellow to deep red.[104] Since no structural information is available for compound **45** $(ClO_4)_2$ an explanation for its vapochromism cannot be provided. It is clear, however, that *intra*molecular stacking leading to closer Pt(II)-Pt(II) contacts after solvent exposure (as observed for the dppm-bridged dinuclear Pt(II) complex **42**) is impossible for complex **45**$^{2+}$ due to the rigidity of the *cis*-1,2-bis(diphenylphosphino)ethylene bridging ligand.

2.4.3 Complexes with 2,6-di(2'-naphthyl)pyridine (C^N^C) ligands

Scheme 20. A vapochromic dinuclear complex with C^N^C ligands.

46
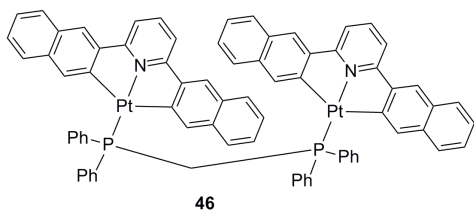
Building on the prior observation of weak vapochromism in the dinuclear dppm-bridged Pt(N^C^N) complex **42** a series of dinuclear Pt(C^N^C) complexes was investigated with a view to obtaining new vapochromic or vapoluminescent materials.[105] It was anticipated that the large π-system of 2,6-di(2'-naphthyl)pyridine would be beneficial for π-π and C-H-π interactions between this ligand and VOCs, and that the disruption of such weak non-covalent interactions would potentially entail a significant vapochromic response. In one out of four investigated complexes of this type (**46**) (Scheme 20) this turned out to be the case.[104] The solvent-free form

of complex **46** is a weak emitter, but exposure to a variety of different VOCs produces an enhancement of its orange-yellow luminescence (λ_{max} = 602 nm) (Figure 22).
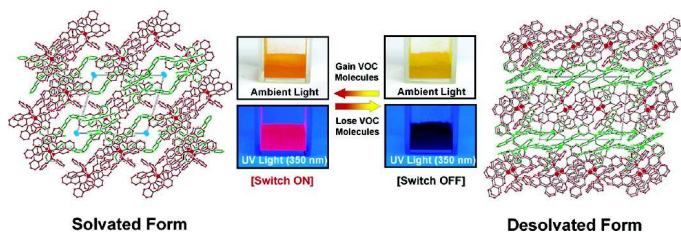
Figure 22. Changes in crystal structure, color, and photoluminescence upon vapor uptake / release by compound **46**. Reprinted with permission from ref. [105]. Copyright 2006 American Chemical Society.

Halogenated vapors (CH_2Cl_2, CH_2Br_2, $CHCl_3$, 1,2-dichloroethane, 1,2-dibromoethane, CH_3I but not CCl_4) lead to particularly strong luminescence enhancements, but small polar VOCs such as acetone, diethyl ether, THF, ethyl acetate also produce a significant response. X-ray diffraction studies on **46**·$6CHCl_3$·C_5H_{12} reveal that both the *syn-* and *anti*-conformations of **46** are present in the combined chloroform/pentane adduct. The most notable feature of this crystal structure is the presence of continuous solvent channels with an aperture size of ca. 6.5 Å × 4.3 Å along the c-axis (Figure 22). Such large channels are absent in the crystal structures of three analogous dinuclear complexes bearing aromatic substituents at the 4-position of the central pyridine ring of the C^N^C ligand, and this may understand why vapoluminescence is observed exclusively for complex **46**.[104] X-ray diffraction of the desolvated form shows that the crystallographic a-axis decreases substantially upon solvent removal, resulting in a reduction of the unit cell volume from 7374 Å^3 to 6188 Å^3. The intramolecular Pt(II)-Pt(II) distance increases from 3.29(3) Å to 3.40(3) Å in the syn form, whereas in the anti-conformer there is an increase

from 5.68(2) Å to 5.40(3) Å. In the desolvated form, individual molecules are held in place by intermolecular π-π interactions (the relevant interplanar separations range from 3.20 Å to 3.47 Å) and by C-H-π interactions. Aggregation of the *syn-* and *anti-*forms in solvent-free **46** is tighter than in **46**·6CHCl$_3$·C$_5$H$_{12}$, and it has been proposed that this is the origin of the luminescence quenching in dry **46**. In other words, the molecular conformations (*syn* or *anti*) do not appear to play a decisive role for the vapoluminescence. Temperature-dependent luminescence studies indicate that there can be emission from a $^3\pi\pi^*$ state of isolated complexes and excimeric $^3\pi\pi^*$ luminescence at longer wavelengths resulting from aggregated complexes; the formation of tight aggregates in the solvent-free form of **46** can red-shift the excimeric $^3\pi\pi^*$ states to the extent that radiative relaxation is no longer competitive with multiphonon relaxation. Sorption of VOCs can then restore the luminescence by disruption of aggregation. The observation that acetonitrile, methanol, and ethanol produce no vapoluminescence response was explained by insufficient hydrophobicity of these solvents, whereas the insensitivity of **46** to benzene, toluene and *n*-hexane was explained by the size of these VOCs.

2.4.4 Complexes with 7,8-benzoquinolinato and 2-phenylpyridine (C^N) ligands

Scheme 21. Two anionic vapochromic Pt(II) complexes.
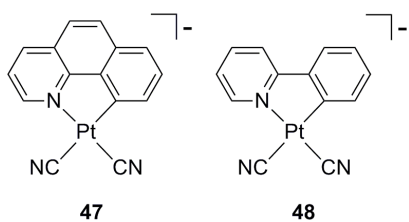
Complexes **47⁻** and **48⁻** (Scheme 21) are two rare examples of anionic Pt(II) complexes exhibiting vapochromism. Their optical spectroscopic properties are strongly dependent on the cation: The tetrabutylammonium salts are yellow, whereas the respective potassium salts are obtained as red and purple solids which are to be formulated as monohydrates (**K47**·H_2O and K**48**·H_2O).[106] When heating to 110 °C the crystal water can be removed, and this procedure induces a change in color from red or purple to yellow (Figure 23).
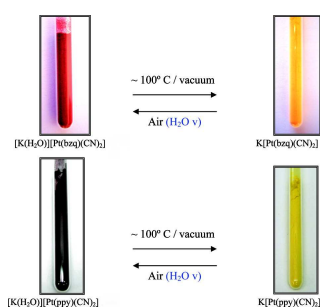
Figure 23. Color changes in K**47**·H_2O and K**48**·H_2O upon water release and uptake. Reprinted with permission from ref. [106]. Copyright 2008 American Chemical Society.

In air, the red and purple forms rapidly regenerate due to spontaneous water uptake. This behavior is opposite to that observed for red [Pt(bpy)(CN)$_2$] which sorbs water to form yellow [Pt(bpy)(CN)$_2$]·H_2O.[38] Apparently, in **K47**·H_2O and K**48**·H_2O short Pt(II)-Pt(II) contacts lead to MMLCT absorptions which are responsible for the red and purple colors of these forms while in the anhydrous yellow forms intermetallic contacts are largely disrupted.[106] Thin films of **K47**·H_2O are responsive to a variety of anhydrous VOCs with response time increasing in the order of methanol (~5 s), ethanol (~10 s), acetonitrile (~30 s), acetone (~2 min), and THF (~45 min). K**48**·H_2O does not respond to any of these anhydrous solvent vapors, perhaps because the

crystal water molecule is more strongly bound to the lattice than in the case of **K47**·H_2O. This interpretation is in line with thermogravimetric analyses.

2.4.5 Pincer complexes

The complexes presented in this chapter are exceptional vapochromic Pt(II) compounds in that they exhibit vapochromism as a result of direct ligation of the analyte to the metal center. Thus, unlike the vast majority of the other compounds from section 2, the pincer complexes in this chapter are type II vapochromic substances according to the definition used in section 1.3.

Scheme 22. Vapochromic pincer complexes, part I.
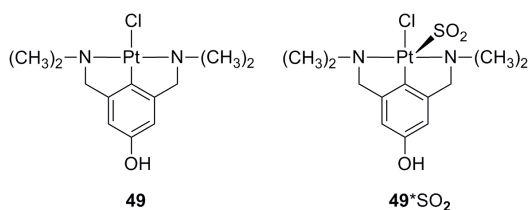
Several square-planar Pt(II) complexes with monoanionic N^C^N pincer ligands were found to be highly selective sensors for gaseous SO_2. Complex **49** (Scheme 22) self-assembles in the solid state to form a network with intramolecular hydrogen-bonds between the chloro-ligand of one complex and the hydroxyl-group of its neighbor (Figure 24).[107] Exposure of **49** to sulfur dioxide for ~1 minute affords the SO_2 adduct **49**·SO_2 in which a sulfur dioxide molecule is ligating to the Pt(II) center. Remarkably, the crystallinity of compound **49** is retained in the course of this process. Associated with the uptake of SO_2 is a change in coordination geometry from square-planar to pyramidal, and this affects the packing index and the density of the material.
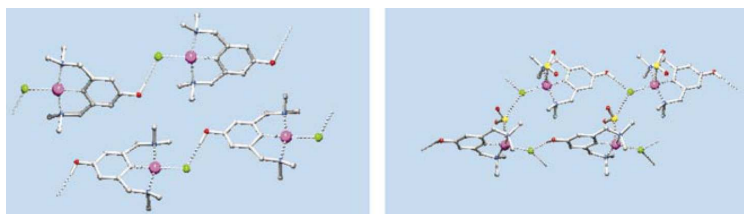
Figure 24. Extracts from the crystal structure of **49** before (left) and after SO$_2$ uptake (right). Reprinted by permission from Macmillan Publishers Ltd: *Nature* 2000, *406*, 970, copyright 2000.

The unit cell volume increases by more than 15% upon SO$_2$ sorption, whereas the density decreases from 2.1606(6) g/cm^3 to 2.1473(6) g/cm^3. The pyramidal complex retains the hydrogen bonds between chloro-ligands and hydroxyl-groups of adjacent ligands (the O-Cl distance remains virtually unchanged: 3.126(8) Å before and 3.127(8) Å after SO$_2$ uptake). In addition there are non-covalent interactions between SO$_2$ and chloro-ligands of adjacent complexes perpendicularly to the hydrogen-bonding network. **49** is colorless while **49**·SO$_2$ is deep orange hence the transformation can easily be detected by naked eye. The recovery of **49** from **49**·SO$_2$ in an atmosphere of air was studied by time-dependent powder X-ray diffraction and infrared spectroscopy (monitoring the SO$_2$ stretching vibrations at 1072 cm^{-1} and 1236 cm^{-1}), and it was concluded that SO$_2$ release follows a zero-order rate law with the absolute rate being strongly dependent on the surface area of the sample. It was assumed that the rate-determining step in SO$_2$ release is the diffusion-controlled transfer of SO$_2$ molecules from one complex to the other from the inner part of the crystalline material to its surface.

Scheme 23. Vapochromic pincer complexes, part II.

50   **51**
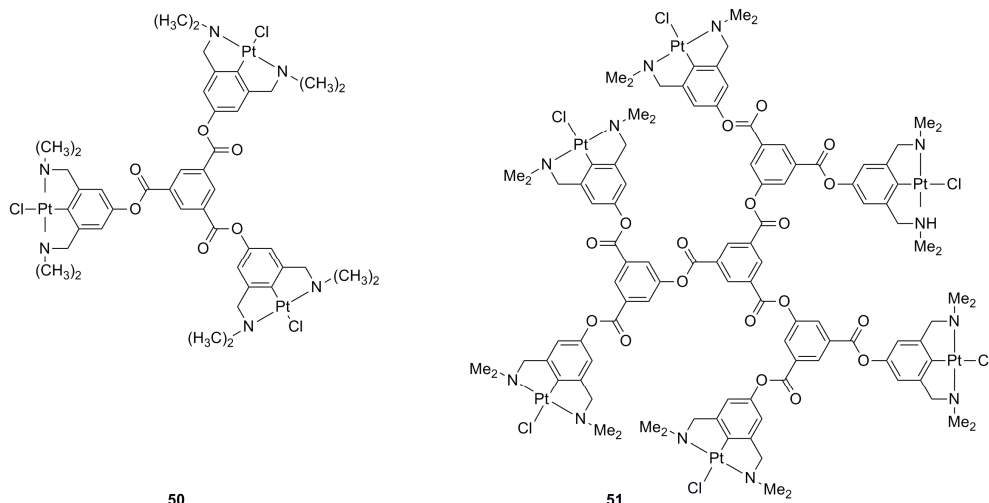
Immobilization of the pincer complex **49** on a surface is of interest for obtaining a functional SO$_2$ sensor device. Instead of layering these complexes into a polymer in which they may be less accessible to SO$_2$ from the atmosphere, functional dendrimers (**50**, **51**) (Scheme 23) with well-defined connectivities were synthesized and explored.[108] According to molecular models, the macromolecular constructs have disk-like structures with diameters of 2.4 nm and 3.4 nm, respectively, and they are found to maintain the high sensitivity for SO$_2$ observed for the monometallic complex **49**. When coating a cellulose surface with dendritic **50** at a density of 20 nm/mm^2 the detection of SO$_2$ at a concentration of 8.5±0.5 µg/cm^3 is possible. Even at 190 K, the response (a change from colorless to orange) occurs within 2 ms. Exposure to SO$_2$-free air regenerates the initial colorless state within a few minutes. A promising resistance against atmospheric impurities such as water and acids has also been noted.

**Scheme 24.** Vapochromic pincer complexes, part III.

52
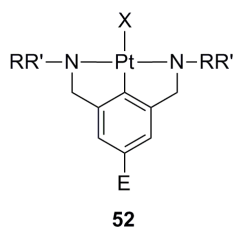
Fundamental studies in which the electronic structure and the steric bulk of mononuclear pincer complexes are varied systematically have been conducted.[109] On the generic structure **52** (Scheme 24) the monodentate ligand X was varied from Cl to Br, I, and *p*-tolyl in order to modulate the electron density at the metal center. The substituents R and R' at the nitrogen donor atoms were varied between methyl and ethyl in order to explore the influence of steric constraints on SO_2 binding. Finally, the *para*-substituent E was varied between H, OH, $OSiMe_2$ and ^tBu in order to tune the electron density in the aromatic system. SO_2 binding is possible irrespective of which of the four monodentate ligands (X) is chosen. However, SO_2 binding is suppressed when all four substituents at the N atoms are ethyl groups. At least one of them has to be a methyl-substituent otherwise there is apparently too much steric bulk. Solution titrations show that the nature of the *para*-substituent E has relatively little influence because the equilibrium constants for SO_2-binding of 7 complexes with variable E are all in the range between 8.48 ± 0.34 M^{-1} and 14.81 ± 0.35 M^{-1} in benzene. Stopped-flow experiments in benzene solution showed that the reaction of pincer complexes with different X, E, and R is complete within 50 μs. In air at room temperature, the complexes lose SO_2 over several weeks, but when heated to 40°C the initial state can be recovered within minutes.

Pt(II) complexes with the anionic N^C^N pincer ligand in the generic complex **52** have an enhanced nucleophilicity when compared to other d^8 metal complexes.[110] This explains why they react with the Lewis acid SO_2, yet the selective recognition of sulfur dioxide even in presence of

other acids such as HCl, CO_2 or H_2O is spectacular. Two additional fundamental observations

are noteworthy: (i) platinum-bound SO_2 does not undergo subsequent reactions such as insertion

into a metal-carbon bond or oxidation to sulfate in air; (ii) in the complexes with X = I there is no

SO_2-binding to the iodide, despite the expected competitive behavior of iodide in terms of

nucleophilicity.[111] In-depth mechanistic studies (theoretical and experimental) lead to the

conclusion that iodide-bound SO_2 does not even play a role as a reaction intermediate during SO_2

uptake or release.[112] Using ^{1}H NMR spectroscopy the exchange rate of the SO_2 ligand on the

complex with X = I, R = CH_3, and E = H was investigated at cryogenic temperatures. When

extrapolating to room temperature, one obtains an exchange rate of $1.5 \cdot 10^8$ s[-1], which is close to

the rate constants for some of the fastest enzymatic reactions. This underscores the point that

these Pt(II) pincer complexes are suitable for on-line monitoring of the SO_2 concentration in air.

   2.4.6 NHC complexes

Scheme 25. Vapochromic Pt(II) complexes with NHC ligands.
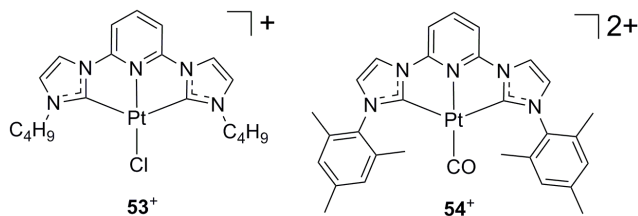
Transition-metal complexes with N-heterocyclic carbenes (NHCs) are playing an increasingly

important role in organometallic chemistry,[113-115] and until now two vapochromic Pt(II)

complexes with such ligands have been reported (Scheme 25).[116, 117] Complex **53**[+] is synthesized

via transmetallation from an Ag(I) precursor complex and crystallizes in two different structures

depending on what solvent is used.[116] Recrystallization from methanol/diethyl ether yields a

hydrated form with the sum formula **53**Cl·2.5H$_2$O, whereas crystallization from CH$_2$Cl$_2$/hexane

affords the anhydrate form **53**Cl. Both crystal structures contain dimers of head-to-tail oriented

complexes with short Pt(II)-Pt(II) contacts (Figure 25). In **53**Cl·2.5H$_2$O the shortest intermetallic

distance is 3.5096(7) Å, in **53**Cl it is 3.5185(19) Å. The interplanar (π-π) stacking distances are

not much different either and vary between 3.342 Å (**53**Cl·2.5H$_2$O) and 3.472 Å (**53**Cl).

However, the hydrate exhibits orange luminescence (λ_{max} = 614 nm) whereas the anhydrate form

emits green (λ_{max} = 555 nm) which is difficult to explain by the observed structural changes. At

any rate, when the green-emitting dehydrated form (**53**Cl) is exposed to moisture, the emission

changes to orange and powder X-ray analysis is in line with the formation of **53**Cl·2.5H$_2$O.
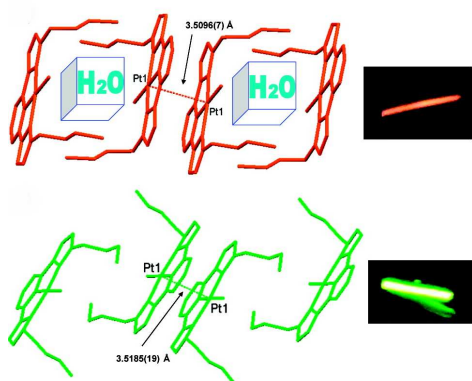
Figure 25. Crystal packing and emission colors of **53**Cl·2.5H$_2$O (top) and **53**Cl (bottom).
Reprinted with permission from ref. [116]. Copyright 2010 American Chemical Society.

Complex **54**$^{2+}$ contains mesityl-substituents instead of *n*-butyl groups and the fourth

coordination site is occupied by a carbonyl instead of a chloro-ligand. The bulky mesityls form a

small pocket which allows VOCs to enter the crystal structure of **54**(PF$_6$)$_2$ in order to form

solvent adducts with different luminescence properties than the desolvated form.[117] The solvent-free form of **54**$(PF_6)_2$ exhibits structured emission with a band maximum at 462 nm but exposure to vapors of small molecules containing nitrogen or oxygen donor atoms such as methanol, water, THF, diethyl ether, DMF, or pyridine leads to a yellow featureless emission with λ_{max} = 529 nm. Small VOCs without donor atoms such as CH_2Cl_2, $CHCl_3$, or benzene do not trigger any response. The exact mechanism for the luminescence vapochromism is not clear, but the crystal structure of **54**$(PF_6)_2 \cdot 2(CH_3)_2CO$ shows signs of solvate/Pt-CO interactions. Specifically, the distance of 2.82 Å between the O-atom of acetone and the C-atom of the carbon monoxide ligand is significantly shorter than what is expected based on the van-der-Waals radii of oxygen and carbon (3.22 Å). Moreover, the CO stretching frequency of the solvated acetone is 10 cm^{-1} lower than that of free acetone, and the CO stretching frequency for the carbon monoxide ligand is 15 cm^{-1} lower in **54**$(PF_6)_2 \cdot 2(CH_3)_2CO$ than in desolvated **54**$(PF_6)_2$.

2.5 Pt(II) complexes with S-, P-, and As-ligand atoms

Scheme 26. *Syn*- and *anti*-isomers of a vapochromic Pt(II) complex with thiolate ligands.

55a   55b
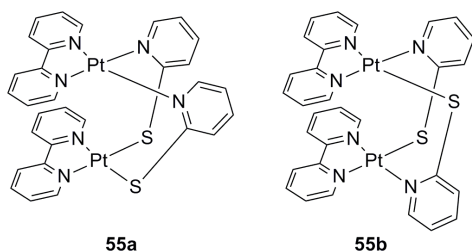
A dinuclear pyridine-2-thiolate bridged Pt(II) bpy complex was obtained both as a *syn*- (**55a**) and an *anti*-isomer (**55b**) (Scheme 26).[118] The *syn*-isomer (**55a**) has one Pt(II) ion in a

coordination sphere of four N-atoms (2 from bpy, 2 from pyridine-2-thiolate), and the second

metal center is coordinated to the two thiolate functions in addition to bpy. In the *anti*-isomer

(**55b**) both Pt(II) centers are coordinated to 3 N-atoms and 1 S-atom. Both isomers exhibit

unusually short (intramolecular) Pt(II)-Pt(II) distances of 2.923(1) Å (*syn*) and 2.997(1) Å (*anti*).

The *syn* isomer changes color from dark red to lighter red upon standing in air, and this is

accompanied by changes in the luminescence properties as illustrated in Figure 26. Exposure to

methanol or acetonitrile reverses the color and luminescence changes.
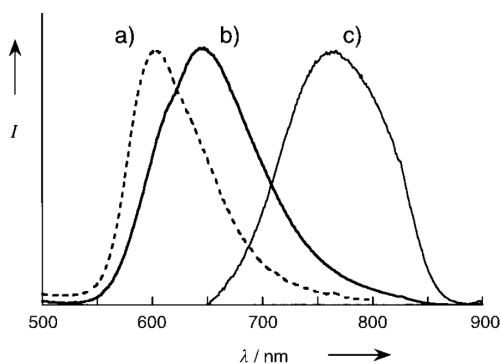
Figure 26. Room-temperature photoluminescence spectra of (a) the *anti*-isomer **55b**, (b) the

desolvated form of the *syn*-isomer **55a**, (c) the solvated form of *syn*-isomer **55a**. (M. Kato, A.

Omura, A. Toshikawa, S. Kishi, Y. Sugimoto: Vapor-Induced Luminescence Switching in

Crystals of the *Syn* Isomer of a Dinuclear (Bipyridine)platinum(II) Complex Bridged with

Pyridine-2-Thiolate Ions. *Angew. Chem. Int. Ed.*, 2000, *41*, 3183-3185. Copyright Wiley-VCH

Verlag GmbH & Co. KGaA. Reproduced with permission.)

The crystal structure of the dark red acetonitrile adduct (**55a**·CH$_3$CN) exhibits short

*inter*molecular Pt(II)-Pt(II) distances of 3.384(1) Å in addition to the short *intra*molecular Pt(II)-

Pt(II) contacts mentioned above. Thus, there is extensive interaction between metal centers along

one dimension, and therefore the strongly red-shifted emission at λ_{max} = 766 nm is most likely due to a low-energy ^{3}MMLCT state. The structure of **55a·CH₃CN** contains channels in which the solvate molecules are located, providing a pathway for them to diffuse in and out of the lattice. The sensitivity of **55a** for VOCs decreases with increasing steric bulk of the solvent vapors, in line with the hypothesis that the adsorbates must be small enough to penetrate these channels. Methanol and acetonitrile produce a rapid response, ethanol and isopropanol lead to slower color and luminescence changes, whereas *t*-butanol triggers no response at all, despite the fact that these five VOCs have similar vapor pressures. The *anti*-isomer (**55b**) is neither vapochromic nor vapoluminescent but emits orange emission (λ_{max} = 603 nm, τ = 240 ns), presumably from a ^{3}MMLCT state resulting from intramolecular Pt(II)-Pt(II) interactions.

Scheme 27. A vapochromic Pt(II) dithiooxamide complex.

Bu   Bu   Bu   Bu
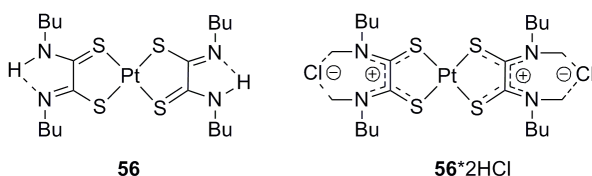
56   **56*2HCl**

The Pt(II) dithiooxamide complex **56** is sensitive to gaseous HCl (Scheme 27).[119] The initial form of this material is orange-red and non-luminescent, but when exposed to HCl it forms an adduct (**56·2HCl**) which is purple-brown and emits in the red spectral range (λ_{max} ≈ 740 nm, τ = 28 ns). According to prior studies of the same process in solution the red emission is due to a charge transfer state in which electron density has been transferred from the Pt/S moiety to the dithiooxamide backbone.[120] In the course of HCl uptake this state shifts to lower energy and begins to emit, whereas in the initial form the CT state is energetically close to other non-

emissive excited states leading to nonradiative energy dissipation. Conversion back from

56·2HCl to **56** is possible either by heating to 80 °C or by exposure to NH_3 vapor.[119]

Scheme 28. Vapochromic Pt(II) complexes with S, P, or As-ligands.
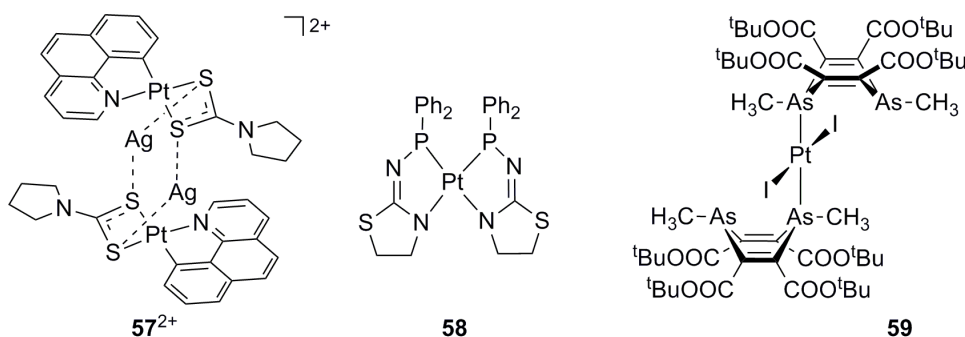
Complex **57**$^{2+}$ is a tetranuclear [Pt$_2$Ag$_2$] cluster made from two Pt(II) benzoquinoline

pyrrolidinedithiocarbamate units bridged via the sulfur atoms through two Ag(I) cations (Scheme

28).[121] The separation distance between the two silver ions (3.0394(18) Å) is significantly shorter

than the sum of their van der Waals radii (3.44 Å), i. e., they show argentophilic interactions. In

the perchlorate salt of complex **57**$^{2+}$ the [Pt$_2$Ag$_2$] clusters form a polymer along the

crystallographic c-axis with short (3.1390(7) Å) Pt(II)-Pt(II) contacts. Consequently, the red

emission of solid **57**(ClO$_4$)$_2$ (λ_{max} = 610 nm) is most likely due to ^{3}MMLCT or excimeric $^3\pi\pi^*$

states. Exposure of solid **57**(ClO$_4$)$_2$ to acetonitrile induces a rapid change in color from orange to

garnet red (Figure 27), but several other vapors (including CH_2Cl_2, methanol, H_2O, acetone,

diethyl ether, DMF, DMSO, toluene, *n*-hexane) produce no response. The origin of the selective

vapochromism with CH_3CN is not known but it has been noted that acetonitrile may replace the

perchlorate anions which are weakly coordinated to the Ag(I) ions. The smaller size of CH_3CN

relative to ClO$_4$ would then allow the individual [Pt$_2$Ag$_2$] clusters to get closer to each other, and

this may well lead to the observed vapochromism. The selectivity of **57**(ClO₄)₂ to acetonitrile is quite unusual, but unfortunately the vapochromic response does not appear to be easily reversible.
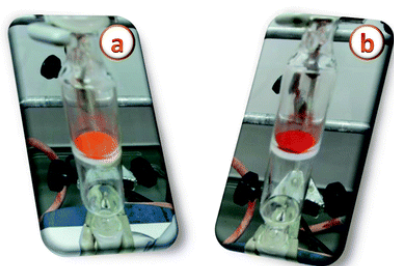
Figure 27. Sample of **57**(ClO₄)₂ before (a) and after (b) exposure to CH₃CN vapor. Reprinted with permission from ref. [121]. Copyright 2008 The Royal Society of Chemistry.

The bischelated Pt(II) complex **58** with two identical aminophosphine ligands was obtained in its *cis*-form and exhibits a vapoluminescence response to small alcohols.[122] Two crystal structures of this complex were studied by X-ray diffraction but none of them contains short Pt(II)-Pt(II) contacts. The shortest intermetallic distances found are 5.9267(2) Å in **58**·C₆H₅CH₃ and 8.9268(2) Å in **58**·2CH₃OH·CH₃CN. The origin of the emission which turns on after methanol exposure is unclear, but given the large intermetallic distances participation of ³MMLCT states appears highly unlikely. It has been speculated that a rigidochromic effect induced by hydrogen-bonding could be the reason why methanol-exposed **58** is emissive. (Rigidochromism is a change of color occurring as a consequence of changes in the rigidity of the surrounding medium). Hydrogen-bond donation from methanol to the aminophosphine ligands may render the overall complex less flexible, making multiphonon relaxation less

efficient. Aside from methanol, ethanol, and (to a lesser extent) isopropanol cause a luminescence turn-on, but *t*-butanol produces no significant response.

The organoarsenic complex **59** can be crystallized either in neat form or as adducts of dichloromethane (**59**·2CH$_2$Cl$_2$), acetone (**59**·2acetone) or toluene (**59**·C$_6$H$_5$CH$_3$).[123] In the crystal structure of **59**·2CH$_2$Cl$_2$ there are no large cavities and the void volume is only 1.1% of the total crystal volume, but in the structure of neat **59** the void volume amounts to 6.0%. Consequently, when exposing neat **59** to vapors of CH$_2$Cl$_2$, acetone, or toluene, these solvent vapors are taken up and the abovementioned adducts are formed rapidly. Vapor sorption is accompanied by the appearance of very intense red luminescene (λ_{max} = 658 nm) within seconds. This emission turn-on has been tentatively explained by a conformational fixation of the emissive species due to tighter crystal packing in the solvent adducts compared to neat **59**.

2.6 MMX chains made from [Pt$_2$(pop)$_4$I]$^{4-}$ units

The photochemistry of the [Pt$_2$(pop)$_4$]$^{4-}$ complex (pop = μ-pyrophoshito) in solution has been explored extensively.[124, 125] This diphosphito-bridged d^8-d^8 dimer exhibits favorable photophysical and photochemical properties due its short (2.925(1) Å) intramolecular Pt(II)-Pt(II) distance.[31] Halogenides can bind to the [Pt$_2$(pop)$_4$]$^{4-}$ core, resulting in so-called MMX compounds in which M = Pt and X = halogenide. A few of these MMX materials were found to exhibit vapochromism.[126-128] The compound [NH$_3$(CH$_2$)$_4$NH$_3$]$_2$[Pt$_2$(pop)$_4$I]·4H$_2$O (**60**) forms linear PtPtI chains along the crystallographic c-axis with Pt(II)-Pt(II) distances of 2.837 Å and Pt(II)-I distances of 2.722 Å, the counter-cations are in the spaces between individual chains.[126] At 296 K there is a single Pt-Pt vibration band at 98 cm^{-1} but upon heating to 340 K the

respective IR signal splits into two separate bands, indicating that there are two kinds of Pt-Pt units at elevated temperatures. Simultaneously, the color of the compound changes from green to red (Figure 28). These observations were explained in terms of a structural transition from a paramagnetic charge-polarization (CP) state to a diamagnetic charge-density-wave (CDW) state. In the initial CP state the individual molecular components are formally best regarded as Pt^{2+}–Pt^{3+}–I units which are linearly linked through weak interactions from the terminal iodo-ligand of one unit to the Pt^{2+} center of the nearest neighbor (Pt^{2+}–Pt^{3+}–I...Pt^{2+}–Pt^{3+}–I). In the CDW state, there are two different kinds of Pt_2 units because this structure is formally best described by alternating Pt^{2+}–Pt^{2+} and I–Pt^{2+}–Pt^{3+}–I units (Pt^{2+}–Pt^{2+}...I–Pt^{2+}–Pt^{3+}–I), resulting in a lower band gap of only 1.12 eV (1110 nm) compared to 2.52 eV (520 nm) in the CP state. In dry atmosphere, the red CDW state remains stable upon cooling from 340 K to room temperature. However, upon exposure of the metastable CDW form to saturated water vapor the CP state is recovered, manifesting itself in a color change from red to green.[126] The anhydrous red form of **60** can be crystallized directly from methanol solution and X-ray diffraction on single crystals confirms the CDW structure of this modification.[128] The difference in lattice volume between anhydrous **60** and **60**·4H_2O amounts to 150 Å^3 whereas the volume of a water molecule is generally approximated to 30 Å^3, suggesting that the total volume of eight H_2O molecules in the unit cell of **60**·4H_2O should be around 240 Å^3. This analysis suggests that crystal packing in anhydrous **60** is not as tight as it could be, and this might account for the facile water uptake in humid atmosphere. The X-ray crystal structure of a methanol adduct (**60**·2CH_3OH) has also been reported,[128] but it is not yet clear whether this material exhibits vapochromism.
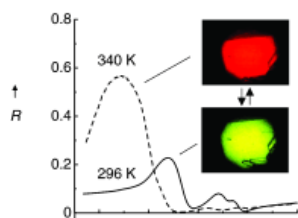
Figure 28. Reflectivity spectra and microscope images of compound **60** at two different temperatures. (Vapochromic Behavior Accompanied by Phase Transition between Charge-Polarization and Charge-Density-Wave States in a Quasi-One-Dimensional Iodine-Bridged Dinuclear Platinum Compound. *Angew. Chem. Int. Ed.*, 2005, *44*, 3240-3243. Copyright Wiley-VCH Verlag GmbH & Co. KGaA. Reproduced with permission.)

When replacing the $[NH_3(CH_2)_4NH_3]^{2+}$ cation of compound **60** by the larger $[NH_3(CH_2)_5NH_3]^{2+}$ cation one obtains another MMX material (**61**) which exhibits an analogous transition from a green CP state to a red CDW state upon heating.[127] However, in this case the transition occurs between 297 K and 308 K, i. e., at significantly lower temperature than in compound **60** (340 K). Thermogravimetric studies show that up to 350 K compound **61** releases four water molecules per formula unit hence the initial CP compound is to be formulated as $[NH_3(CH_2)_5NH_3]_2[Pt_2(pop)_4I] \cdot 4H_2O$ (**61**·$4H_2O$). Anhydrous **61** sorbs water readily from air at room temperature whereas anhydrous **60** requires water-saturated atmosphere. The higher sensitivity of **61** compared to **60** has been explained by the larger distances between individual MMX chains (caused by the larger cation), facilitating water diffusion into the crystal structure.

3. Gold(I) compounds

3.1 Dicyanoaurates

When reacting $Cu(ClO_4)_2$ with $KAu(CN)_2$ in DMSO, two different polymorphs of

$Cu[Au(CN)_2]_2(DMSO)_2$ (**62**·$(DMSO)_2$) can be obtained.[129] Reactant concentrations below 0.2 M

lead to a green polymorph, whereas blue crystals of a second polymorph are obtained at

concentrations above 0.5 M. This concentration dependence suggests that the blue material is a

kinetic reaction product while the green polymorph is presumably the thermodynamically more

stable form. The X-ray crystal structures of the two forms are significantly different, one of the

most evident differences is the five-fold (square-pyramidal) coordination of Cu(II) in the green

polymorph compared to the six-coordinate Cu(II) center in the blue form (Figure 29).
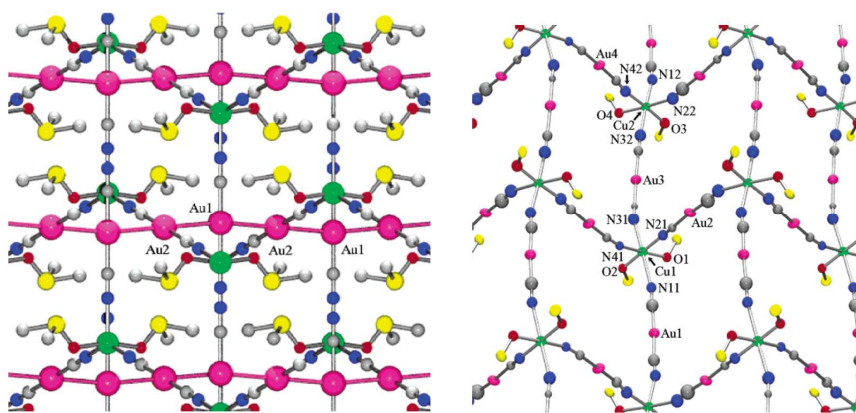
Figure 29. Extracts of the crystal structures of the green (left) and blue (right) polymorph of

$Cu[Au(CN)_2]_2(DMSO)_2$ (**62**·$(DMSO)_2$). Reprinted with permission from ref. [129]. Copyright 2004

American Chemical Society.

The green structure exhibits an extended 1D zigzag chain structure in which Cu(II) bridges

between individual $Au(CN)_2^-$ units. Each chain is connected to four neighboring chains through

Au(I)-Au(I) interactions occurring through an intermetallic contact of 3.22007(5) Å. The DMSO

molecules, ligated to Cu(II), occupy the voids between the chains. The blue polymorph contains

2-D layers of interconnected Au(CN)$_2$⁻ units and octahedral Cu(II) complexes, individual layers are stacked through aurophilic interactions of 3.419(3) Å to yield a 3-D network. The different colors of the two polymorphs are due to the different coordination numbers (5 or 6) and geometries (square-pyramidal vs. octahedral) of the Cu(II) ions, causing substantially different crystal field splittings of the d-d excited states. Both polymorphs are thermally stable up to 100 °C, but they easily sorb a variety of different small molecules with N- or O-atoms and thereby release DMSO. Specifically water, acetonitrile, DMF, dioxane, pyridine, and NH$_3$ were tested. A combination of elemental analysis, thermogravimetry, X-ray diffraction, and IR spectroscopy leads to the conclusion that the compounds generated by vapor uptake are identical to those that can be obtained directly from solutions containing the respective N- or O-atom-containing small molecules. A key finding is that all adsorbed solvent molecules are ligated to Cu(II) by replacing some or all of the initially present DMSO molecules. This behavior is in clear contrast to many other vapochromic materials in which adsorbed VOCs are loosely trapped in channels or voids of the crystalline host lattice. The ratio of adsorbed molecule to Cu(II) varies between 1:1 (DMF), 2:1 (H$_2$O, CH$_3$CN, pyridine), and 4:1 (NH$_3$), producing color changes which are easily detectable (Figure 30): The maximum visible reflectance varies between 433±7 nm for Cu[Au(CN)$_2$]$_2$(NH$_3$)$_4$ and 560±20 nm for solvent-free Cu[Au(CN)$_2$]$_2$. As the color variations are entirely due to changes in the Cu(II) coordination number and geometry it might be argued that Cu[Au(CN)$_2$]$_2$ is a copper- rather than gold-based vapochromic material. However, on the one hand the aurophilic interactions between individual cyanoaurate units are crucial for obtaining the vapor-responsive structures of Cu[Au(CN)$_2$]$_2$,[17] and on the other hand the Au(CN)$_2$⁻ units provide a spectroscopic handle which is at least as sensitive to solvent uptake as the changes in the UV-vis (reflectance) spectrum. Specifically, the CN stretching frequency is very susceptible

to π-backbonding from the Cu(II) center to the cyano-groups, producing shifts between 10 cm^{-1}

and 40 cm^{-1} depending on solvent.[129]
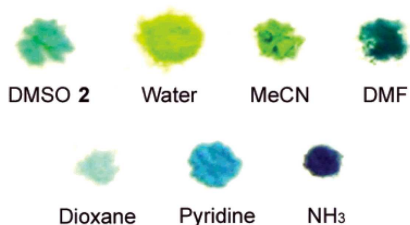
Figure 30. Vapochromic response of Cu[Au(CN)$_2$]$_2$(DMSO)$_2$ (**62**·(DMSO)$_2$) to different vapors. Reprinted with permission from ref. [129]. Copyright 2004 American Chemical Society.

The solvent exchange on Cu(II) is completely reversible, permitting dynamic vapor sensing, at least for H$_2$O, CH$_3$CN, DMF, and dioxane.[14] The stronger pyridine and NH$_3$ ligands are less easily replaced by other solvents hence in the case of Cu[Au(CN)$_2$]$_2$(pyridine)$_2$ and Cu[Au(CN)$_2$]$_2$(NH$_3$)$_4$ thermal treatment is necessary to reactivate the vapochromic behavior.

The strong binding of NH$_3$ to Cu(II) in **62** was one of the motivations for investigating analogous zinc(II) compounds in which the reversibility of NH$_3$ uptake was anticipated to be better. The second reason why Zn[Au(CN)$_2$]$_2$ (**63**) was studied is that in this material no d-d absorptions of the 3d metal can mask any gold-localized emission.[130] A vapoluminescence response in lieu of a vapochromic effect would potentially increase the detection sensitivity. Depending on reaction conditions (starting material, solvent, concentration) four different polymorphs of compound **63** were obtained. Particularly noteworthy is the fact that even the counterions of the zinc(II) and Au(CN)$_2^-$ starting materials influence which polymorph is formed even though these counterions are not incorporated into the final product. Despite careful

systematic investigations the rationale behind the preferential formation of a particular polymer under a given set of conditions has not become clear. All four polymorphs of $Zn[Au(CN)_2]_2$ have been characterized structurally. They all have Zn(II) in tetrahedral coordination geometry, and they all exhibit short Au(I)-Au(I) contacts in the range of 3.11 – 3.34 Å. Two polymorphs exhibit diamond-like networks, among the other two polymorphs there is a quartz-like and a herringbone-like network with different degrees of interpenetration. Because of the presence of aurophilic interactions, UV excitation leads to photoluminescence in three of the four polymorphs. One polymorph shows even two emissions, namely a short-lived (τ = 240 ns) band at 390 nm attributed to fluorescence and a longer lived (τ = 930 ns) band at 480 nm assigned to phosphorescence. Along the series of the three emissive polymorphs the phosphorescence energy is inversely proportional to the Au(I)-Au(I) distance, as expected.[131, 132]
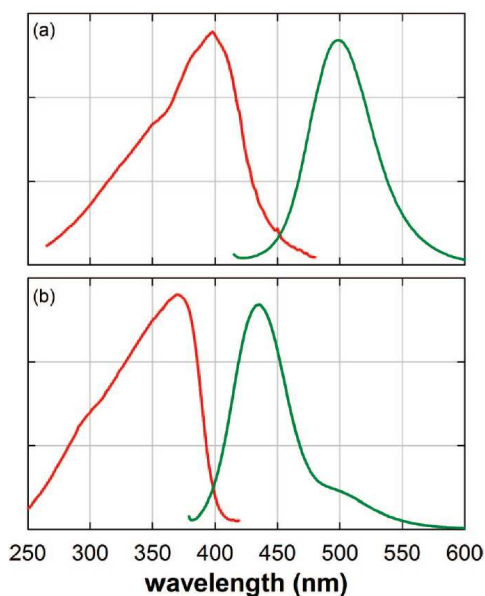

Figure 31. Excitation and emission spectra of (a) $[Zn(NH_3)_2][Au(CN)_2]_2$ and (b) $[Zn(NH_3)_4][Au(CN)_2]_2$ illustrating the vapochromic and vapoluminescent response of compound

62 to ammonia vapor. Reprinted with permission from ref. [130]. Copyright 2008 American Chemical Society.

Exposure of any of the four polymorphs to ammonia vapors produces a new emission with a band maximum at 430 nm (Figure 31).[130] The resulting species, identified as $[Zn(NH_3)_4][Au(CN)_2]_2$, decomposes fairly rapidly once it is removed from ammonia-rich atmosphere, and the $[Zn(NH_3)_2][Au(CN)_2]_2$ compound with a lower ammonia content emitting at 500 nm is formed. In IR spectroscopy the CN stretch of $[Zn(NH_3)_2][Au(CN)_2]_2$ shows up as a single band at 2158 cm^{-1}, and there is evidence for metal-bound NH_3, suggesting that Zn(II) is either octahedrally or tetrahedrally coordinated by ammonia. From powder X-ray diffraction data it was inferred that $[Zn(NH_3)_2][Au(CN)_2]_2$ contains Zn(II) centers in D_{4h} local symmetry with NH_3 ligands in *trans*-disposition and four equatorial N-bound cyanides. When $[Zn(NH_3)_2][Au(CN)_2]_2$ was left standing in air for 30 minutes, neat $Zn[Au(CN)_2]_2$ was formed, i. e., the vapoluminescence response has the anticipated higher reversibility compared to $Cu[Au(CN)_2]_2$. Although all four polymorphs of $Zn[Au(CN)_2]_2$ show vapoluminescence behavior, the material made from $Zn(NO_3)_2$ and $[(n\text{-}Bu)_4N][Au(CN)_2]$ exhibits the highest sensitivity for ammonia with a detection limit of 1 ppb.[17] The permissible long-term exposure limit for NH_3 is 20 ppm, the human nose starts sensing ammonia at concentrations of 50 ppm.[133]

3.2 Di- and trinuclear Au(I) complexes

Reaction of $KS_2CN(C_5H_{11})_2$ with "$AuCl_2^-$" generated in situ from $K[AuCl_4]$ and $Na_2S_2O_3$ affords a dimeric gold(I) dithiocarbamate complex (Scheme 29), $[Au(S_2CN)(C_5H_{11})_2]_2$ (**64**),

which exhibits reversible vapoluminescence upon exposure to polar aprotic molecules such as

acetone, CH_3CN, CH_2Cl_2, $CHCl_3$.[134] Vapors of protic solvents such as methanol or ethanol

produce no response. X-ray diffraction of single crystals of **64**·DMSO and **64**·CH_3CN shows that

there are infinite chains of Au atoms along the crystallographic c-axis with *inter*molecular Au(I)-

Au(I) contacts of 2.9617(7) Å (**64**·DMSO) and 3.0241(12) Å (**64**·CH_3CN). The *intra*molecular

Au(I)-Au(I) distances in the two solvates are 2.7690(7) Å and 2.7916(12) Å. In solvent-free **64**

the intramolecular metal-metal contacts are equally short (2.7653(3) Å), but the closest

intermolecular Au(I)-Au(I) distance increases to 8.135 Å hence there is no infinite chain of

mutually interacting gold atoms. Thus, the orange emission (λ_{max} = 604 nm) is only observed

when *inter*molecular Au(I)-Au(I) interactions between dimers are present, and the emissive

excited states are likely to have either $(d\sigma^*)^1(p\sigma)^1$ or $(d\delta^*)^1(p\sigma)^1$ valence electron

configurations.[135]

Scheme 29. Dinuclear gold(I) complexes exhibiting vapochromism and tribochromism.
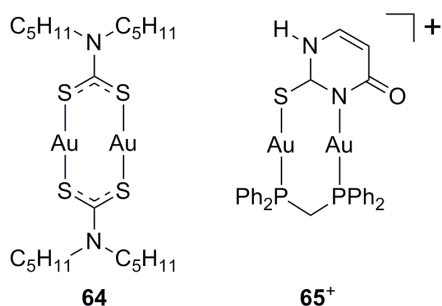
A gold(I) 2-thiouracilato complex with a bridging bis(diphenylphosphino)methane (dppm)

ligand (**65a**·CF_3COO) exhibits a somewhat longer (2.8797(4) Å) intramolecular Au(I)-Au(I)

distance than complex **64**.[136] The helical supramolecular arrangement in the crystal structure of

65a·CF$_3$COO precludes the formation of extended chains of interacting gold atoms (Figure 32), and the substance is not luminescent. When it is gently crushed with a spatula blue photoluminescence (λ_{max} = 483 nm) can be detected, i. e., the substance shows luminescence tribochromism.[137] The emissive form can also be obtained upon gentle heating (37 °C) or by sonication,[136] and in the course of this treatment acid is released as monitored by using pH paper. When compound **65a**·CF$_3$COO is stirred in CH$_2$Cl$_2$/CH$_3$OH solutions over Na$_2$CO$_3$ it is possible to obtain the deprotonated product **65b** which consists of dimers held together with short (2.9235(4) Å) intermolecular Au(I)-Au(I) contacts (Figure 32), i. e., the crystal packing is completely different. The available experimental evidence including powder X-ray analysis of crushed **65a**·CF$_3$COO supports the hypothesis that **65b** is the emissive material resulting from mechanical (or thermal) treatment of **65a**·CF$_3$COO. Thus it appears that the tribochromism is due to rearrangement of the molecules in the crystal lattice coupled to release of volatile acid. Exposure of **65b** to CF$_3$COOH vapor leads (very slowly) to a loss of the photoluminescence, but the emission can be recovered by subsequent exposure to triethylamine vapor. The C-O bond lengths in the crystal structures of **65a**·CF$_3$COO and **65b** are similar hence the probable site of protonation in **65b** is most likely the uncoordinated pyrimidine N-atom.
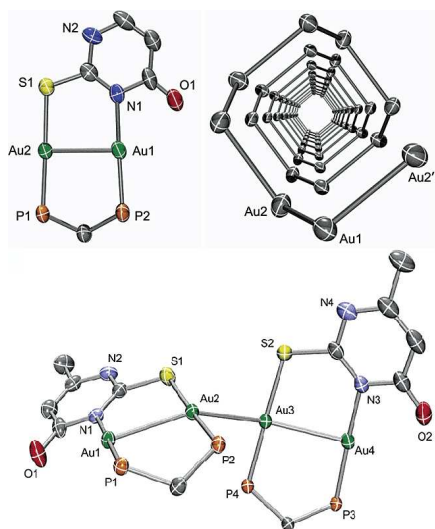
Figure 32. Top left: Crystal structure of compound **65a**·CF$_3$COO. Top right: helical arrangement of gold atoms in **65a**·CF$_3$COO. Bottom: Dimers of complexes in compound **65b**. Reprinted with permission from ref. [136]. Copyright 2003 American Chemical Society.

Scheme 30. Trinuclear gold(I) complexes.
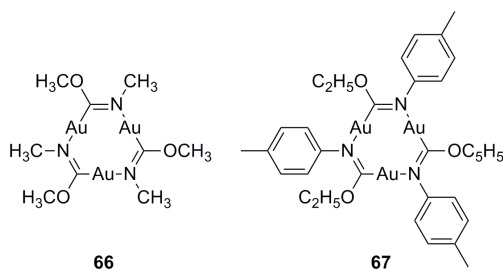
The trinuclear gold(I) complex **66** (Scheme 30) exhibits the unusual phenomenon of solvent-stimulated luminescence.[138, 139] This means that emission is triggered when liquids are brought into contact with crystals of **66** that have been previously irradiated at 366 nm. Compound **66** features short intra- (3.308(2) Å) and intermolecular Au(I)-Au(I) interactions (3.346(1) Å), and thus it seems plausible that aurophilic interactions are important for the luminescence behavior

of **66**, particularly in view of the fact that a reference compound without any short intermetallic contacts is non-emissive. In the crystal structure of **66** there are extended stacks of individual molecules along the c-axis, and it has been speculated that upon UV irradiation energy might be stored in these stacks in the form of electron-hole pairs which only recombine following addition of solvent. This tentative explanation is plausible because one would expect relatively facile charge migration along these stacks,[140] and electrons or holes can easily be trapped at defect sites. Solvent addition can then trigger minor structural changes such that the electrons and holes are released from the defect sites. Interestingly, $CHCl_3$ and CH_2Cl_2 in which compound **66** has the highest solubility produce the strongest luminescence. It has been noted that the solvent-stimulated luminescence of **66** is related to the phenomenon of lyoluminescence,[141] in which light emission occurs when dissolving a solid that has been previously exposed to ionizing radiation – with the important difference that radiation of much lower energy is required to induce emission in compound **66**.[138] The solvoluminescence from planar trigold(I) complexes has been reviewed.[142]

The charge mobility in microwires of compound **66** has been explored with a view to obtaining materials with vapor-sensitive conductive properties.[143] For this purpose a CH_2Cl_2 solution of **66** was drop-cast between two gold electrodes on a SiO_2 surface, and the resulting microwires formed from stacks of **66** were found to bridge the 150 μm gap between the two gold electrodes. Hole mobilities on the order of 0.2 cm^2 V^{-1} s^{-1} were determined for 10 devices of this type. At a voltage of 1.5 V between the two gold electrodes currents on the order of 0.6 nA flow through the microwires. Exposure to ethanol vapor decreases the flowing current by two orders of magnitude, but this decrease is reversible when purging with pure N_2 afterwards. In addition to ethanol, THF, CH_3CN, acetone, methanol, *n*-propanol, *n*-butanol, *n*-pentanol, benzene, and *p*-

xylene have been tested, but only ethanol, methanol and CH_3CN were found to produce a significant response. It has been argued that hydrogen-bonding interactions between compound **66** and adsorbed VOCs might disturb the 1D-stacking of the complexes and thereby disrupt efficient charge transfer pathways.[143]
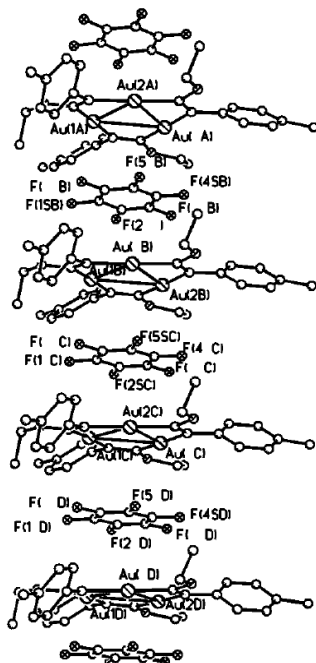
Figure 33. Columnar structure of **67**·C_6F_6. Reprinted with permission from ref. [144]. Copyright 2001 American Chemical Society.

The trinuclear gold(I) complex **67** differs from compound **66** mainly in that the N-atoms bear *p*-tolyl groups instead of methyl-substituents. Solid **67** exhibits blue photoluminescence ($\lambda_{max} \approx$ 440 nm), but when exposed to vapor of C_6F_6 the emission is quenched.[144] X-ray structural investigations provide a plausible explanation for this behavior. Neat **67** crystallizes in such a way that dimers of **67** with short intermolecular Au(I)-Au(I) contacts are formed,[145] whereas the

crystal structure of **67**·C$_6$F$_6$ consists of 1D-chains of alternating gold complexes and hexafluorobenzene molecules interacting with each other through (Lewis) acid-base interactions (Figure 33).[144] Thus, uptake of C$_6$F$_6$ disrupts intermolecular Au(I)-Au(I) contacts, and this is likely the reason for the emission quenching described above.

A chemically related trinuclear Au(I) complex with imidazolate instead of carbeniate ligands forms analogous 1D chains with intercalating TCNQ molecules, but for the respective complex no vapoluminescence behavior has been reported.[144]
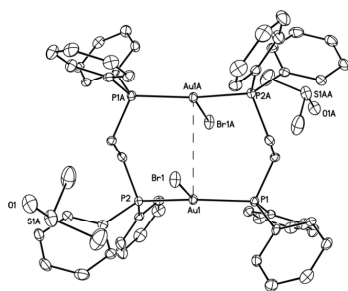
Figure 34. Drawing of the structure of **68**·2DMSO (type A representative). Reprinted with permission from ref. [146]. Copyright 2010 American Chemical Society.

The dimer Au$_2$(μ-bis-(diphenylphosphino)ethane)$_2$Br$_2$ (**68**) was found to exhibit remarkable molecular flexibility and for this reason may be regarded as a molecular accordion with vapoluminescent properties.[146] Depending on crystallization conditions three different types of structures of the same compound are obtained. Type A crystals are obtained for **68**·2DMSO, **68**·2Me$_2$CO, **68**·2CH$_2$Cl$_2$, **68**·2DMF and contain discrete Au$_2$ dimers (Figure 34). They are colorless and exhibit orange emission (λ_{max} = 620 – 640 nm) upon UV excitation. The intramolecular Au(I)-Au(I) distances in type A crystals are relatively long and range from 3.8479(3) Å for **68**·2DMSO to 3.5142(3) Å in **68**·2DMF. The expected Au(I)-Au(I) separation

based on the van der Waals radius is about 3.6 Å,[147] i. e., there are little to no aurophilic interactions in these crystals. The solvent molecules merely fill space in the crystal structures but do not interact with the metal centers. Type B crystals are green photoluminescent (λ_{max} = 550 nm) and exhibit aurophilic interactions within discrete dimers since there are short Au(I)-Au(I) contacts between 3.3249(2) Å and 3.09841(18) Å in **68**·2CH$_3$CN and **68**·0.5Et$_2$O. Type C crystals are polymers which are not considered further here because they are not vapochromic or vapoluminescent. The finding of intermolecular Au(I)-Au(I) distances varying between 3.09841(18) Å and 3.8479(3) Å for the same compound is highly unusual and justifies usage of the term "molecular accordion".
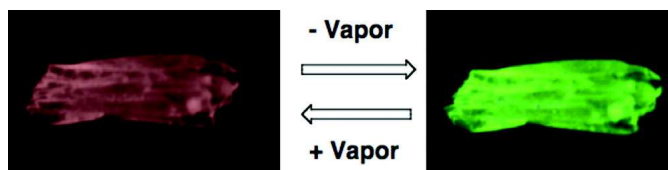
Figure 35. Vapor-induced luminescence changes in compound **68**. Reprinted with permission from ref. [146]. Copyright 2010 American Chemical Society.

When drying type A crystals of **68**·2CH$_2$Cl$_2$ and **68**·Me$_2$CO their orange emission disappears, and they begin to exhibit the green luminescence observed for type B crystals (Figure 35). Subsequent exposure to acetone or CH$_2$Cl$_2$ vapor recovers the orange emission of the initial type A material, but no vapoluminescence response is observed for acetonitrile, diethyl ether, DMF, DMSO, benzene, pyridine, nitrobenzene, and carbon disulfide. It seems quite obvious that the remarkable flexibility of the Au$_2$(μ-dppe)$_2$Br$_2$ molecule is responsible for the vapoluminescence

behavior. The different luminescence colors between type A (orange) and type B (green) seem to

be primarily an effect of a smaller Stokes shift in type B crystals.
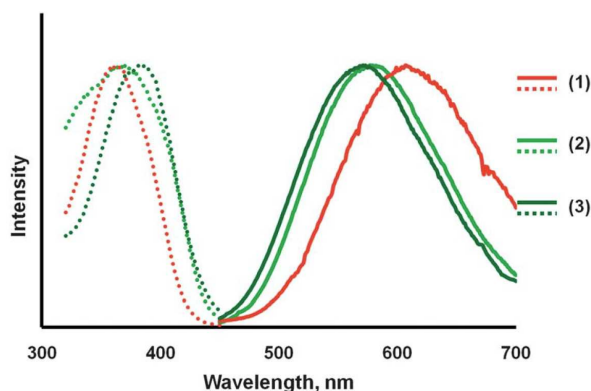
Figure 36. Excitation (dotted lines) and emission (solid lines) spectra of (a) the α-polymorph of

69·2Me$_2$CO; (b) the β-form obtained after gentle drying of α-**69**·2Me$_2$CO (light green traces); (c)

the material obtained after drying of α-**69**·2Me$_2$CO for three hours (dark green traces). Reprinted

with permission from ref. [148]. Copyright 2012 The Royal Society of Chemistry.

An analogous gold(I) dimer with iodo- instead of bromo-ligands, Au$_2$(μ-bis-

(diphenylphosphino)ethane)$_2$I$_2$·2Me$_2$CO (**69**·2Me$_2$CO), exhibits similarly spectacular

behavior.[148] Depending on crystallization conditions two different polymorphs of **69**·2Me$_2$CO

can be obtained: The α-polymorph luminesces in the orange spectral range (λ_{max} = 607 nm),

whereas the β-polymorph is a green emitter (λ_{max} = 577 nm) (Figure 36). The two polymorphs

can be reversibly converted into one another. Gentle drying of α-**69**·2Me$_2$CO crystals in air

transforms them into the green-emitting β-form, and subsequent exposure to acetone or CH$_2$Cl$_2$

vapor converts them back to the orange-glowing α-polymorph. This single crystal to single

crystal conversion does not involve any loss or uptake of acetone, but it is possible to remove 2

molecules of acetone from the β-polymorph by prolonged drying. In the course of the conversion

of the α- to the β-form the intramolecular Au(I)-Au(I) distance decreases from 3.6720(2) Å to

3.3955(2) Å.

Scheme 31. Di- and trinuclear gold complexes.
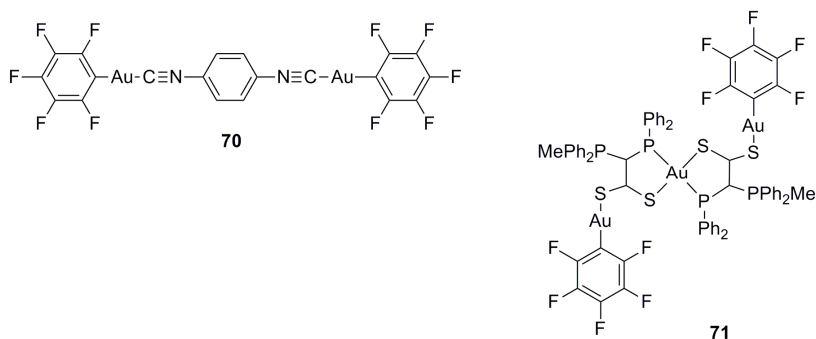
When reacting C_6F_5Au(tetrahydrothiophene) with 1,4-diisocyanobenzene in CH_2Cl_2 one

obtains the dinuclear gold(I) complex **70** (Scheme 31) which is a mechanochromic and

vapochromic substance.[149] The blue photoluminescence of untreated powder or crystals of **70**

was attributed to ligand-localized π-π* transitions. X-ray diffraction on a single crystal shows

that the shortest intermolecular Au(I)-Au(I) distance is 5.19 Å, i. e., there are no aurophilic

interactions between individual molecules. When grinding a sample of **70** in an agate mortar the

luminescence changes to yellow (Figure 37). Powder X-ray diffraction shows that an amorphous

material is formed, and it has been speculated that the yellow luminescence of this material

might be due to aurophilic interactions that arise from rearrangement of the individual molecules

relative to each other. Significant changes in the N≡C stretching frequencies upon mechanical

grinding suggest that the coordination mode of the isocyanide ligands is altered, and this could

indeed be due to the formation of aurophilic bonds.[150] When exposing a ground sample of **70** to

CH_2Cl_2 vapor the blue luminescence is restored, indicating that the structural transformation is reversible.[149] A simple slipping motion of the planar molecules appears as the most plausible molecular rearrangement accompanying mechano- and vapochromism in compound **70**.
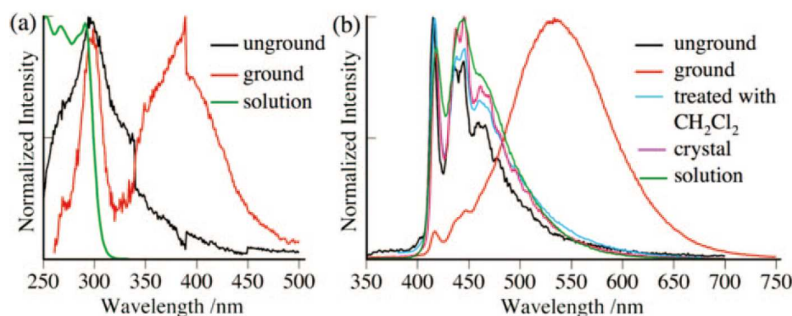
Figure 37. (a) Absorption and (b) photoluminescence spectra of compound **70** in various states. Reprinted with permission from ref. [149]. Copyright 2008 American Chemical Society.

The dinuclear complex **71** changes color from orange to black when exposed to vapors of acetone, CH_2Cl_2, or $CHCl_3$.[151, 152] This behavior was exploited for the construction of VOC-sensitive optical fibers. The sensors consisted of a standard 1.3 μm optical fiber onto which the vapochromic material was deposited at one end. Since the vapochromic material undergoes a change in refractive index upon solvent exposure, the reflectance of the overall optical fiber changes dramatically in the 500 – 1800 nm wavelength range when the material is exposed to VOCs. Changes of up to 13.5 dB in the transmitted optical power were detected for acetone and CH_2Cl_2, but the devices respond to other solvents as well, for example to $CHCl_3$, dichloroethane, ethanol, ethyl acetate, THF, and toluene.[151, 152]

3.3 Gold-thallium complexes

When equimolar quantities of $[NBu_4][Au(C_6Cl_5)_2]$ and $TlPF_6$ are brought to reaction in THF one obtains $[Tl[Au(C_6Cl_5)_2]]_n$ (**72**) as a pale yellow solid.[153] This vapochromic material contains linear chains of alternating (and nearly planar) $[Au(C_6Cl_5)_2]^-$ anions and Tl^+ cations along the crystallographic z-axis with unsupported Au(I)-Tl(I) interactions at distances of 3.044(5) and 2.9726(5) Å. Theoretical studies lead to the conclusion that this heterobimetallic d^{10}-s^2 interaction (of Lewis acid – Lewis base type) is associated with a stabilization energy of about 275 kJ/mol.[154] Between individual Au(I)-Tl(I) chains there are channels with hole diameters as large as 10.471 Å running parallel to the z-axis hence there is considerable room for incorporation of solvent guests. Compound **72** changes color from yellow to red when exposed to vapors of acetylacetone or pyridine but stays yellow upon exposure to acetone, acetonitrile, THF, triethylamine, 2-fluoropyridine, or tetrahydrothiophene. However, all of these VOCs produce detectable vapoluminescence responses with emission maxima ranging from 507 nm (THF) to 650 nm (acetylacetone) compared to λ_{max} = 531 nm for neat **72** (Figure 38).[153]
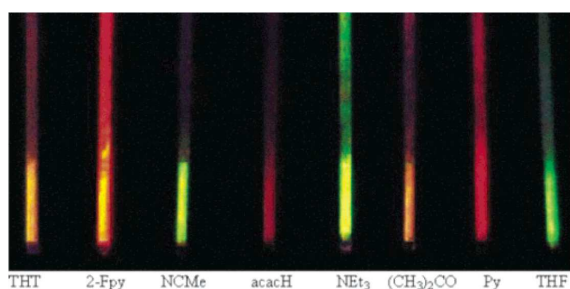
Figure 38. Luminescence vapochromism of compound **72** observed after exposure to various VOCs. Reprinted with permission from ref. [155]. Copyright 2004 American Chemical Society.

Using the appropriate VOCs as solvents, it is possible to synthesize a range of solvent adducts with the general stoichiometry $[TlL_2[Au(C_6Cl_5)_2]]_n$ ($\mathbf{72}L_2$), two of which have been structurally characterized ($\mathbf{72}$(tetrahydrothiophene)$_2$, $\mathbf{72}$(2-fluoropyridine)$_2$).[155] The respective structures contain polymeric chains of cations and anions with unsupported Au(I)-Tl(I) contacts at distances between 2.90894(5) and 3.1981(4) Å which are close to the sum of thallium and gold metallic radii (3.034 Å). The tetrahydrothiophene and 2-fluoropyridine molecules ligate to Tl(I) which is now in pseudo trigonal-bipyramidal coordination with a vacant equatorial coordination site occupied by a lone pair. As a consequence, the Au(I)-Tl(I)-Au(I) interaction is no longer as linear as in neat $\mathbf{72}$ but more zigzag-like (the Au(I)-Tl(I)-Au(I) angle is 164°). The emission of the individual solvent adducts undergoes a significant red-shift between room temperature and 77 K, suggesting that the luminescence of $[Tl[Au(C_6Cl_5)_2]]_n$ has its origin in gold-thallium interactions. Time-dependent DFT supports this hypothesis. The geometrical changes around the Tl(I) cation in the course of solvent uptake lead to a change in HOMO-LUMO energy gap because the Au(I)-Tl(I) interaction is perturbed by solvent ligation to the Lewis acid. Importantly, the vapoluminescence response of compound $\mathbf{72}$ is reversible: Heating of the $\mathbf{72}L_2$ compounds to 100°C for a few minutes regenerates the solvent-free starting material.

Scheme 32. Vapochromic substances ($\mathbf{73a}/\mathbf{73b}$) based on ketimine formation ($\mathbf{74a}/\mathbf{74b}$).

$\mathbf{73a}$ X = F
$\mathbf{73b}$ X = Cl

$\mathbf{74a}$ X = F
$\mathbf{74b}$ X = Cl
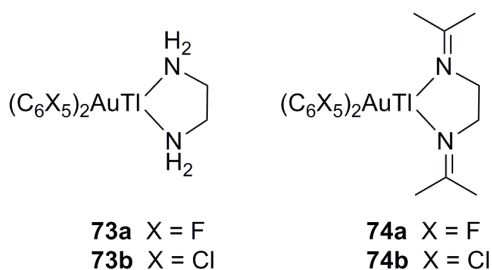
When reacting equimolar amounts of $[Tl[Au(C_6X_5)_2]]_n$ (X = F, Cl) and 1,2-ethylenediamine

(en) one obtains $[Tl(en)[Au(C_6F_5)_2]]_n$ (**73a**) and $[Tl(en)[Au(C_6Cl_5)_2]]_n$ (**73b**) as green and white

solids, respectively.[156] The ethylenediamine ligand ligates to Tl(I), leading to the pseudo

trigonal-bipyramidal coordination geometry discussed above for the $72L_2$ compounds. When

exposing solid **73a** to acetone or acetophenone vapor it changes color from green to yellow,

whereas **73b** changes from white to red with acetone and from white to orange with

acetophenone. In order to understand this vapochromic behavior it is important to know that the

reaction of **73a** or **73b** with 2 (or more) equivalents of acetone in THF solution yields

compounds **74a** and **74b** which are ketimines formed through reaction of the ethylenediamine

ligand and acetone. The vapochromism of solids of **73a** and **73b** is most likely due to the same

reaction because IR spectroscopy provides clear evidence for the disappearance of the amine N-

H stretch in the course of VOC exposure with the simultaneous appearance of imine C=N

stretches near 1650 cm^{-1}. Solid **73a/74a** and **73b/74b** are brightly luminescent in different colors

hence the compounds can also be used as vapoluminescent sensors. The absorption and emission

color changes following ketimide formation have been attributed to perturbation of excitonic

states along Tl(I)-Au(I) chains caused by changes in the Tl(I) coordination environment.

3.4 Gold-silver complexes

Bimetallic gold-silver compounds of the general formula $[Au_2Ag_2(C_6F_5)_4L_2]_n$ (**75L$_2$**) with a

variety of different donor ligands L exhibit vapochromic behavior.[12, 157] Structural studies of the

systems with L = Et$_2$O (**75(Et$_2$O)$_2$**), Me$_2$CO (**75(Me$_2$CO)$_2$**), THF (**75(THF)$_2$**), and CH$_3$CN

(**75(CH$_3$CN)$_2$**)) reveal that this class of compounds contains tetranuclear Au$_2$Ag$_2$ units linked to

each other along the crystallographic z axis through unsupported Au(I)-Au(I) interactions at distances between 3.1674(11) Å and 3.1959(3) Å, resulting in extended linear-chain compounds (Figure 39).[158]
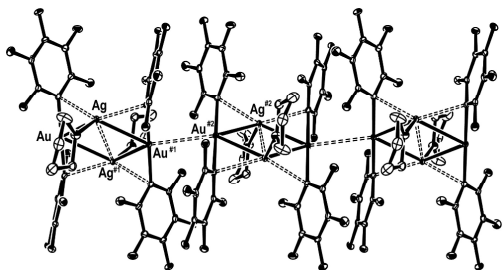
Figure 39. Extract of the crystal structure of compound **75**(THF)$_2$). Reprinted with permission from ref. [158]. Copyright 2008 American Chemical Society.

Compound **75**(Et$_2$O)$_2$ is obtained by reacting equimolar quantities of [Bu$_4$N][Au(C$_6$F$_5$)$_2$] and AgClO$_4$ in a CH$_2$Cl$_2$/Et$_2$O solvent mixture and can be used as a starting material for the syntheses of the other **75**L$_2$ compounds.[159, 160] Moreover, exposure of solid **75**(Et$_2$O)$_2$ to vapors of acetone, THF or acetonitrile produces rapid color changes that are consistent with replacement of Et$_2$O by the respective other VOCs (Figure 40).
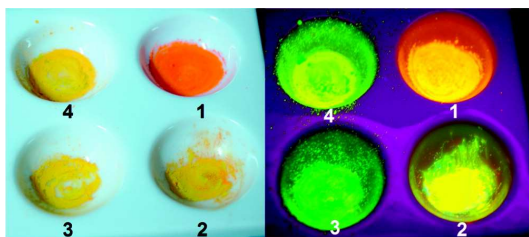
Figure 40. Left: Samples of compound **75**(Et$_2$O)$_2$ before (1) and after exposure to vapors of acetone (2), THF (3), CH$_3$CN (4). Right: Reprinted with permission from ref. [158]. Copyright 2008 American Chemical Society.

IR spectroscopy provides clear evidence for the substitution of the initial O-donor by the stronger N-donor ligand. The exchange ability of the individual VOCs follows the order CH$_3$CN > Me$_2$CO > THF > Et$_2$O, i. e., acetonitrile is able to replace all oxygen donor ligands but not vice versa. This observation suggests that true ligand substitution reactions take place at the Au$_2$Ag$_2$ core and that the vapochromic behavior of this class of compounds is not simply due to adsorption of the VOCs into the crystal lattice. Thermogravimetric analyses of the **75**L$_2$ compounds reveal significant differences between the temperatures at which the donor ligands (L) are lost, and these variations were interpreted in terms of different boiling points of the individual VOCs and the strengths of their interactions with the Ag(I) centers.[158] The **75**L$_2$ compounds are emissive at room temperature and 77 K, presumably involving electronic transitions on the Au$_2$Ag$_2$ core which may be perturbed by changes in the Au(I)-Au(I) and Au(I)-Ag(I) interactions.

Scheme 33. Vapochromic Au$_2$Ag$_2$ compounds. R = C$_6$F$_5$.

76   **77**
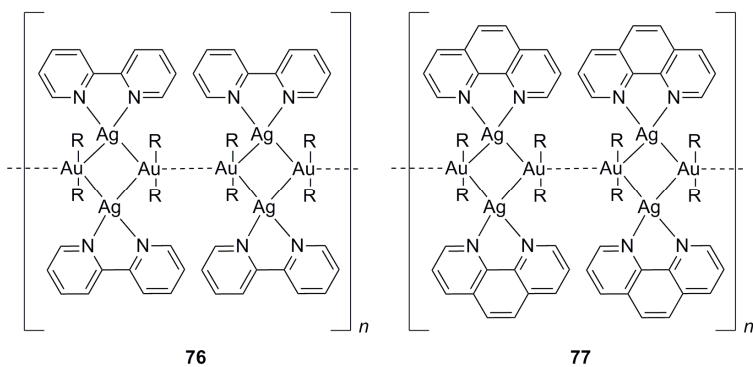
Several compounds of the stoichiometry $[Au_2Ag_2(C_6F_5)_4L_2]_n$ have been the subject of more application-oriented studies in which these vapochromic materials were deposited on optical fibers. [161-163] VOC-induced changes in reflected optical power on the order of 2.5 dB − 4 dB were detected.[161-163] In one set of experiments it was possible to distinguish isopropanol from ethanol and methanol, but discrimination between the two shorter alcohols proved more difficult.[12] In several of these vapochromic sensor materials the donor ligand L was a bidentate 2,2'-bipyridine (bpy) or 1,10-phenanthroline (phen) ligand, i. e., these materials can be formulated as $[Au_2Ag_2(C_6F_5)_4(bpy)_2]_n$ (**76**) and $[Au_2Ag_2(C_6F_5)_4(phen)_2]_n$ (**77**) (Scheme 33).[12, 162] Prior to VOC exposure many of these materials are bright yellow but then turn colorless upon sorption of different donor solvents. The loss of color has been attributed to the rupture of intermolecular Au(I)-Au(I) contacts between individual Au_2Ag_2 metallacycles.[157, 159, 162]

The reaction between $[Bu_4N][Au(4-C_6F_4I)_2]$ and $AgClO_4$ affords a creme-colored solid which can be identified as $[Au_2Ag_2(4-C_6F_4I)_4]_n$ (**78**).[164] Utilization of the $4-C_6F_4I$ group instead of C_6F_5 was motivated by the possibility that the *p*-iodo-substituent might form noncovalent halogen-bonds to Lewis donor atoms.[165] Compound **78** is vapochromic toward Me_2CO, THF, or CH_3CN, but no response is detected for non-coordinating solvents such as diethyl ether or toluene. Solvates of compound **78** with the general formula $[Au_2Ag_2(4-C_6F_4I)_4L_2]_n·xL$ (**78**L_2·xL) are

readily obtained when reacting $[Au_2Ag_2(4\text{-}C_6F_4I)_4]_n$ in Me_2CO, THF, or CH_3CN. The respective

substances are brightly colored and contain the desired halogen bonds with I-O, I-F, and I-N

distances in the range from 2.837(23) to 3.494(15) Å.[164] The acetone solvate

($78(Me_2CO)_2·2Me_2CO$)) and the THF solvate ($78(THF)_2$)) can both be converted to the

acetonitrile solvate ($78(CH_3CN)_2$)) by exposure to vapors of CH_3CN, manifesting in an emission

color change from red to bright yellow. Combined structural and emission studies (the latter in

fluid solution) lead to the conclusion that two factors drive the vapoluminescence response: (i)

the degree of aggregation of individual Au_2Ag_2 clusters into polymeric chains, and (ii) the

geometry of the Au_2Ag_2 clusters itself.[164] The aggregation of individual clusters results from an

interplay between aurophilic interactions (with Au(I)-Au(I) distances in the range from

2.7853(14) to 2.9481(3) Å) and noncovalent halogen bonds. TD-DFT calculations indicate that

in the acetone solvate the HOMO is mostly spread over the $4\text{-}C_6F_4I$ ligands with a some

contribution of $5d_{z2}\sigma^*$ character from interacting Au(I)-Au(I) centers. The LUMO is a mixture of

$5p\sigma$ bonding density between the Au(I) and Ag(I) centers.

Analogous tetranuclear Au_2Ag_2 compounds with vapochromic properties can be obtained

when using $3,5\text{-}C_6Cl_2F_3$ or C_6Cl_5 groups as ligands to the gold atoms.[166] From Et_2O/CH_2Cl_2

solution one obtains compounds with the formulas $[Au_2Ag_2(3,5\text{-}C_6Cl_2F_3)_4(Et_2O)_2]_n$ ($79(Et_2O)_2$)

and $[Au_2Ag_2(C_6Cl_5)_4(Et_2O)_2]_n$ ($80(Et_2O)_2$).[166] Upon exposure to the respective VOCs the diethyl

ether molecules in $79(Et_2O)_2$ and $80(Et_2O)_2$ can be replaced with THF, acetone or acetonitrile,

manifesting itself in a vapochromic response. X-ray crystal structure analyses of $[Au_2Ag_2(3,5\text{-}$

$C_6Cl_2F_3)_4(THF)_2]_n$ and $[Au_2Ag_2(3,5\text{-}C_6Cl_2F_3)_4(toluene)_2]_n$ demonstrate that there are polymeric

chains of Au_2Ag_2 units held together via aurophilic interactions. The intermolecular Au(I)-Au(I)

distances are 2.8617(7) and 2.8863(7) Å in $79(THF)_2$ which is appreciably shorter than in the

related pentafluorophenyl derivative with THF (**75**(THF)$_2$) (3.1959(3) Å). However, the compounds with the 3,5-C$_6$Cl$_2$F$_3$ ligand were found to exhibit a relatively poor thermal stability when compared to the pentachlorophenyl derivatives. Contrary to the behavior of compound **75** which has a strong preference for acetonitrile over Et$_2$O, THF, or acetone (see above),[158] in the [Au$_2$Ag$_2$(3,5-C$_6$Cl$_2$F$_3$)$_4$(CH$_3$CN)$_2$]$_n$ material acetonitrile is displaced by vapors of THF or acetone.[166] Similarly, the THF molecules of **79**(THF)$_2$ can be displaced by acetone from the gaseous phase, but exposure to vapors of acetonitrile leads only to solvate mixtures and incomplete THF substitution.
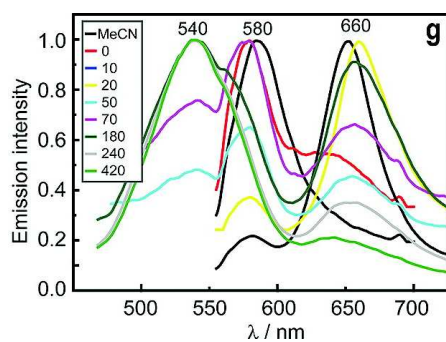
Figure 41. Luminescence changes of compound **81** observed in the course of solvation with fluid CH$_3$CN. The inset marks the reaction time in minutes. Reprinted with permission from ref. [167]. Copyright 2011 American Chemical Society.

When using 2-C$_6$F$_4$I instead of 4-C$_6$F$_4$I as a ligand to gold(I), the iodine-atom can ligate to Ag(I), thereby mitigating the propensity for polymerization of this class of materials.[167] Accordingly, reaction of Ag(tfa) (tfa = trifluoroacetate) with an equimolar amount of NBu$_4$[Au(2-C$_6$F$_4$I)$_2$] in CH$_2$Cl$_2$ affords (NBu$_4$)$_2$[Au$_2$Ag$_2$(2-C$_6$F$_4$I)$_4$](tfa)$_2$ (**81**) which is comprised of tetranuclear monomers with Au(I)-Ag(I) distances in the range from 2.7738(7) to 2.9269(7) Å.

Both 2-C_6F_4I ligands of Au(I) coordinate to Ag(I) with Ag-I distances of 2.7987(9) − 2.9011(9)

Å. Solvation of green emitting **81** with fluid CH_3CN leads to the rapid formation of a yellow

glowing intermediate (Figure 41), and finally a red luminescent polymeric compound of

stoichiometry $[Au_2Ag_2(2\text{-}C_6F_4I)_4(CH_3CN)_2]_n$ is obtained. The yellow intermediate is believed to

be a material of stoichiometry $[Au_2Ag_2(2\text{-}C_6F_4I)_4]_2$ (**82**) composed of dimers of tetranuclear

Au_2Ag_2 clusters. The dimer compound **82** can be obtained from reaction of $NBu_4[Au(2\text{-}C_6F_4I)_2]$

with $AgClO_4$ and is selectively vapochromic toward coordinating solvents such as CH_3CN, THF,

and acetone. The fact that the Ag(I) ions in **82** are coordinatively unsaturated seems to be key to

the vapochromic behavior.

   3.5 Other Au(I) complexes

Scheme 34. Solvoluminescent gold(I) complexes.
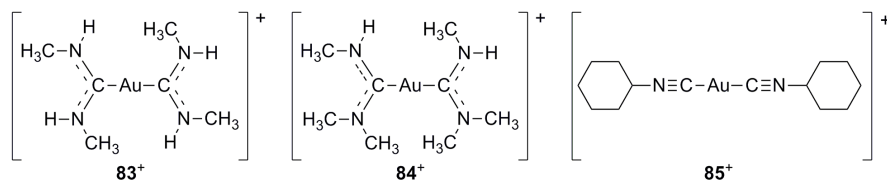
Three carbene complexes of gold(I) (**83**PF_6, **83**BF_4, **84**PF_6) (Scheme 34) are frequently cited in

the context of vapochromism even though they show the phenomenon of solvoluminescence

rather than true vapochromism or vapoluminescence.[168] The 77 K emission of **83**PF_6 is green in

acetonitrile, blue in DMSO and pyridine, and orange in acetone (Figure 42).
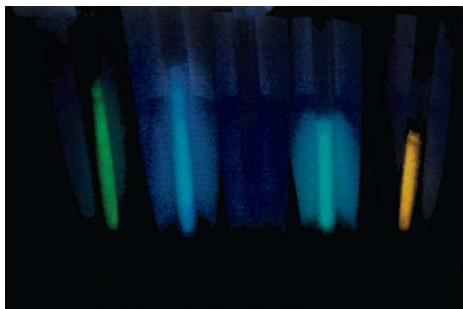
Figure 42. Photoluminescence of frozen solutions of compound **83**PF$_6$ in CH$_3$CN, DMSO, DMF, pyridine, and acetone. Reprinted with permission from ref. [168]. Copyright 2002 American Chemical Society.

Detailed structural and spectroscopic studies lead to the conclusion that the emission changes induced by concentration and temperature variation are due to the formation of aggregates (dimers, trimers, and higher oligomers) of emissive gold(I) complexes. Thus it appears that aurophilic attractions can overcome the Coulomb repulsion between individual cationic complexes. This can lead to the formation of a band of orbitals made from overlapping (filled) 5d$_{z2}$ orbitals of interacting Au(I) centers and a corresponding unoccupied band made from 6p$_z$ orbitals of gold. The X-ray crystal structure of **83**PF$_6$·0.5(Me$_2$CO) features extended columns of cations with an Au(I)-Au(I) separation of only 3.1882(1) Å. Hydrogen-bonding interactions between the emissive cations and the anions could potentially play an important role for the emission properties, at least this would explain the observable differences between **83**PF$_6$ and **83**BF$_4$. The observation of a hydrogen-bonding network in the abovementioned crystal structure supports this interpretation.

The [(cyclohexyl-isocyanide)$_2$Au](PF$_6$) compound (**85**PF$_6$) exhibits similarly spectacular solvoluminescence behavior as the carbene compounds **83**PF$_6$, **83**BF$_4$, and **84**PF$_6$.[150] A colorless

polymorph of the isocyanide compound **86**PF$_6$ exhibits linear chains with regular Au(I)-Au(I)

distances of 3.1822(3) Å, whereas the structure of a yellow polymorph is more complicated with

4 independent Au(I)-Au(I) contacts ranging from 2.9643(6) to 2.9803(6) Å. Such distances are

clearly on the short end of known aurophilic interactions.[28]

Scheme 35. A vapochromic Cu(I)-Au(I)-Cu(I) complex (**86**$^{3+}$) and its reaction product (**87**$^{3+}$)

after exposure to MeOH vapor.
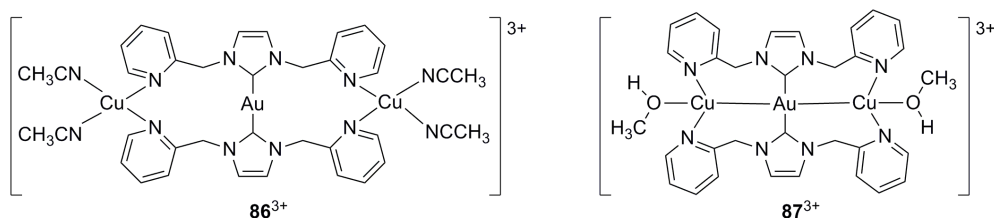
The heterotrinuclear Cu(I)-Au(I)-Cu(I) complex **86**$^{3+}$ (Scheme 35) is one out of comparatively

few vapochromic substances in which the VOC-induced color change is a direct consequence of

a ligand exchange reaction.[169] This complex formed by addition of [Cu(CH$_3$CN)$_4$](PF$_6$) to an

acetonitrile solution of the gold(I) imidazole (im) complex [Au(im(CH$_2$-py)$_2$)$_2$](PF$_6$) which has

pendant pyridine (py) units that can bind to copper(I). The intermetallic distances are long (~ 4.6

Å) and presumably repulsive. Single crystals of **86**(PF$_6$)$_3$ grown from acetonitrile solution

contain two lattice CH$_3$CN molecules which are lost upon evacuation or prolonged exposure to

air, resulting in solvent-free and blue photoluminescent **86**(PF$_6$)$_3$. Subsequent exposure of dry

86(PF$_6$)$_3$ to methanol, H$_2$O, or acetone causes a change in luminescence color from blue to green

(Figure 43). THF and CH$_2$Cl$_2$ do not induce any change in emission behavior. Crystallization of

the trinuclear complex from MeOH/Et$_2$O mixture directly yields the green emitting compound,

which has been identified as **87**(PF$_6$)$_3$. X-ray diffraction on single crystals of **87**(PF$_6$)$_3$ reveals the

presence of short (2.7915(7) Å) Au(I)-Cu(I) distances. This attractive interaction between

individual metals is likely the consequence of the replacement of two CH_3CN molecules per

Cu(I) center by only one methanol ligand, making one coordination site of the tetrahedral

copper(I) centers available for metal-metal bonding. Compound **87**$(PF_6)_3$ can be converted to

86$(PF_6)_3$ by exposure to CH_3CN vapor, i. e., the vapoluminescence is reversible.
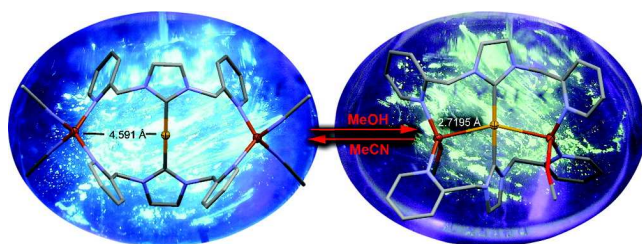
Figure 43. Crystal structures and emission colors of complexes **86**$^{3+}$ and **87**$^{3+}$. Reprinted with

permission from ref. [169]. Copyright 2010 American Chemical Society.

Scheme 36. A cationic gold(I) complex whose vapochromic properties strongly depend on the

counter-anion.
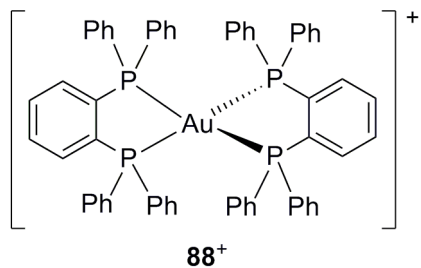
The tetrahedral gold(I) complex $[Au(dppb)_2]^+$ (**88**$^+$) (Scheme 36) with two bidentate dppb

(dppb = 1,2-bis-(diphenylphosphino)benzene) ligands was isolated   with seven different

anions.[170] Small anions such as NO_3^-, Cl^- or BF_4^- permit symmetrical coordination of the two

dppb ligands to the Au(I) center in the crystal lattice, resulting in blue phosphorescence for

88NO$_3$ (Figure 44), **88**Cl, and **88**BF$_4$. Larger cations (e. g., PF$_6$ or B(4-C$_6$H$_4$F)$_4^-$) enforce small

conformational changes of the dppb ligands in the solid state, resulting in yellow-orange

phosphorescence for **88**PF$_6$ and **88**B(4-C$_6$H$_4$F)$_4$. The nitrate salt is a vapoluminescent substance

(Figure 44).[170] Solid **88**NO$_3$ emits blue light, and the luminescence spectrum is similar to that of

free dppb, indicative of ligand-localized phosphorescence (τ = 3.3 μs). Exposure of

microcrystalline **88**NO$_3$ to vapors of ethanol and methanol leads to a rapid change in emission

color from blue to orange-yellow (Figure 44), but longer alcohols trigger no response. The

respective solvent adducts (**88**NO$_3$·2EtOH and **88**NO$_3$·3MeOH) were characterized by single

crystal X-ray diffraction and were found to contain structurally distorted [Au(dppb)$_2$]$^+$ units

similar to what has been noted above for larger anions. When heating the solvent adducts to 100

°C for ~20 minutes, blue-emitting neat **88**NO$_3$ is restored.
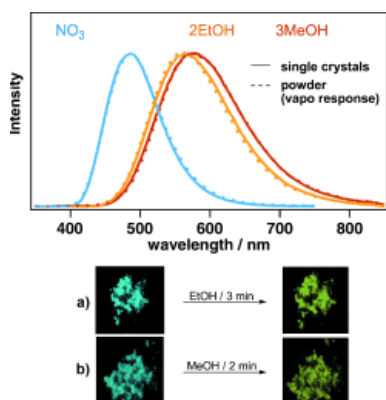
Figure 44. Vapochromic response of **88**NO$_3$ to ethanol and methanol. (M. Osawa, I. Kawata, S.

Igawa, M. Hoshino, T. Fukunaga, D. Hashizume: Vapochromic and Mechanochromic

Tetrahedral Gold(I) Complexes Based on the 1,2-Bis(diphenylposphino)benzene Ligand. *Chem.*

Eur. J., 2010, *16*, 12114-12126. Copyright Wiley-VCH Verlag GmbH & Co. KGaA. Reproduced with permission.)

The tetrafluoroborate salt of **88**$^+$ exhibits mechanochromism.[170] Upon extensive grinding the emission color eventually changes from blue to yellow-orange, suggesting that a conformational change of the [Au(dppb)$_2$]$^+$ complex can be induced mechanically. Ground **88**BF$_4$ is vapoluminescent and exhibits the reverse emission color change following exposure to vapors of acetone, acetonitrile, CH$_2$Cl$_2$, diethyl ether, and THF.

A referee of this review article speculated that the cations in some of the emissive salts formed with **88**$^+$ have gold(I) only in a three-coordinate state, because luminescence is a common phenomenon for three-coordinate Au(I) but almost unknown for four-coordinate Au(I). Potentially, a hydrogen bond from an alcohol to an anion or to a phosphorus atom can give rise to structural changes, and mechanical stress might cause a flattening of the cations from a quasi-tetrahedral structure.

4. Compounds with metals other than platinum or gold

Most of the platinum compounds and many of the gold materials from the previous two sections are type I vapochromic systems according to the definition used in section 1.3, i. e., changes in weak intermolecular interactions (e. g., metal-metal interactions, π-stacking, hydrogen-bonding, or C-H-π interactions) as a result of analyte uptake trigger the vapochromic response. This common theme and the large number of platinum and gold based vapochromic

substances compared to other VOC-sensitive materials provided the rationale for grouping them into two separate sections.

Section 4 contains many 3d metal complexes which are inherently more labile than complexes of 4d or 5d elements. As a consequence type II vapochromic behavior, defined in section 1.3 as the vapochromism or vapoluminescence response triggered by analyte-induced changes in the first coordination sphere of the metal, is a unifying theme for many of the VOC-sensitive materials in this section. Specifically, this encompasses roughly 20 compounds which are treated in subsection 4.1, sorted along the metal component from vanadium to cobalt, nickel, copper, and tin; an additional short chapter on metalloporphyrins with various metal centers concludes this subsection on type II vapochromic materials containing metals other than Pt or Au. In the majority of the compounds presented in section 4.1, vapochromism is a *direct* consequence of changes in the ligand field around the metal leading to significant changes in the d-d and/or MLCT absorptions.

Subsection 4.2 contains about 15 coordination compounds in which the vapochromism is the result of changes in weak intermolecular interactions. As a matter of fact, the origin of the vapochromism in these 15 type I materials is quite diverse, and the identification of common themes for the different classes of materials presented in this subsection is rather difficult; an attempt to do so has resulted in the division of subsection 4.2 into 5 individual chapters.

4.1 Vapochromism as a result of analyte-induced changes in the first coordination sphere of the metal

4.1.1 A vanadium complex

1
2
3
4
5
6
7
8
9
10
11
12
13
14
15
16
17
18
19
20
21
22
23
24
25
26
27
28
29
30
31
32
33
34
35
36
37
38
39
40
41
42
43
44
45
46
47
48
49
50
51
52
53
54
55
56
57
58
59
60

Scheme 37. A vapochromic oxovanadium(IV) complex.

89
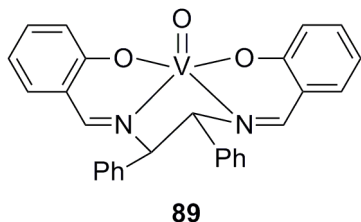
The oxovanadium(IV) complex **89** (Scheme 37) is the only vapochromic vanadium complex known to date.[171] Green crystals are obtained from chloroform solution (**89**·CHCl$_3$) whereas recrystallization from acetonitrile affords orange crystals (**89**·CH$_3$CN). The two forms can be converted into one another and contain either monomeric complexes or polymeric chains thereof.[172-174] In the monomeric green form, the vanadium(IV) center is in square-pyramidal coordination with the V=O group in apical position, in the orange form the vanadyl oxygen atom of one complex ligates to the sixth coordination site of the neighboring vanadium center, resulting in an infinite -V=O-V=O- chain. The polymeric acetonitrile adduct (**89**·CH$_3$CN) contains two independent molecules per unit cell with V=O bond distances of 1.625(5) and 1.636(5) Å, the distances between the vanadium center and the oxygen atom of a neighboring vanadyl group are 2.188(5) and 2.196(5) Å. When exposing orange crystals of **89**·CH$_3$CN to chloroform vapor they turn green (Figure 45). Conversely, green crystals of **89**·CHCl$_3$ change color to orange when exposed to acetonitrile vapor. Due to changes in V=O stretching frequencies the interconversion between the two forms can also be detected by IR spectroscopy. Another interesting observation is the occurrence of mechanochromism in the orange form: Grinding of **89**·CH$_3$CN affords a green powder, and subsequent addition of a small volume of

CH₃CN regenerates the initial orange material. Thermochromism is observed for the green form

as it turns orange when heated to 120 °C for a few minutes. [171]
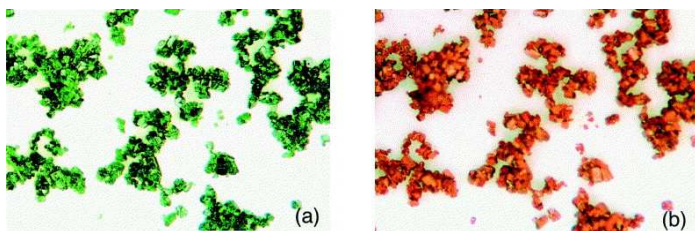
Figure 45. Vapochromism of compound **89** observed following exposure to CH₃CN (green to

orange) or CHCl₃ (orange to green). Reprinted with permission from ref. [171]. Copyright 2003

Elsevier.

4.1.2 Cobalt complexes

Cobalt(II) complexes are known to undergo relatively facile inter-conversion between

octahedral and tetrahedral coordination geometries accompanied by drastic color changes.[175]

This property forms the basis of the vapochromic behavior of a few compounds in which

octahedral clusters of $[Re_6S_8(CN)_6]^{4-}$ or $[Re_6Se_8(CN)_6]^{4-}$ connect partially hydrated Co(II)

complexes in extended solid frameworks with porous structures.[176] The crystal structure of

$[Co_2(H_2O)_4][Re_6S_8(CN)_6]\cdot 12H_2O$ (**90**$\cdot$12H₂O) exhibits a three-dimensional network comprised of

$[Re_6S_8]^{2+}$ and $[Co_2(\mu-OH_2)_2]^{4+}$ cations linked by cyanides (Figure 46).
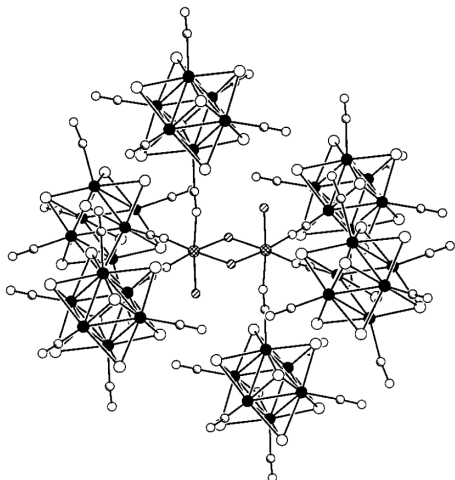
Figure 46. Extract from the crystal structure of (**90**·12H$_2$O) showing the [Co$_2$(μ-OH$_2$)$_2$] in the middle and the [Re$_6$S$_8$]$^{2+}$ clusters around it. Reprinted with permission from ref. [176]. Copyright 2000 American Chemical Society.

The Co(II) ions are in *fac*-configuration with three N-atoms from cyanide and three water ligands, each Re$_6$ moiety is in turn connected to six Co$_2$ clusters yielding a Prussian blue type structure. The relatively large size of the [Re$_6$S$_8$]$^{2+}$ and [Co$_2$(μ-OH$_2$)$_2$] cations entails the formation of large cube-like cages within the Prussian blue type structure comprising a volume of 258 Å^3. Each of these cages contains 6 water molecules. The structure of [Co(H$_2$O)$_3$]$_4$[Co$_2$(H$_2$O)$_4$][Re$_6$Se$_8$(CN)$_6$]$_3$·44H$_2$O (**91**·44H$_2$O) contains a mixture of isolated Co(II) complexes with octahedral coordination and [Co$_2$(μ-OH$_2$)$_2$]$^{4+}$ clusters which are linked via cyanide to the [Re$_6$Se$_8$]$^{2+}$ units. All framework atoms together occupy only 56% of the total volume of this structure hence the large content of crystal water. Exposure of **90**·12H$_2$O or **91**·44H$_2$O to vapors of diethyl ether leads to a rapid change in color from orange to blue-violet and blue, exposure to THF induces a change to violet or green (Figure 47).

Figure 47. Powder samples of **90**·12H$_2$O (upper line) and **91**·44H$_2$O (lower line) treated with water (as prepared), THF, and diethyl ether (from left to right). Reprinted with permission from ref. [176]. Copyright 2000 American Chemical Society.

A range of VOCs influence the absorption properties of these two compounds, but diethyl ether leads to the most rapid response. For **90**·12H$_2$O substantial color changes are detected by the naked eye for nitromethane, THF, acetone, propionitrile, *n*-octanol, *n*-propanol, ethyl acetate, isopropanol, and diethyl ether. For **91**·44H$_2$O the most important color changes occur upon exposure to vapors of triethylamine, acetonitrile, THF, EtOH, DMF, acetone, propionitrile, *n*-octanol, methyl *tert*-butyl ether, ethyl acetate, *n*-propanol, isopropanol, and diethyl ether. The changes in the optical absorption spectrum following VOC exposure are fully consistent with inter-conversion of some or all of the Co(II) ions from octahedral to tetrahedral coordination geometry. Specifically, one observes the characteristic $^4T_1(F) \leftarrow {}^4A_2$ and $^4T_1(P) \leftarrow {}^4A_2$ transitions of tetrahedral $e^4t_2^3$ species. As far as the mechanism of this conversion is concerned, it has been proposed that VOCs enter the cavities and channels of compounds **90**·12H$_2$O and **91**·44H$_2$O, thereby disrupting the hydrogen-bonding network which stabilizes the octahedral coordination of Co(II). With bulkier VOC molecules present, labile water ligands are released and the tetrahedral coordination geometry is adopted.

Reaction of CoSO$_4$·7H$_2$O with the N,N'-ditopic 2-aminopyrazine (ampyz) ligand in aqueous solution gives a coordination framework with the composition [Co(H$_2$O)$_4$(ampyz)$_2$][Co(H$_2$O)$_6$](SO$_4$)$_2$(H$_2$O)$_2$ (**92**).[177] Intermolecular hydrogen-bonding and π-π interactions lead to the formation of 2D sheets with the sulfate anion playing a key role as a structural element. In diffuse reflectance one detects d-d absorptions of high-spin Co(II) at ~9000 cm^{-1} and 19500 – 22000 cm^{-1} due to $^4T_{2g} \leftarrow {}^4T_{1g}$ and $^4T_{1g}$ (P) $\leftarrow {}^4T_{1g}$ transitions. When heating compound **92** to 220 °C, a color change from orange to purple occurs, accompanied by a loss in crystallinity due to collapse of the supramolecular framework. The color change is most likely the result of a change in the coordination environment of the Co(II) centers, leading to shifts of the d-d absorption bands. Thermogravimetric analysis reveals that the resulting material has the composition [Co$_2$(ampyz)$_2$](SO$_4$)]. Exposure of the dehydrated compound to laboratory air during 8 hours restores the initial orange crystalline material. An isostructural Fe(II) compound and a mixed Co(II)/Fe(II) compound exhibit similar behavior, but their water-vapor sensing properties are less favorable because the color changes occurring upon water uptake are minor.[177]

4.1.3 Nickel complexes

Scheme 38. A vapochromic Ni(II) complex (**93**) and its reaction product with acetonitrile (**94**).
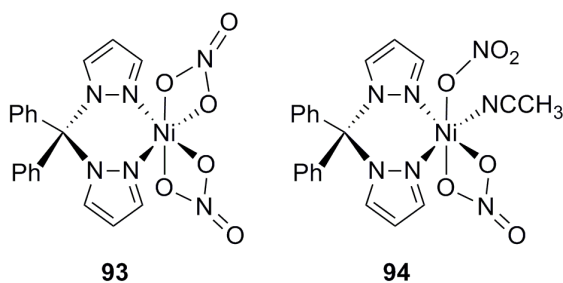
A nickel(II) complex with a chelating diphenyl(dipyrazolyl)methane and two nitrate ligands (**93**) (Scheme 38) shows enough flexibility in its coordination sphere that one of the nitrates can undergo a change in hapticity from η^2 to η^1 as a function of temperature or acetonitrile vapor pressure.[178] This ability makes complex **93** a thermochromic and vapochromic substance because the conversion of **93** into **94** is associated with a color change from green to blue. Shifts in d-d absorption bands due to electronic transitions from the $^3A_{2g}$ ground state to $^3T_{2g}$, $^3T_{1g}$ (^3F), and $^3T_{1g}$ (^3P) excited states are responsible for this change in color. The nitrate hapticity switch is further associated with a change in the IR spectrum. Complexes **93** and **94** were both characterized structurally, and their most notable feature is the small bite angle of the bidentate nitrate ligands leading to *cis*-O-Ni-O angles of about 62°, causing significant distortions from the ideal octahedral geometry. The vapor-induced conversion from **93** to **94** can be reversed by heating to 100 °C for a few minutes. The formation of the η^2 complex is favored at higher temperatures due to entropic effects associated with the release of CH_3CN and chelation of the nitrate ligand.

Scheme 39. Vapochromic Ni(II) complexes.

95

96^{2+}
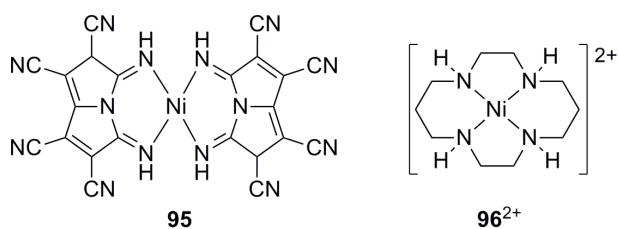
The bis(pyrrolizinato)nickel(II) complex **95** (Scheme 39) acts as a vapochromic substance in polyvinylbutyral (PVB) matrices.[179] The initially prepared spin-coated film containing about

0.02 moles of **95** per liter of PVB is light blue but changes to colorless on heating to 90 °C for a few minutes. The colorless state persists at room temperature unless the films are exposed to vapors of various VOCs with alcohols triggering the most rapid response and manifesting in the appearance of an absorption maximum at 661 nm. It is believed that the blue form of **95** is in fact an octahedral complex with two solvent molecules completing the coordination sphere of Ni(II) whereas the colorless form corresponds to the four-coordinate NiN$_4$ complex represented by structure **95**. The selectivity for alcohols has been attributed to their coordinating ability, the poor response to acetonitrile vapor has been explained by the observation that this solvent shows little tendency to coordinate to **95** even in solution. Curiously, toluene triggers a vapochromic response as well, but this has been ascribed to the affinity of the PVB matrix for this particular solvent.
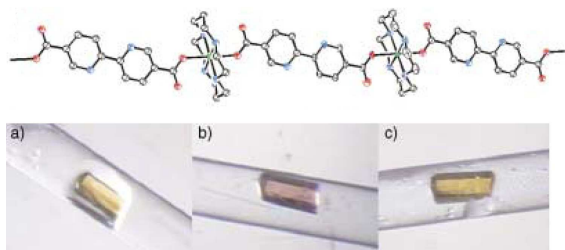
Figure 48. Top: 1D chain structure of [Ni(cyclam)]$^{2+}$ and 5,5'-dcbpy^{2-}. Bottom: (a) Crystal of [Ni(cyclam)(dcbpy)]·5H$_2$O in the mother liquor; (b) same crystal after evacuation at 150°C; (c) same crystal after subsequent exposure to water vapor. (E. Y. Lee, M. P. Suh: A Robust Porous Material Constructed of Linear Coordination Polymer Chains: Reversible Single-Crystal to Single-Crystal Transformation upon Dehydration and Rehydration. *Angew. Chem. Int. Ed.*, 2004, *43*, 2798-2801. Copyright Wiley-VCH Verlag GmbH & Co. KGaA. Reproduced with permission.)

The [Ni(cyclam)]$^{2+}$ complex (**96^{2+}**) and 2,2'-bipyridine-5,5'-dicarboxylate (5,5'-dcbpy^{2-}) form together a robust metal-organic open framework of composition [Ni(cyclam)(dcbpy)]·5H$_2$O which is able to undergo reversible single crystal to single crystal transformations.[180] The Ni(II) center is octahedrally coordinated with axial 5,5'-dcbpy^{2-} ligands binding in monodentate fashion and resulting in a linear coordination polymer chain (Figure 48). Individual chains are linked to each other through C-H-π interactions involving a carbon atom of the macrocycle and the pyridyl rings of 5,5'-dcbpy^{2-}. When heating single crystals of [Ni(cyclam)(dcbpy)]·5H$_2$O to 150 °C under 10^{-5} Torr for several hours there is a color change from yellow to pink. The packing of the porous framework stays intact, and it appears that the C-H-π interactions are largely responsible for this. The Ni-O(carboxylate) bonds shorten by 0.025 Å upon dehydration which may be responsible for the observed color change. In this sense, complex **96^{2+}** is not a clear type II vapochromic substance (according to the definition used in section 1.3), yet the metal-ligand bond length change is clearly a significant modification of the first coordination sphere of the metal center. When exposing the pink dehydrated crystals to air the yellow color is restored within minutes with retention of single crystallinity.

4.1.4 Copper complexes

When adding excess 4-picoline (4-pic) to a solution of CuI in concentrated aqueous KI one obtains the material [CuI(4-pic)]$_\infty$ (**97**) which crystallizes in a double-zigzag configuration with -Cu(I)-I-Cu(I)- connections propagating along the crystallographic b axis (Figure 49). The shortest Cu(I)-Cu(I) distances in this compound are 2.8087(8) Å,[181, 182] and this polymeric

material is blue photoluminescent (λ_{max} = 437 nm) due to the presence of an emissive XLCT (halogen-to-ligand charge transfer) state.[20] When exposing it to toluene vapors in a sealed vial for 2 days, it converts into [CuI(4-pic)]$_4$·2C$_6$H$_5$CH$_3$ (**98**·2C$_6$H$_5$CH$_3$). The tetrameteric copper(I) species of the toluene adduct exhibits comparatively short Cu(I)-Cu(I) distances ranging from 2.651 to 2.735 Å, and the yellow emission of this compound (λ_{max} = 580 nm) has been attributed to a cluster-centered (^{3}CC) electronic transition.[20] The incorporation of toluene molecules permits arrangement of the tetrameric units into chains without leaving too many voids between them, and this fact presumably facilitates the conversion of [CuI(4-pic)]$_4$·2C$_6$H$_5$CH$_3$ back to [CuI(4-pic)]$_\infty$ occurring upon exposure to pentane vapor, simply because the copper units are already pre-arranged into chains. It has been noted that for practical sensing applications the slowness of the VOC-induced chemical conversions between **97** and **98**·2C$_6$H$_5$CH$_3$ is a problem.
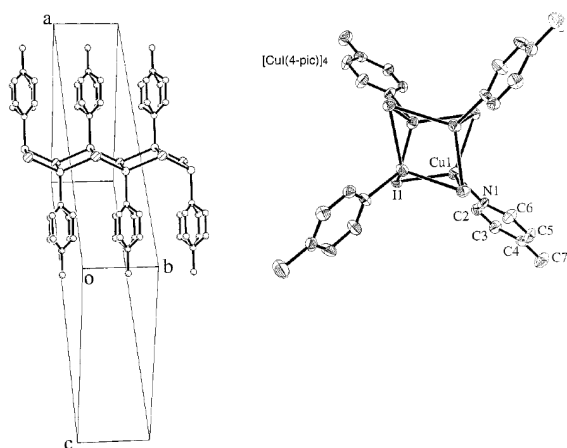
Figure 49. Left: Polymer chain of [CuI(4-pic)]$_\infty$ (**97**) propagating along the b-axis. Right: Structure of the [CuI(4-pic)]$_4$ (**98**) cluster. Reprinted with permission from ref. [180]. Copyright 2000 American Chemical Society.
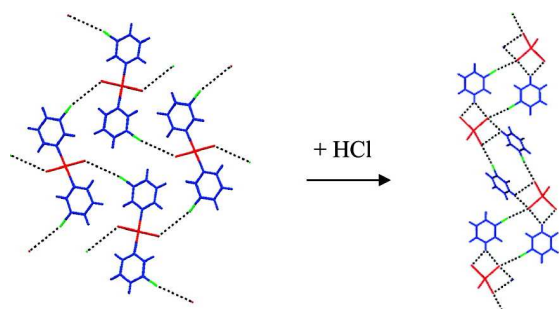
Figure 50. 2D network of compound **99** (with square-planar Cu(II)) and 1D network of compound **100** (with tetrahedral Cu(II). Reprinted with permission from ref. [182]. Copyright 2007 American Chemical Society.

Reaction of $CuCl_2$ and 3-chloropyridine (3-Clpy) in methanol solution affords the charge-neutral coordination compound *trans*-$[CuCl_2(3\text{-}Clpy)_2]$ (**99**) in which the copper(II) center is in square planar coordination.[183, 184] This material is blue and reacts with gaseous HCl to form the yellow salt $(3\text{-}ClpyH)_2[CuCl_4]$ (**100**) in which Cu(II) is tetrahedrally coordinated. This vapor-induced conversion is remarkable because it not only involves cleavage of two Cu-N coordination bonds but also the rupture of the covalent H-Cl bonds to form two new Cu-Cl and N-H bonds. The crystal structure changes from a 2D-network propagated via Cu-Cl – Cl-C halogen bonds (**99**) (Figure 50) to a 1D-network propagated via N-H – Cl_2Cu hydrogen bonds and Cu-Cl – Cl-C halogen bonds (**100**). HCl uptake has been monitored by FTIR spectroscopy from which an equilibrium constant of $1.03(5)\cdot10^{-5}$ was determined, indicating good sensitivity for HCl detection in the 200 – 20000 ppm concentration range. Temperature dependent FTIR studies show that HCl extrusion is endothermic. X-ray diffraction at a synchrotron facility was used to search for intermediate crystalline phases present at small concentrations but occurring in the process of interconversion between **99** and **100**. However, no such phase could be found and

Rietveld analysis of X-ray powder patterns gave an excellent fit to a two-phase model without

the need for involvement of an intermediate (amorphous) phase. This study shows that the

molecular solid state can be far more flexible and dynamic that it is generally perceived to be.[183,]

[184]
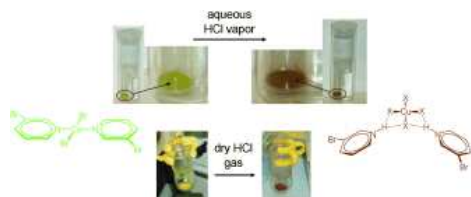
Figure 51. Reaction of *trans*-[CuBr$_2$(3-Brpy)$_2$] (**101**) to (3-BrpyH)$_2$[CuBr$_2$Cl$_2$] (**102**). (G.

Mínguez Espallargas, J. van de Streek, P. Fernandes, A. J. Florence, M. Brunelli, K. Shankland,

L. Brammer: Mechanistic Insights into a Gas-Solid Reaction in Molecular Crystals: The Role of

Hydrogen Bonding. *Angew. Chem. Int. Ed.*, 2010, *49*, 8892-8896. Copyright Wiley-VCH Verlag

GmbH & Co. KGaA. Reproduced with permission.)

Subsequent related work focused on the isostructural *trans*-[CuBr$_2$(3-Brpy)$_2$] (**101**) complex

and its reaction with gaseous HCl.[185] This study provided significant new insight into the

mechanism of HCl uptake. One important observation is that upon conversion of green **101** to

brown (3-BrpyH)$_2$[CuBr$_2$Cl$_2$] (**102**) (Figure 51) the initially present bromo-ligands are not lost. It

has been hypothesized that insertion of HCl into Cu-N bonds of **101** is followed by a structural

reorientation of the [CuBr$_2$Cl$_2$]$^{2-}$ anions which is driven by the formation of hydrogen bonds and

halogen bonds. Indeed it was found that the chloride population of a given crystallographic site

correlates with the total number of strong intermolecular interactions formed, either hydrogen or

halogen bonds. Thus, the hypothesis from above makes sense because the respective noncovalent

(and mainly electrostatically driven) interactions are expected to be stronger with chloride than with bromide due to the more negative electrostatic potential of Cl⁻. Methodologically, the reaction of *trans*-[CuBr$_2$(3-Brpy)$_2$] with HCl resembles isotope labeling experiments only that Cl and Br exhibit sufficiently different X-ray scattering power that differentiation of the two halides becomes easily possible with X-ray diffraction.

Green *trans*-[CuBr$_2$(3-Brpy)$_2$] (**101**) reacts with HBr to brown (3-BrpyH)$_2$[CuBr$_4$], but this material has a different crystallographic structure with different supramolecular connections than **100** and **102**.[186] However, release of HBr from (3-BrpyH)$_2$[CuBr$_4$] or HCl from **100/102** leads to an isostructural series of compounds.

Scheme 40. Vapochromism based on ligand flip isomerization.
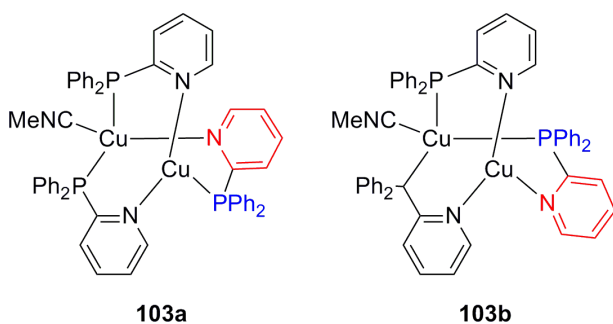
An interesting case of linkage isomerism has been reported for [Cu$_2$(dppy)$_3$(CH$_3$CN)](BF$_4$)$_2$ (dppy = diphenylphosphino-pyridine) (Scheme 40).[187] This binuclear complex has its dppy ligands arranged in head-to-tail fashion with two phosphorus atoms binding to one copper(I) center and the third to the other one (**103a**). Recrystallization of **103a** from a mixture of CH$_2$Cl$_2$ and CH$_3$OH affords the methanol adduct (**103b**·CH$_3$OH) which has one of its dppy ligands flipped, resulting in head-to-head orientation of all three ligands. Because of the hemilability of

the dppy ligand it is further possible to convert blue photoluminescent **103a** (λ_{max} = 489 nm) into green emissive **103b·CH₃OH** (λ_{max} = 520 nm) by exposure of solid **103a** to methanol vapor, and this process can be fully reversed when heating the methanol adduct to 203 °C. The linkage isomerization reaction is accompanied by a significant increase of the Cu(I)-Cu(I) separation from 2.721(3) Å in **103a** to 2.7961(4) Å in **103b·CH₃OH** and by an increase of π-π interactions manifesting by short distances between the phenyl and pyridyl planes in the methanol adduct. These two structural changes are most likely jointly responsible for the shift in emission wavelength upon CH₃OH uptake.

Scheme 41. A copper complex exhibiting concentration lumichromism.

104
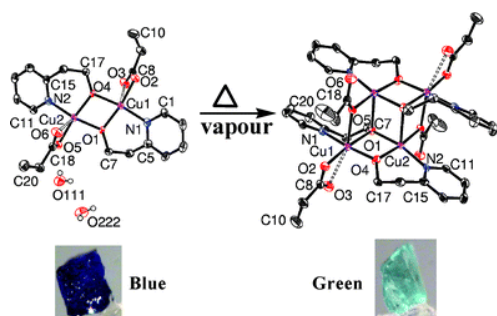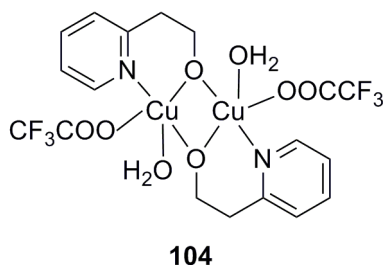
Figure 52. Conversion of dimeric blue **104·2H₂O** to a tetrameric green product. Copyright 2010 The Royal Society of Chemistry.

A dinuclear copper(I) complex with 2-(2-hydroxyethyl)pyridine (μ-hep) and *n*-propionate (O^{n}Pr) ligands (**104**) shows the unusual phenomenon of a vapor-induced single crystal to single crystal transformation.[188] Initially the [(O^{n}Pr)Cu(μ-hep)$_2$Cu(O^{n}Pr)] complex is obtained as a di-hydrate (**104**·2H$_2$O). When heated to 110 °C this blue compound releases water and undergoes a structural change to a green tetrametric complex under retention of its crystallinity (Figure 52). The tetramer has the structure of a double open cubane. The same structural conversion can be induced at room temperature when exposing **104**·2H$_2$O to various VOCs, albeit with different response times. Whereas CH$_3$OH produces a response within 5 minutes, ethanol, isopropanol, and acetonitrile require exposure times of 2 hours, 24 hours, and 8 days, respectively. In view of the fact that multiple bond breaking and bond making processes must occur, this structural conversion in the single crystalline state is remarkable. However, the overall process is irreversible. Analogous compounds with acetate instead of *n*-propionate were also investigated but did not show vapochromic behavior.[188]
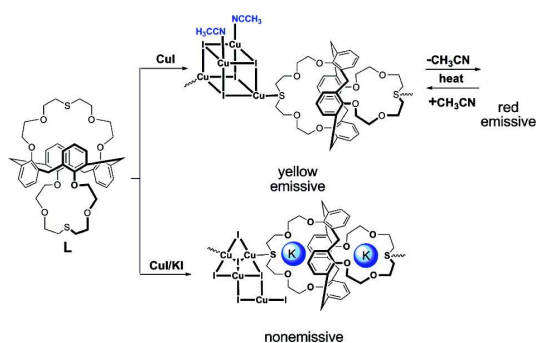
Figure 53. Reactivity and luminescence behavior of [(Cu$_4$I$_4$)L(CH$_3$CN)$_2$]$_n$ (**105**·(CH$_3$CN)$_2$). Reprinted with permission from ref. [189]. Copyright 2008 American Chemical Society.

Reaction of a calix[4]-*bis*-monothiacrown (L) with CuI in acetonitrile leads to the formation of a 1D polymeric material with the formulation $[(Cu_4I_4)L(CH_3CN)_2]_n$ (**105·(CH_3CN)_2**) (Figure 53).[189] It contains cubane-like Cu_4I_4 clusters which are linked to one another by the calix[4]-*bis*-monothiacrown ligands through two of the four Cu(I) ions, while the two other metal centers bear acetonitrile ligands. The yellow photoluminescence of compound **105** (λ_{max} = 567 nm) was assigned to a cluster-centered excited state with admixed halide-to-metal charge transfer (XLCT) character. Addition of KI leads to the incorporation of K^+ ions into the thiacrowns, a process which is accompanied by emission quenching, perhaps because of η^5-type cation – π interactions. When heating potassium-free samples to 150 °C for 1 hour the acetonitrile ligands are released, producing a red photoluminescent (λ_{max} = 600 nm) compound. Bulk crystallinity is maintained and thus the process is reversible, manifesting in a vapoluminescence response upon exposure of the de-solvated material to CH_3CN.

Six different coordination compounds have been isolated as products from the reaction between CuI and triphenylphosphine (PPh_3).[190] One out of two cubane-type polymorphs with the stoichiometry $[CuI(PPh_3)_4]$ (**106a**) converts to an isomer when exposed to vapors of acetonitrile, dichloromethane or ethanol. In the product (**106b**), two opposite edges of the cubane-like structure are broken up, and a molecular structure resembling that of cyclooctane is formed. Compound **106a** emits green light (λ_{max} = 518 nm, τ = 3.2 μs) upon UV excitation at room temperature whereas its isomer **106b** is essentially nonluminescent under these conditions, paving the way to vapor-induced luminescence on/off switching.

Copper(I) cyanide (**107**) reacts with a variety of different amines (both in the liquid and vapor phase) to produce adducts of the stoichiometry $CuCN·L_n$ with n = 0.75 – 2.0.[191-193] Neat CuCN emits at the edge of the visible spectral range with λ_{max} = 392 nm, but the solvent adducts

luminesce with different colors throughout the visible spectral range with λ_{max} depending on the exact nature of the amine (L) (Figure 54).[191] The CuCN·L$_n$ adducts can be obtained on the preparative scale by heating CuCN suspensions in neat amines and hence can be characterized structurally. Single crystals suitable for X-ray diffraction were obtained with L = pyridine, 2-methylpyridine, 4-methylpyridine, 3-ethylpyridine, 4-(*t*-butyl)pyridine, piperidine, *N*-methylmorpholine, and *N,N*-dimethylcyclohexane. Each of these structures contains chains of CuCN with the cyano C/N positions disordered in most cases, and in each structure (except for CuCN·4-(*t*-butyl)pyridine) the amine is directly bonded to copper(I). Depending on the amine content (n), the Cu(I) centers are either 3- or 4-coordinate. The photoluminescence behavior of these authentic solvent adducts is identical to that observed for samples of CuCN that have been exposed to vapors of the respective amines. However, powder X-ray diffraction reveals that only a fraction of vapor-exposed CuCN reacts to the adduct CuCN·L$_n$, and thus it seems that only the surface of CuCN is able to react with the amine vapors. This interpretation is compatible with the high reversibility of the vapoluminescent response. Based on DFT calculations the HOMO of the CuCN·L$_n$ compounds is mostly comprised of the $3d_{z2}$ orbital of the metal while the LUMO is a mixture of 4p orbitals of Cu(I) and π* orbitals of the cyano ligand,[194] and consequently it might be argued that the emission has mixed d-d and MLCT character.
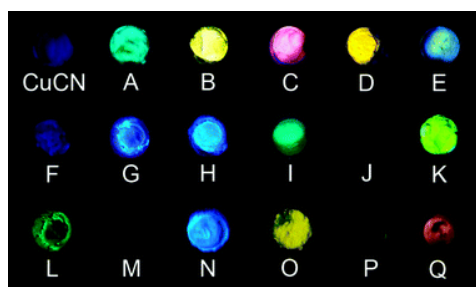
Figure 54. Luminescence of neat CuCN (upper left) and various solvent adducts of CuCN (A-Q). Copyright 2010 The Royal Society of Chemistry.

The reaction of CuI with selected *N,N'*-disubstituted piperazines (pip) in acetonitrile yields $(CuI)_2(pip)$ compounds consisting of chains with piperazine-linked Cu_2I_2 rombs.[195] These structures with 3-coordinate Cu(I) are obtained only for sterically crowded *N,N'*-diethylpiperazine (Et$_2$pip), *N,N'*-dibenzylpiperazine (Bnpip), *N,N'-bis*-phenylethylpiperazine (PhEtpip), producing compounds $(CuI)_2(Et_2pip)$ (**108a**), $(CuI)_2(Bn_2pip)$ (**108b**), and $(CuI)_2((PhEt)_2pip)$ (**108c**), whereas sterically less demanding piperazines lead to structures with 4-coordinate Cu(I). The Cu(I)-Cu(I) distances in **108a-c** range from 2.4716(11) to 2.4837(14) Å and are significantly below the van der Waals distance (~2.80 Å), indicative of substantial metallophilic interactions. Exposure of **108a** and **108b** to vapors of amine and sulfide nucleophiles (Nu) leads to brightly photoluminescent materials which show identical luminescence properties as the respective $(CuI)_4(Nu)_4$ compounds, suggesting that Nu vapor exposure induces the reaction 2 $(CuI)_2(pip)$ + 4 Nu → $(CuI)_4(Nu)_4$ + 2 pip. Depending on the nucleophile, luminescent materials with emission colors ranging from blue (Nu = 2-methylpyridine) to red (Nu = morpholine) are obtained. Other nucleophiles which give a vapoluminescence response are pyridine, 3-methylpyridine, , piperidine, pyrrolidine, pyrrolidine, diethylamine, dimethyl sulfide.[195] Vapors of 2-chloropyridine, 3-chloropyridine, and *N*-methylpiperidine yield non-emissive compounds.

4.1.5 Tin

Four commercial tin(II) salts were found to be useful for optical sensing of amine vapors at concentrations as low as 100 ppb.[196] Specifically, tin(II) sulfate (SnSO$_4$, **109a**), tin(II) methanesulfonate (Sn(CH$_3$SO$_3$)$_2$, **109b**), tin(II) triflate (Sn(OTf)$_2$, **109c**), and tin(II) fluorophosphate (SnPO$_3$F, **109d**) were found to display visible room temperature emission after exposure to vapors of NH$_3$, EtNH$_2$, Et$_2$NH, Et$_3$N, or N(C$_5$H$_5$)$_3$. Importantly, each of the four tin(II) salts responds differently to the five amines, and consequently similar analytes can be distinguished from each other rather easily. Many other nucleophilic analytes have little impact on the emission properties, but it has been noted that for real-world applications the water-sensitivity of several of the tin(II) salts is problematic. For instance the emission intensity of amine-vapor exposed Sn(CH$_3$SO$_3$)$_2$ and Sn(OTf)$_2$ drops considerably in presence of atmospheric humidity. The fundamental reasons for the luminescence turn-on response in presence of amines is unclear,[196] it was merely noted that tin(II) is known to form complexes with amine-containing molecules.[197, 198]

4.1.6 Metalloporphyrins

Due to their intense colors and the presence of axial binding sites metalloporphyrins are of interest for sensing of coordinating VOCs. An application-oriented study falling into the category of "electronic nose" research made use of arrays containing 11 different tetraphenylporphyrin-based compounds for achieving chemoselective vapor visualization. The tetraphenylporphyrin was either used as a free base, or with Sn(IV), Co(III), Cr(III), Mn(III), Fe(III), Co(II), Cu(II), Ru(II), Zn(II) and Ag(II).[199] These metals span a wide range of ligand affinity which opens the possibility for obtaining unique color fingerprints upon VOC exposure

at analyte concentrations below 2 ppm. A wide range of ligating solvents including alcohols, amines, thiols, thioethers, and phosphines can be detected and distinguished from each other by taking the difference before and after vapor-exposure of the scanned images of the arrays. The porphyrins were dissolved in dibutylphtalate in polystyrene matrix, and deposition of small spots with 0.5 mm diameter was found to optimize the response time. The porphyrin spots can be deposited using an ink-jet technique in order to obtain cheap disposable sensor arrays.

Zinc(II) tetraphenylporphyrin (**110**) dissolved in silicone rubber can be used for detection of ammonia vapor at concentrations as low as 0.7 ppm.[200] In the course of NH_3 ligation to ZnTPP the Soret band shifts from 414 to 424 nm, and similar spectral changes were observed on exposure to triethylamine. Silicone films of ZnTPP produce significantly better results than Nafion or ethyl cellulose support matrices. The latter is apparently impermeable for ammonia gas while the Nafion films were very thin (10 μm) and resulted in weak absorption.

4.2 Vapochromism as a result of indirect analyte-metal interactions

This subsection treats the remainder of metal-containing vapochromic substances that cannot easily be grouped according to a single unifying theme. These materials contain different metals and their vapochromism has diverse origins. The division into 5 chapters is an attempt to group these substances according to common themes and/or origin of their vapochromic properties.

4.2.1 Vapochromism as a consequence of a change in spin state

A single crystal to single crystal transformation has been reported for the spin-crossover compound Fe(tpa)(NCS)$_2$ (**111**) (tpa = tris-(2-pyridylmethyl)amine).[201] This molecule crystallizes in a relatively open structure with individual molecules arranged via π-π interactions in one direction and hydrogen bonds in a second direction. The Fe-N distances are between 1.977(8) to 2.091(6) Å, which is typical for low-spin Fe(II)-N bonds. Exposure to methanol vapor leads to a new compound which is best formulated as [Fe(tpa)(NCS)$_2$]·[Fe(tpa)(NCS)$_2$·CH$_3$OH] (**111**·[**111**·CH$_3$OH]). In the crystal structure determined at 120 K this methanol adduct exhibits Fe-N distances contracted by about 0.2 Å, indicating that a low-spin to high-spin transition has taken place. The change in spin state has been confirmed by Mössbauer spectroscopy and is accompanied by a change in color from yellow (**111**) to red (**111**·[**111**·CH$_3$OH]) (Figure 55). Remarkably, the methanol molecule is not directly interacting with any of the two metal centers, but it merely changes the way individual molecules interact with each other yet this suffices to induce the spin transition. As an additional subtlety the two crystallographically distinct iron centers give rise to three different spin crossover phases: At 120 K both metal centers are low-spin, at 298 K one Fe(II) is high-spin while the other is low-spin, and at 350 K both metals are high-spin.
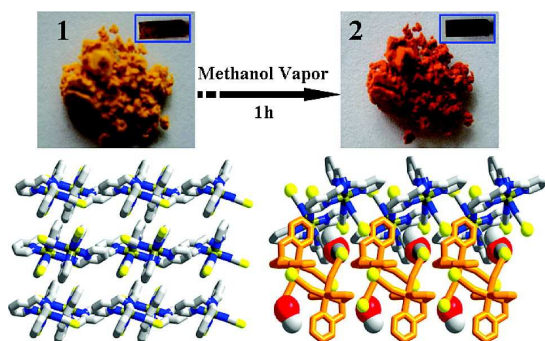
Figure 55. Change in appearance and crystal structure of compound **111** upon exposure to MeOH vapor. The red form contains two crystallographically distinct types of Fe complexes and is best formulated as **111**·[**111**·CH_3OH]. Reprinted with permission from ref. [201]. Copyright 2010 American Chemical Society.

Ethanol gives an adduct of similar stoichiometry as methanol (**111**·[**111**·C_2H_5OH]), i. e., a compound with two crystallographically distinct Fe(II) centers. By contrast, all other tested solvents (*n*-PrOH, *i*-PrOH, CH_3CN, CH_2Cl_2, and $CHCl_3$) yield adducts of the same stoichiometry as the solvent-free parent compound (**111**) in which all Fe(II) centers are identical.[202] Adducts of **111** with any of the latter five solvents undergo a color change from yellow/brown to red following exposure to ethanol vapor, indicating that a similar low-spin to high-spin transition as discussed above for methanol is occurring. When **111**·[**111**·C_2H_5OH] is exposed to vapors of CH_2Cl_2 or $CHCl_3$ the color reverts to yellow. Comparison of magnetic and structural properties within this family of materials has led to the conclusion that hydrogen-bonding interactions between solvent molecules and the metal complexes tend to enhance the ligand field exerted on the Fe(II) center, and this obviously plays a key role for the spin-crossover behavior.[203]

4.2.2 Hydrogen-bonded proton transfer assemblies
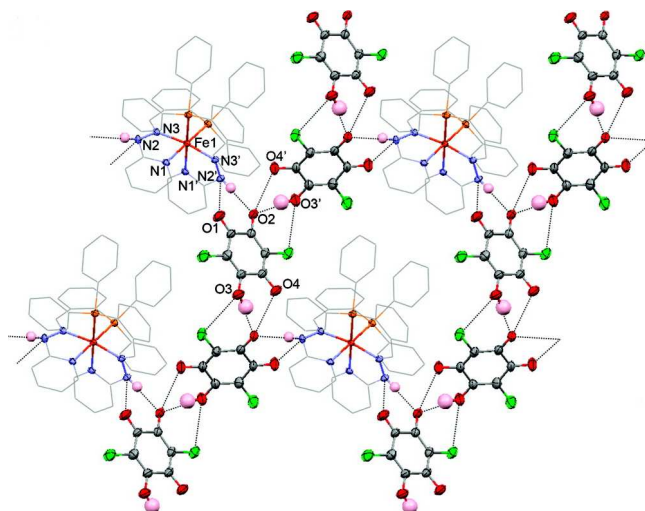
Figure 56. Extract from the crystal structure of **112**·2THF. Reprinted with permission from ref. [204]. Copyright 2011 American Chemical Society.

A vapochromic hydrogen-bonded proton transfer (HBPT) assembly is obtained from reaction between Fe(pbph)$_2$·3H$_2$O (pbph = 2-(diphenylphosphino)benzaldehyde-2-pyridylhydrazone) and chloranilic acid (H$_2$CA) in THF.[204] The stoichiometry of the final compound is Fe(Hpbph)$_2$(HCA)$_2$·2THF (**112**·2THF), i. e., two protons are transferred from two chloranilic acid molecules to the pbph ligands. In the crystal structure of this compound (Figure 56) there are two 2D hydrogen-bonded sheets containing interactions between cationic metal complexes and HCA$^-$, as well as interactions between individual HCA$^-$ anions. The THF guest molecules are located between these sheets. When **112**·2THF is heated to 158 °C all THF molecules are eliminated from the lattice. Subsequent exposure to vapors of THF restores the initial assembly. Adduct **112**·2THF itself is susceptible to various organic vapors including aprotic and protic solvents. Diffuse reflectance reveals spectral changes around 610 nm with CH$_2$Cl$_2$ and Et$_2$O producing distinctly different changes than MeOH, EtOH or acetic acid. The spectral changes

occurring with the protic solvents are perceived as a color change from brick-red to orange, resulting presumably from perturbation of hydrogen-bonding interactions in the HBPT assembly. The iron(II) center does not appear to be directly involved in the vapochromic behavior.

Palladium has also been incorporated into a vapochromic hydrogen-bonded proton transfer (HBPT) assembly.[205] Specifically, a Pd(II)-hydrazone complex (PdBr(Hmtbhp); Hmtbhp = 2-(2-(2-methylthio)benzylidene)hydrazinyl)pyridine) was combined with bromanilic acid (H_2BA), a widely used building block for supramolecular architectures known for its ability to accept one electron and donate two protons.[206, 207] The HBPT assembly **113** ([PdBr(Hmtbhp)]$_2$(HBA)$_2$(H_2BA)) can uptake CH_3CN reversibly, resulting in a color change from reddish purple to dark red. In the resulting solvent adduct the acetonitrile molecules form 1D channels along the crystallographic b-axis (Figure 57), and upon heating to 100 °C in argon atmosphere the guest-free assembly can be recovered.
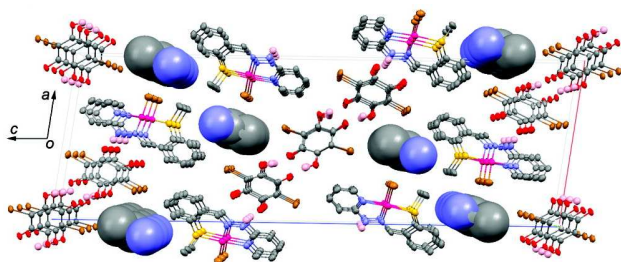
Figure 57. Packing diagram of HBPT assembly **113** with CH_3CN guest molecules shown as space filling models. Reprinted with permission from ref. [205]. Copyright 2010 American Chemical Society.

However, acetonitrile removal alters the powder X-ray diffraction pattern significantly, indicating that the supramolecular assembly is not robust enough to retain its structure without

the CH$_3$CN guests. Depending on what solvent vapors HBPT assembly **113** is exposed to, the lowest energetic absorption band either blue-shifts (DMF, pyridine, dimethylacetoamide, DMSO) or red-shifts (1,4-dioxane, CH$_3$CN, MeOH, EtOH). The absorption band shifts seem to correlate with Gutmann donor and acceptor numbers of the solvents.[208] Presumably, the hydrogen-bonding mode of the supramolecular assembly is fundamentally changed upon sorption of solvents with a high donor number, and such proton-accepting solvents seem to be adsorbed more easily than proton-donating solvents with a large acceptor number. Palladium does not appear to be directly involved in the vapochromic behavior of assembly **113**; in this regard the classification of this material as a Pd-based vapochromic substance is not optimal.

4.2.3 Metallophilic, π-π, and donor-acceptor interactions

A zinc(II) complex of 1,3,5-tris(p-(2,2'-dipyridylamino)phenyl)benzene (TPDPB) (Scheme 42) can selectively detect benzene vapors at concentrations of ~500 ppm.[209] Depending on crystallization conditions, two different forms are obtained. When using a small amount of benzene in CH$_2$Cl$_2$, form A with the composition [(ZnCl$_2$)$_3$(TPDPB)]·3CH$_2$Cl$_2$·0.25C$_6$H$_6$ (**114**·3CH$_2$Cl$_2$·0.25C$_6$H$_6$) crystallizes, whereas a 1:1 mixture of benzene and CH$_2$Cl$_2$ affords form B with the composition [(ZnCl$_2$)$_3$(TPDPB)]·3C$_6$H$_6$ (**114**·3C$_6$H$_6$). In the crystal structure of form A individual molecules of **114** build pairs with a separation of 3.85(1) Å between their central phenyl rings, and the TPDPB ligands are rotated by 120° relative to each other to give a staggered face-to-face orientation. Benzene guest molecules are sandwiched between two pairs of host molecules, undergoing π-π stacking with the central phenyl rings of **114** at an interplanar distance of 3.60(1) Å. In form B the molecular packing is fundamentally different with both

edge-to-edge and face-to-face interactions between benzene and the host present. The occurrence

of two forms of benzene inclusion structures was taken as evidence for the affinity of **114** for

benzene, and hence the benzene-sensing properties of this compound were tested by depositing it

onto a polydimethylsiloxane (PDMS) bead which was attached onto an optical fiber tip. In the

solid state, **114** is blue photoluminescent (λ_{max} = 430 nm) with an emission band resembling that

of the free TPDPB ligand, only red-shifted by ~30 nm. Upon exposure to vapors of benzene the

emission is quenched, presumably because the benzene guests undergo π-π stacking with the

host, similar to what is observed in the two crystal structures discussed above. Interestingly,

toluene, xylene, and ethyl benzene induce a much weaker response, similar to what is observed

for hexane, cyclohexane, methanol, ethanol, CH_2Cl_2, trichloroethylene, or perchloroethylene.

Thus, compound **114** exhibits a remarkable selectivity for benzene vapors.

Scheme 42. Zinc(II) complexes investigated in the context of vapochromism.
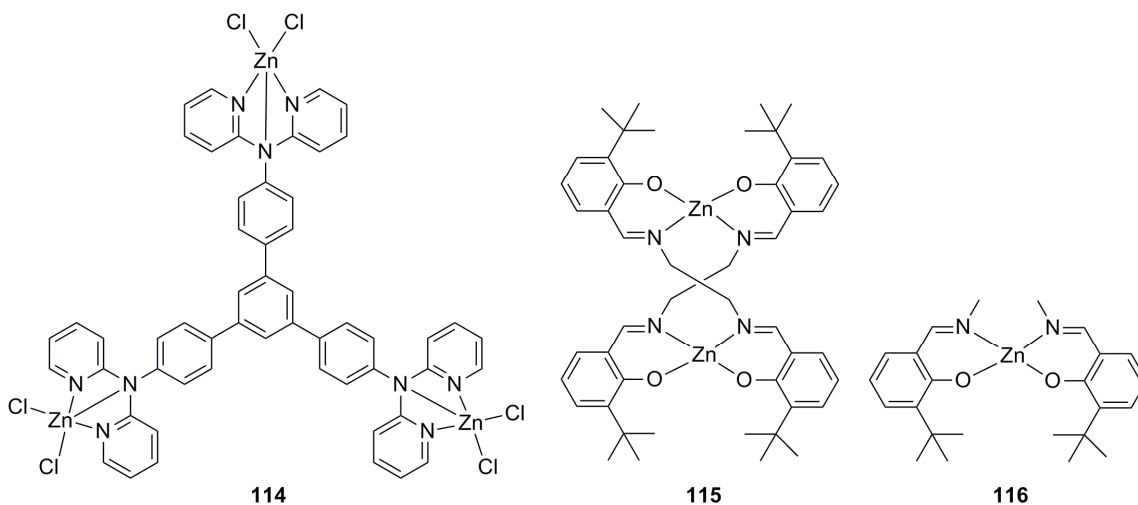
A helical zinc(II) dimer complex with two 3,3'-di-*tert*-butylsalen (*t*Busalen) ligands (**115**)

shows mechanochromic and vapochromic behavior.[210] The [Zn₂(*t*Busalen)₂] complex is green

photoluminescent (λ_{max} = 473 nm), quite different from its monomer analogue (**116**) which emits

blue light upon UV irradiation (λ_{max} = 456 nm). The X-ray crystal structure of the dimer

complex **115** reveals significant intramolecular π-π stacking interactions between individual

phenyl rings of the ^{t}Busalen ligands. Mechanical grinding of **115** or exposure to THF vapor

produces a blue luminescent substance, suggesting at first glance that these external stimuli

disrupt the intramolecular π-π interactions, leading to non-interacting luminophors which exhibit

similar emission properties as the monomer reference substance (**116**). However, careful analysis

of X-ray diffraction and emission data of **115**·THF and **115**·MeOH reveals that the emission

color is in fact correlated with the crystal packing structure and that *inter*molecular π-π stacking

is the key to the change in photoluminescence color.[210]

Scheme 43. A vapochromic silver(I) complex.

117
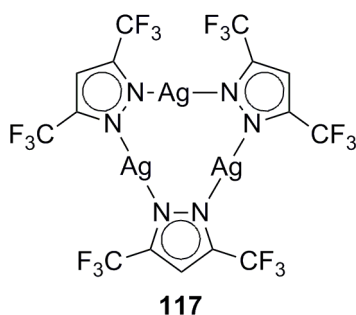
The trinuclear pyrazolyl-bridged silver(I) complex [[3,5-(CF$_3$)$_2$pz]Ag]$_3$ (**117**) (Scheme 43)

forms π-acid/π-base binary adducts with benzene and some of its methylated derivatives.[211] X-

ray crystal structure analysis of a benzene adduct reveals the presence of discrete tetramolecular

units comprised of a benzene/**117**/**117**/benzene sequence. Being a stronger π-base than benzene,

mesitylene is able to overcome the argentophilic interactions between neighboring complexes,

and consequently an infinite chain of **117**/mesitylene/**117**/mesitylene units is formed with this compound. This difference in packing structure between benzene and mesitylene adducts has important implications for the photoluminescence behavior. While neat **117** is non-emissive, the benzene adduct shows green luminescence ($\lambda_{max} \approx 520$ nm) and the mesitylene adduct emits in the blue spectral range ($\lambda_{max} \approx 410$ nm). The green luminescence has been attributed to excimeric states involving argentophilic interactions,[212] the disruption of these intermetallic contacts in the mesitylene adduct leads to blue emission. Thin films of **117** respond to vapors of benzene, toluene, and mesitylene with a luminescence turn-on response, in line with the formation of the solvent adducts described above. Aromatic solvents with electron-withdrawing substituents such as chlorobenzene and hexafluorobenzene do not switch on the luminescence. Similarly, non-aromatic solvents such as acetone, methanol, and THF do not trigger a response. These observations support the notion of π-acid/π-base interactions in the benzene, toluene, and mesitylene adducts.

Hupp and coworkers explored a variety of molecular rectangles based on rhenium(I) tricarbonyl diimines,[213] and one of them exhibits vapoluminescence.[214] Notably, it is a charge-neutral compound (**118**) (Scheme 44) in which no counterions are blocking the channels formed within and between individual rectangles. The crystal structure of [Re(CO)$_3$(bibzim)(4,4'-bpy)Re(CO)$_3$]$_2$ (**118**) (bibzim = 2,2'-bibenzimidazole) contains both intra- and intermolecular vacancies of rectangular shape and similar size (~10 Å × 6 Å). The emission intensity of **118** changes upon exposure to various VOCs, the affinity of thin films of **118** for aromatic compounds decreases along the series toluene > 4-fluorotoluene > benzene > fluorobenzene > hexafluorobenzene. This order suggests that electron donor/acceptor (host/guest) interactions might play an important role for guest uptake. The host/guest stoichiometry can exceed unity,

indicating that the guest molecules fill both intra- and intermolecular cavities. The estimated internal surface area is ~120 m^2/g.

Scheme 44. Vapochromic rhenium(I) and iridium(III) complexes.

118   **119**
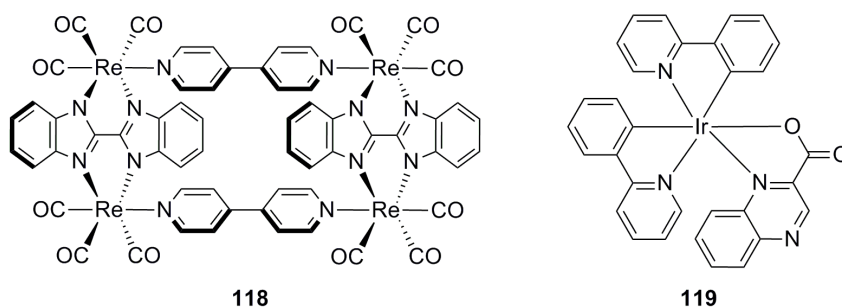
Many cyclometalated iridium(III) complexes exhibit favorable emission properties which makes them interesting for triplet harvesting in OLEDs.[215, 216] The [Ir(ppy)$_2$(qxn)] (ppy = 2-phenylpyridine, qxn = quinoxaline-2-carboxylate) complex (**119**) can be crystallized in two differently colored forms one of which can be converted into the other by exposure to CH$_3$CN vapor.[217] From mixed ethanol/chloroform solution one obtains black crystals of **119**·0.25EtOH·0.5CHCl$_3$ while from acetonitrile/chloroform red crystals of **119**·CH$_3$CN are formed. In the black form there are π-π interactions between qxn ligands from different complexes which may lead to an energetic stabilization of the ligand-based LUMO with respect to the red structure in which such π-π interactions are absent hence the different colors of the two forms. The black form is weakly emissive with λ_{max} = 692 nm and a decay time of only 43 ns, but the red form exhibits intense photoluminescence at 654 nm with a lifetime of 130 ns. Exposure of black **119**·0.25EtOH·0.5CHCl$_3$ to acetonitrile vapor converts it to the red form within ~1 minute while several other VOC vapors (propionitrile, acetone, acetic acid, ethyl

acetate, methanol, ethanol, 2-propanol, pyridine, THF, diethyl ether, CH_2Cl_2, $CHCl_3$, CH_3I, hexane, benzene) gave no response. Reconversion of the red form to the black form does not occur as easily, and the most efficient procedure is to dissolve the complex in $CHCl_3$ followed by subsequent evaporation of the solvent.

4.2.4 Vapochromism in coordination polymers and metal-organic frameworks

Figure 58. Left: Anhydrous $Cu(pz)_2$ (**120**); middle: $Cu(pz)_2 \cdot H_2O$ (**120·H$_2$O**); right: $Cu(pz)_2 \cdot NH_3$ (**120·NH$_3$**). Reprinted with permission from ref. [218]. Copyright 2009 American Chemical Society.

The $Cu(pz)_2$ compound (pz = pyrazolato) (**120**) is most easily obtained in the form of a pink hydrate (**120·H$_2$O**). This material forms a 1D coordination polymer with weakly bound water molecules and Cu-O distances of 2.913(4) Å.[219] Gentle heating leads to the anhydrous beige form. In humid air the beige substance readily reconverts to the pink hydrate but under dry conditions anhydrous **120** can be used for detection of NH_3, methylamine, methanol, ethanol, acetonitrile, and pyridine vapors. The resulting materials are solvent adducts of the general formula **120·solvent** and exhibit colors ranging from pink (methanol and acetonitrile adduct) to blue (other adducts). However, vapor uptake is slow and requires between 20 minutes (NH_3) and 2 days (ethanol) in order to be complete.

The structural changes accompanying water sorption of **120** have been studied in detail.[218] Interestingly the anhydrous form has no pores yet H_2O uptake occurs with remarkable ease (within 2 minutes), and hence it has been noted that this material exhibits "porosity without pores".
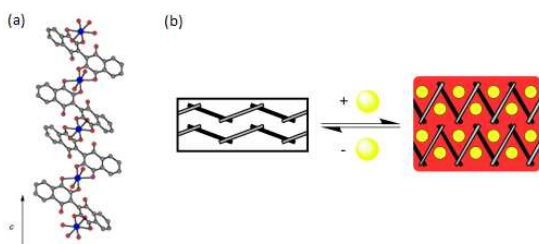
Figure 59. (a) Chain of $[Cu(bhnq)(H_2O)_2]$ complexes in (**121**·H_2O·3EtOH); (b) schematic representation of the hinge-like behavior of the 2,2'-bi(3-hydroxy-1,4-naphthoquinone) ligand upon VOC uptake. (K. Yamada, S. Yagishita, H. Tanaka, K. Tohyama, K. Adachi, S. Kaizaki, H. Kumagai, K. Inoue, R. Kitaura, H.-C. Chang, S. Kitagawa, S. Kawata: Metal-Complex Assemblies Constructed From the Flexible Hinge-Like Ligand H_2bhnq: Structural Versatility and Dynamic Behavior in the Solid State. *Chem. Eur. J.*, 2004, *10*, 2647-2660. Copyright Wiley-VCH Verlag GmbH & Co. KGaA. Reproduced with permission.)

When reacting $CuSO_4$ and the 2,2′-bi(3-hydroxy-1,4-naphthoquinone) ligand (H_2bhnq) in water-ethanol mixtures one obtains a coordination polymer of formulation $[[Cu(bhnq)(H_2O)_2(H_2O)(EtOH)_3]_n$ (**121**·H_2O·3EtOH) which has infinite 1D chains of $[Cu(bhnq)(H_2O)_2]$ units (Figure 59) with interstitial ethanol and water molecules.[220] The chelating bhnq^{2-} ligands bridge neighboring Cu(II) centers in an *anti* fashion to form zigzag

chains, the coordination sphere around each metal is a distorted octahedron with four O-atoms from two bhnq^{2-} ligands and two water molecules. Once removed from the mother liquor red crystals of **121**·H$_2$O·3EtOH turn black due to loss of ethanol, but this process is reversible for example when using MeOH or EtOH vapor. Crystallographic investigations show that the Cu(II)-Cu(II) distance shortens when going from the black to the red form, the reason being that sorbed EtOH molecules establish a hydrogen-bonding network with the bhnq^{2-} ligands and the coordinated waters. These noncovalent interactions lead to a contraction of the 1D chains which is possible thanks to the flexible hinge-like structure of the bhnq^{2-} ligand (Figure 59).

In THF the reaction between CuSO$_4$ and the H$_2$bhnq ligand leads to the compound [[Cu(bhnq)(THF)$_2$](THF)]$_n$ (**122**·THF).[221] This material forms similar 1D chains as compound **121**·H$_2$O·3EtOH only with THF ligands and additional interstitial THF molecules which can be removed in vacuum. The de-solvated form has a longer Cu(II)-Cu(II) distance than the THF solvate (6.45 vs. 7.8 Å), and a shift of the absorption band maximum in the visible spectral range from 500 to 540 nm accompanies de-solvation. THF uptake restores the initial material, and the reversibility of this transformation has been attributed to the hinge-like bhnq^{2-} ligand.

Depending on reaction conditions two different forms of a vapochromic metal-organic framework (MOF) can be obtained from the reaction of CuI with 1,4-diazabicyclo[2.2.2]octane (DABCO).[222] In both forms DABCO completes the coordination sphere of Cu(I) by ligating to four corners of the Cu$_4$I$_4$ cubane-like clusters. In form A (obtained from aqueous solution) the supertetrahedral [Cu$_4$I$_4$(DABCO)$_4$] units are arranged in a self-interpenetrating network (**123a**). In form B (obtained from CH$_3$CN solution, **123b**) two independent networks interpenetrate each other. In both forms there is ~20% of volume accessible for solvent molecules because there are channels of ~7 Å diameter propagating through the crystalline lattices. Both forms exhibit long-

lived (τ = 8.0, 13.4 μs) emission from cluster-centered excited states (^{3}CC) which might have some admixture from XMCT states resulting from iodide-to-copper charge transfer. Emission occurs with large Stokes shifts (11400 and 10700 cm^{-1}) indicative of strong excited-state distortions and significant structural reorganization of the photoexcited cubane-like clusters. The clusters are not exactly identical in both forms, consequently, the emission occurs at slightly different wavelengths (form A: λ_{max} = 580 nm; form B: λ_{max} = 556 nm). This fact can be exploited for vapoluminescence sensing because exposure of form A to vapors of acetonitrile induces a structural conversion to form B.
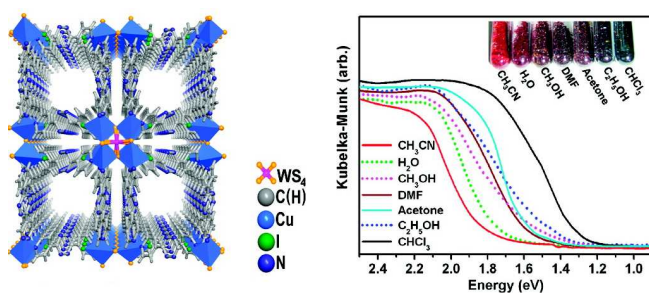
Figure 60. Left: Nanotubular structure of $[(WS_4Cu_4)I_2(dptz)_3]_n$ (**124**); right: UV-Vis spectra and photographs of different solvent adduct of **124**. Reprinted with permission from ref. [223]. Copyright 2011 American Chemical Society.

Reaction of $(NH_4)_2WS_4$, CuI, and dptz (dptz = 3,6-(dipyridin-4-yl)-1,2,4,5-tetrazine) in DMF yields a nanotubular metal-organic framework with the stoichiometry $[[(WS_4Cu_4)I_2(dptz)_3]\cdot DMF]_n$ (**124**·DMF) in which each WS_4^{2-} anion chelates four Cu(I) cations (Figure 60).[223] Each Cu(I) center is tetrahedrally coordinated, individual $WS_4Cu_4^{2+}$ units are paired up by pyrazines which exhibit π-π interactions at interplanar distances of 3.578(2) Å.

There are square-shaped (5.4 × 5.3 Å) nanotubes along the c-axis containing DMF guests which can be removed at 100 °C. Immersion of the de-solvated MOF into various organic solvents causes significant color changes that can also be induced by exposure to the respective vapors, albeit leading to a much slower response. Systematic studies revealed a negative solvatochromic effect with a solvent-induced absorption band shift of 245 nm between CH_3CN and $CHCl_3$ (Figure 60). Moreover, there is a good correlation between the magnitude of the absorption band shift and the Reichardt solvent polarity parameter.[224] The strong π-acceptor property of the dptz ligand is believed to play a key role for this solvatochromic and vapochromic behavior, a structurally analogous MOF with 2,2'-bipyridine instead of dptz does not show such behavior.[223]

4.2.5 Vapochromism in cyanometallates

2,2'-Bipyridinetetracyanoruthenate(II) complexes exhibit strongly solvent-dependent absorption and luminescence properties,[225-229] and a few of them (or closely related complexes) are sensitive to *vapors* of certain chemical substances. For instance, the $Ru(4,4'-{}^tBubpy)_2(CN)_2$ complex (**125**) is responsive to water vapor.[230] **125**, **125**·H_2O, and **125**·$2H_2O$ exhibit luminescence band maxima at 740, 685, and 640 nm, i. e., there is a correlation between emission peak and number of crystal waters. Simultaneously, the increase in the number of crystal waters is accompanied by a decrease of the CN stretching frequency in the IR spectrum. Thin films of **125** are most sensitive to moisture, operating at water vapor pressures as low as 10^{-2} Pa. Complex **125** is also responsive to vapors of various VOCs.[231] Neat **125** has an emission band maximum at 740 nm, but λ_{max} shifts to 700 nm when exposed to benzene, to 660 nm for quinoline, 650 nm for CH_2Cl_2, and 640 nm for MeOH and pyridine. Thus, complex **125** has a

certain discrimination capability for several VOCs, which parallels its solvatochromic behavior. In fluid solution there is a good correlation between the MLCT energy and the acceptor number (AN)[232] of the solvent, furthermore the CN stretching frequencies correlate with AN.

The tetrakis(bis-3,5-trifluoromethylphenylborate) (tfpb⁻) salt of tris(5,6-dimethyl-1,10-phenanthroline)ruthenium(II) (**126**) is an excellent sensor for benzene vapors at concentrations down to 7600 ppm.[233] The vapoluminescence effect manifests in a rapid spectral change dominated by a shift in emission band maximum from 572 to 558 nm. The most interesting aspect of $[Ru(5,6-Me_2phen)_3](tfpb)_2$ is its cross-sensitivity for the simultaneous sensing of benzene and oxygen. O_2 quenches the luminescence of neat **126**, but simultaneous exposure to vapors of benzene and O_2 leads to benzene uptake and very little emission quenching is observed. A crystal structure of $\mathbf{126} \cdot 1.5C_6H_6$ reveals that benzene guest molecules block channels in the crystal structure in such a way that oxygen diffusion can be suppressed.

5. Summary of detectable VOCs

Even though many of the vapochromic and vapoluminescent coordination complexes from the previous sections cannot realistically be used in real-world applications for reasons explained for each individual case above, a summary of analytes which can be detected and, where available, quantitative information regarding sensitivity is given in Table 1. The table lists the vapochromic substances in the same order as they appear in the text, for the abbreviations used the reader is referred to the text.

Table 1. Summary of vapochromic sensing materials and analytes considered in this review.

sensing material	analyte
[Pt(bpy)(CN)$_2$] (**1**)	HF, H$_2$O, H$_2$S [35, 38]
[Pt(5,5'-Me$_2$bpy)(CN)$_2$] (**5**)	H$_2$O [37]
[Pt(4,4'-H$_2$dcbpy)(CN)$_2$] (**6**)	DMSO, DMF, CH$_3$CN, EtOH, MeOH, Me$_2$CO, CH$_2$Cl$_2$, CHCl$_3$, CH$_3$COOH, CCl$_4$, C$_6$H$_6$ [13, 39]
Na$_2$[Pt(dcbpy)(CN)$_2$]·2H$_2$O (**7**·2H$_2$O)	MeOH, Me$_2$CO, DMF [40]
[Pt(4,4'-H$_2$dcbpy)(SCN)$_2$] (**8**)	DMSO, DMF, dimethylacetamide, MeOH, EtOH, Me$_2$CO, CH$_3$CN [50]
Zn[Pt(5,5'-dcbpy)(CN)$_2$] (Zn**9**)	H$_2$O [41]
Mg/Ca/Sr/Ba[Pt(5,5'-dcbpy)(CN)$_2$] (Mg/Ca/Sr/Ba**9**)	H$_2$O, MeOH [42]
[Pt(^{t}Bu$_2$bpy)(4-ethynylpyridine)$_2$] (**10**)	CH$_2$Cl$_2$ (25 ppm), CHCl$_3$ (450 ppm) [59]
[Pt(^{t}Bu$_2$bpy)(C≡C-C$_6$F$_5$)$_2$] (**11**)	CH$_2$Cl$_2$ [59]
Pt(^{t}Bu$_2$bpy)(ethynyltriarylboron)$_2$] (**12**)	CH$_2$Cl$_2$, CHCl$_3$, Me$_2$CO, EtOH, CH$_3$CN, THF: green luminescence; toluene, hexane, MeOH: luminescence quenching; benzene, cyclohexane: red emission [60]
[Pt(5,5'-bis(TMS-C≡C)-bpy)$_2$(5-ethynyl-bpy)$_2$] (**13**)	Me$_2$CO, CH$_2$Cl$_2$, *n*-hexane, and many others [66]
[Pt(5,5'-bis(TMS-C≡C)-bpy)$_2$(C≡CC$_6$H$_5$)$_2$] (**14**)	CH$_2$Cl$_2$, CHCl$_3$, CH$_3$I [67]
[Pt(5,5'-bis(TMS-C≡C)-bpy)$_2$(C≡CC$_6$H$_4$F-3)$_2$] (**15**)	CHCl$_3$ [68]
[Pt(5,5'-bis(TMS-C≡C)-bpy)$_2$(C≡CC$_6$H$_4$F-4)$_2$] (**16**)	CH$_2$Cl$_2$, CHCl$_3$ [68]
[Pt(5,5'-bis(TMS-C≡C)-bpy)$_2$(C≡CC$_6$H$_4$-CF$_3$-4)$_2$] (**17**)	dioxane, THF, THP [69]
cis-[Pt(CN-C$_6$H$_4$-C$_2$H$_5$)$_2$(CN)$_2$], (*cis*-**18**)	toluene, benzene, chlorobenzene, *p*-xylene, mesitylene, EtOH [70]
cis-[Pt(CN-^{i}C$_3$H$_7$)$_2$(CN)$_2$] (*cis*-**19**)	benzene (selective) [72]
[Pt(CN-^{t}Bu)$_2$(CN)$_2$] (**20**)	MeOH, CH$_3$CN, toluene; no response to: THF, Me$_2$CO, EtOAc, Et$_2$O, petroleum

	ether, hexane, CH_3NO_2, NH_3, chlorobenzene, cyclohexane, CH_2Cl_2, $CHCl_3$, N_2H_4 [73, 74]
$[Pt(CN-^iC_3H_7)_4][Pt(CN)_4]$ (**21**)	H_2O, MeOH, CF_3CH_2OH, $CHCl_3$ [75]
$[Pt(CN-C_6H_4-C_{10}H_{21})_4][Pd(CN)_4]$ (**23**)	$CHCl_3$ (response time 350 ms), MeOH, CH_2Cl_2, acetone ;[76, 77] detection limit for $CHCl_3$: a few mg/m^3
$[Pt(CN-C_6H_4-C_{10}H_{21})_4][Pt(CN)_4]$ (**24c**)	$CHCl_3$ (response time 500 ms), CH_2Cl_2, MeOH, EtOH, 2-propanol, Et_2O, CH_3CN, hexanes, acetone, C_6H_6 [78]
$[Pt(CN-C_6H_4-C_{10}H_{21})_4][Pt(NO_2)_4]$ (**25**)	Me_2CO [81]
electronic nose made from **26**, **27**, **28**	$CHCl_3$, H_2O, MeOH, CH_2Cl_2, 1-PrOH, *n*-hexane, cyclohexane [83]
electronic nose made from **26**, **27**, **29**	Me_2CO (12% saturation, 75g/m^3), MeOH (3% saturation, 6 g/m^3) [84]
$[Pt(CN-cyclododecyl)_4][Pt(CN)_4]$ (**30**)	H_2O (unique two-step response); $CH_2Cl_2/CHCl_3$ (weaker two-step response); benzene, toluene, *p*-xylene (one-step response) [86]
$[Pt(R/S-\beta-methylphenethylisocyanide)_4][Pt(CN)_4]$ (**31**)	differentiates between *R*-2-BuOH and *S*-2-BuOH at 90% confidence level [87]
$[Pt(R-tpy)Cl]X$ (R = H, OC_4H_9, OC_6H_{13}, OC_8H_{17}, $OC_{12}H_{25}$; X = Cl$^-$, ClO_4^-, PF_6^- (**32**$^+$X$^-$); $[Pt(^tBu_3-tpy)Cl]X$ (X = Cl$^-$, ClO_4^-, PF_6^-) (**33**$^+$X$^-$)	CH_3CN, piperidine, DMF, and other VOCs with lone pairs[88]
$[Pt(Cl-tpy)Cl]Cl$ (**34**Cl)	MeOH (selective) [90]
$[Pt(tpy)(NCS)]SCN$ (**35**SCN)	MeOH, two-step response [91]
$[Pt(tpy)(NCS)]SCN$ (**35**SbF$_6$)	selective for CH_3CN, DMF, pyridine [92]
$[Pt(tpy-nicotinamide)Cl](PF_6)_2$ (**37**(PF$_6$)$_2$)	MeOH, CH_3CN, pyridine [93]
$[Pt(pentaphenyl-benzene-tpy)Cl]Cl$ (**38**)	selective for CH_2Cl_2, EtOH, CH_3CN, EtOAc [94]
$[Pt(Me_2bzimpy)Cl]Cl$ (**39**Cl)	MeOH, EtOH, $CHCl_3$, CH_3CN [95]
$[Pt(Me_2bzimpy)Cl]PF_6$ (**39**PF$_6$)	CH_3CN, DMF (unresponsive to H_2O, MeOH, EtOH, 2-PrOH, Et_2O, CH_2Cl_2, $CHCl_3$, CCl_4, Me_2CO, hexanes, benzene) [95,]

	97
[Pt(Me$_2$bzimpy)Cl]Cl in ZrP (**39$^+$** in ZrP)	H$_2$O, MeOH, CH$_3$CN, Me$_2$CO, CH$_2$Cl$_2$, THF, benzene, toluene, *n*-hexane [98]
[Pt(R$_2$bzimpy)Cl]X (**40a**: R = C$_8$H$_{17}$, **40b**: C$_{12}$H$_{25}$, **40c**: C$_{16}$H$_{33}$; X = Cl, PF$_6$, BF$_4$, ClO$_4$, OTf, OAc)	Me$_2$CO, CH$_3$CN, MeOH, EtOH, CH$_2$Cl$_2$, CHCl$_3$, EtOAc, benzene [99]
[Pt(2,6-bis (1*H*-imidazol-2-yl)pyridine)Cl]Cl (**41**)	CH$_2$Cl$_2$, CH$_3$CN, CH$_3$OH, Me$_2$CO [100]
[(Pt(2,6-diphenylpyridine))$_2$(dppm)] (**42**)	CH$_2$Cl$_2$, CH$_3$OH, Me$_2$CO, benzene, pentane [101]
[Pt(2,6-di(hexanoylamide-phenyl)pyridine)] (**43**)	DMF, CH$_3$OH [102]
[Pt(4,6-di(phenyl)-2,2'-bipyridine)] (**44**) on silica gel	pentane, benzene, CH$_2$Cl$_2$, CHCl$_3$ [103]
[(Pt(C^N^N))2(*cis*-1,2-bis(diphenylphosphino)ethylene)](ClO$_4$)$_2$ (**45**(ClO$_4$)$_2$)	CH$_3$CN, EtOH, Et$_2$O, THF, EtOAc, CH$_2$Cl$_2$, CHCl$_3$ [104]
[(Pt(2,6-di(2'-naphthyl)pyridine))$_2$(dppm)] (**46**)	strong response: CH$_2$Cl$_2$, CH$_2$Br$_2$, CHCl$_3$, ClCH$_2$CH$_2$Cl, BrCH$_2$CH$_2$Br, CH$_3$I; weak response: Me$_2$CO, Et$_2$O, THF, EtOAc; no response: CH$_3$CN, MeOH, EtOH, benzene, toluene, *n*-hexane [105]
K[Pt(bzq)(CN)$_2$]·H$_2$O (K**47**·H$_2$O)	MeOH (response time: ~5 s), EtOH (~10 s), CH$_3$CN (~30 s), Me$_2$CO (~2 min), THF (~45 min) [106]
K[Pt(bzq)(CN)$_2$] (K**47**)	H$_2$O [106]
K[Pt(ppy)(CN)$_2$] (K**48**)	H$_2$O [106]
[Pt(NCN-pincer)Cl] (**49**)	SO$_2$ [107]
[Pt(NCN-pincer)Cl]$_3$-dendrimers (**50** and **51**)	SO$_2$ at conc. of 100 μM (6 μg SO$_2$ cm^{-3}), response time: 2 ms [108]
[Pt(NHC-butyl$_2$)Cl]Cl (**53**)	H$_2$O [116]
[Pt(NHC-mesityl$_2$)(CO)](PF$_6$)$_2$ (**54**)	MeOH, H$_2$O, THF, Et$_2$O, DMF, pyridine; no response to CH$_2$Cl$_2$, CHCl$_3$, benzene [117]
[Pt(bpy)(pyridine-2-thiolate)](PF$_6$)$_2$ (**55**)	Rapid response: MeOH, CH$_3$CN; slow response: EtOH, *^{i}*PrOH; no response: *^{t}*BuOH [118]

[Pt(dithiooxamide)$_2$] (**56**)	HCl [119]
[Pt$_2$Ag$_2$] cluster made from two Pt(II) benzoquinoline pyrrolidinedithiocarbamate units (**57**(ClO$_4$)$_2$)	CH$_3$CN; does not respond to MeOH, H$_2$O, CH$_2$Cl$_2$, Et$_2$O, DMF, DMSO, n-hexane, toluene [121]
cis-[Pt(aminophosphine)$_2$] (**58**)	MeOH, EtOH, ^{i}PrOH; no response: ^{t}BuOH [122]
[PtI$_2$(diarsinine)$_2$] (**59**)	CH$_2$Cl$_2$, Me$_2$CO, toluene [123]
[NH$_3$(CH$_2$)$_4$NH$_3$]$_2$[Pt$_2$(pop)$_4$I] (**60**)	H$_2$O [126, 128]
[NH$_3$(CH$_2$)$_5$NH$_3$]$_2$[Pt$_2$(pop)$_4$I] (**61**)	H$_2$O [127]
Cu[Au(CN)$_2$]$_2$(DMSO)$_2$ (**62**·(DMSO)$_2$)	H$_2$O, CH$_3$CN, DMF, dioxane, morpholine pyridine, NH$_3$ [14, 129]
Zn[Au(CN)$_2$]$_2$ (**63**)	NH$_3$ (1 ppb detection limit) [17, 130]
[Au(S$_2$CN(C$_5$H$_{11}$)$_2$)]$_2$ (**64**)	Me$_2$CO, CH$_3$CN, CH$_2$Cl$_2$, CHCl$_3$, insensitive to: MeOH, EtOH [134]
[Au$_2$(μ-thiouracilato)(μ-dppm)CF$_3$COO (**65**CF$_3$COO)	Et$_3$N vs. CF$_3$COOH [136]
[Au$_3$(CH$_3$N=COCH$_3$)$_3$] (**66**)	solvent-stimulated luminescence strongest with CHCl$_3$ and CH$_2$Cl$_2$ [138]
[Au$_3$(CH$_3$N=COCH$_3$)$_3$] (**66**)	conductivity in microwires (not vapochromism): significant response for: MeOH, EtOH, CH$_3$CN; no response: THF, acetone, n-PrOH, n-BuOH, n-pentanol, benzene, and p-xylene [143]
[Au$_3$(H$_3$C-p-C$_6$H$_4$-N=COC$_2$H$_5$)$_3$] (**67**)	C$_6$F$_6$ [144]
Au$_2$(μ-bis-(diphenylphosphino)ethane)$_2$Br$_2$ (**68**)	CH$_2$Cl$_2$, Me$_2$CO; no response to: CH$_3$CN, Et$_2$O, DMF, DMSO, benzene, pyridine, nitrobenzene, CS$_2$ [146]
Au$_2$(μ-bis-(diphenylphosphino)ethane)$_2$I$_2$·2Me$_2$CO (**69**·2Me$_2$CO)	CH$_2$Cl$_2$, Me$_2$CO [148]
[(C$_6$F$_5$Au)$_2$(μ-1,4-diisocyanobenzene)] (**70**)	CH$_2$Cl$_2$ [149]
[Au(PPh$_2$C(CSSAuC$_6$F$_5$)PPh$_2$Me)$_2$](ClO$_4$) (**71**)	Me$_2$CO, CH$_2$Cl$_2$, CHCl$_3$, ClCH$_2$CH$_2$Cl, EtOH, EtOAc, THF, toluene [151, 152]
[Tl[Au(C$_6$Cl$_5$)$_2$]]$_n$ (**72**)	Me$_2$CO, Hacac, CH$_3$CN, THF, Et$_3$N,

	pyridine, 2-fluoropyridine, or tetrahydrothiophene [153, 155]
[Tl(en)[Au(C$_6$X$_5$)$_2$]]$_n$ (**73a** X = F; **73b** X = Cl)	Me$_2$CO, acetophenone [156]
[Au$_2$Ag$_2$(C$_6$F$_5$)$_4$L$_2$]$_n$ (L = Et$_2$O) (**75**(Et$_2$O)$_2$)	Me$_2$CO, THF, CH$_3$CN [158]
[Au$_2$Ag$_2$(C$_6$F$_5$)$_4$(bpy)$_2$]$_n$ (**76**)	MeOH, EtOH, ^{i}PrOH [12]
[Au$_2$Ag$_2$(C$_6$F$_5$)$_4$(phen)$_2$]$_n$ (**77**)	MeOH, EtOH, Me$_2$CO [162]
[Au$_2$Ag$_2$(4-C$_6$F$_4$I)$_4$]$_n$ (**78**)	Me$_2$CO, THF, CH$_3$CN; insensitive to: Et$_2$O, toluene [164]
[Au$_2$Ag$_2$(4-C$_6$F$_4$I)$_4$(Me$_2$CO)$_2$]$_n$·2Me$_2$CO (**78**(Me$_2$CO)·2Me$_2$CO)	CH$_3$CN [164]
[Au$_2$Ag$_2$(4-C$_6$F$_4$I)$_4$(THF)$_2$]$_n$ (**78**(THF)$_2$)	CH$_3$CN [164]
[Au$_2$Ag$_2$(3,5-C$_6$Cl$_2$F$_3$)$_4$(Et$_2$O)$_2$]$_n$ (**79**(Et$_2$O)$_2$)	Me$_2$CO, THF, CH$_3$CN [166]
[Au$_2$Ag$_2$(3,5-C$_6$Cl$_2$F$_3$)$_4$(THF)$_2$]$_n$ (**79**(THF)$_2$)	Me$_2$CO, partial reaction with CH$_3$CN [166]
[Au$_2$Ag$_2$(3,5-C$_6$Cl$_2$F$_3$)$_4$(CH$_3$CN)$_2$]$_n$ (**79**(CH$_3$CN)$_2$)	Me$_2$CO, THF [166]
[Au$_2$Ag$_2$(C$_6$Cl$_5$)$_4$(Et$_2$O)$_2$]$_n$ (**80**(Et$_2$O)$_2$)	Me$_2$CO, THF, CH$_3$CN [166]
[Au$_2$Ag$_2$(2-C$_6$F$_4$I)$_4$]$_2$·4NBu$_4$ClO$_4$·THF (**81**·4NBu$_4$ClO$_4$·THF)	Me$_2$CO, THF, CH$_3$CN [167]
[Au(im(CH$_2$-py)$_2$)$_2$(Cu(CH$_3$CN)$_2$)$_2$](PF$_6$)$_3$ (**86**)	MeOH, H$_2$O, Me$_2$CO; insensitive to: THF, CH$_2$Cl$_2$ [169]
[Au(im(CH$_2$-py)$_2$)$_2$(Cu(CH$_3$OH))$_2$](PF$_6$) (**87b**)	CH$_3$CN [169]
[Au(dppb)$_2$](NO$_3$) (**88**NO$_3$)	MeOH, EtOH; insensitive to longer alcohols [170]
[Au(dppb)$_2$](BF$_4$) (**88**BF$_4$)	Me$_2$CO, CH$_3$CN, CH$_2$Cl$_2$, Et$_2$O, THF [170]
[VO(sal-(R,R)-stien)]· CHCl$_3$] (**89**·CHCl$_3$)	CH$_3$CN [171]
[VO(sal-(R,R)-stien)]· CH$_3$CN] (**89**· CH$_3$CN)	CHCl$_3$ [171]
[Co$_2$(H$_2$O)$_4$][Re$_6$S$_8$(CN)$_6$]·12H$_2$O (**90**·12H$_2$O)	CH$_3$NO$_2$, Me$_2$CO, CH$_3$CH$_2$CN, n-octanol, 1-PrOH, 2-PrOH, EtOAc, Et$_2$O, THF [176]
[Co(H$_2$O)$_3$]$_4$[Co$_2$(H$_2$O)$_4$][Re$_6$Se$_8$(CN)$_6$]$_3$·44H$_2$O (**91**·44H$_2$O)	Et$_3$N, CH$_3$CN, CH$_3$CH$_2$CN, THF, EtOH, DMF, Me$_2$CO, n-octanol, MTBE, EtOAc, 1-PrOH, 2-PrOH, Et$_2$O [176]

[Co$_2$(ampyz)$_2$](SO$_4$)] (= dry form of **92**)	H$_2$O [177]
[(dpdpm)Ni(η^2-NO$_3$)$_2$] (**93**)	CH$_3$CN [178]
Bis(1,2,6,7-tetracyano-3,5-dihydro-3,5-diiminopyrrolizinido)nickel(II) (**95**)	CH$_3$OH, toluene; poor response to CH$_3$CN [179]
[Ni(cyclam)(dcbpy)] (**96**(dcbpy))	H$_2$O [180]
[CuI(4-pic)]$_\infty$ (**97**)	toluene [181, 182]
[CuI(4-pic)]$_4$·2C$_6$H$_5$CH$_3$ (**98**·2C$_6$H$_5$CH$_3$)	pentane [181, 182]
trans-[CuCl$_2$(3-Clpy)$_2$] (**99**)	HCl [184]
trans-[CuBr$_2$(3-Brpy)$_2$] (**101**)	HCl, HBr [185, 186]
[Cu$_2$(dppy)$_3$(CH$_3$CN)](BF$_4$)$_2$ (**103**)	CH$_3$OH [187]
[(O^{n}Pr)Cu(μ-hep)$_2$Cu(O^{n}Pr)]·2H$_2$O (**104**·2H$_2$O)	MeOH, EtOH, ^{i}PrOH, CH$_3$CN with response times of 5 min, 2 h, 24 h, 8 d [188]
[(Cu$_4$I$_4$)(calix[4]-*bis*-monothiacrown)]$_n$ (**105**)	CH$_3$CN [189]
[CuI(PPh$_3$)$_4$] (**106a**)	CH$_3$CN, CH$_2$Cl$_2$, EtOH [190]
CuCN (**107**)	amines (Py, 2-MePy, 3-MePy, 4-MePy, 3-EtPy, 4-EtPy, 4-^{t}BuPy, piperidine, *N*-methylpiperidine, *N*-ethylpiperidine, Me$_2$NCy) and other nucleophilic VOCs (N-methylmorpholine) [191]
(CuI)$_2$(Et$_2$pip) (**108a**), (CuI)$_2$(Bn$_2$pip) (**108b**)	Py, 2-MePy, 3-MePy, pyrrolidine, pyrrolidine, morpholine, Et$_3$N, dimethyl sulfide [195]
SnSO$_4$ (**109a**), Sn(CH$_3$SO$_3$)$_2$ (**109b**), Sn(OTf)$_2$, (**109c**), SnPO$_3$F (**109d**)	NH$_3$, EtNH$_2$, Et$_2$NH, Et$_3$N, N(C$_5$H$_5$)$_3$ [196]
Zn(II)tetraphenylporphyrin (**110**)	NH$_3$, Et$_3$N [200]
Fe(tris-(2-pyridylmethyl)amine)(NCS)$_2$ (**111**)	MeOH [201]
[Fe(tpa)(NCS)$_2$]·[[Fe(tpa)(NCS)$_2$]·EtOH] (**111**·[**111**·EtOH])	CH$_2$Cl$_2$, CHCl$_3$ [202]
Fe(Hpbph)$_2$(HCA)$_2$·2THF (**112**·2THF)	CH$_2$Cl$_2$, Et$_2$O, MeOH, EtOH, CH$_3$COOH [204]
Fe(Hpbph)$_2$(HCA)$_2$ (**112**)	THF [204]

[PdBr(Hmtbhp)]$_2$(HBA)$_2$(H$_2$BA) (**113**)	DMF, pyridine, dimethylacetoamide, DMSO, 1,4-dioxane, CH$_3$CN, MeOH, EtOH; with discrimination ability [205]
[(ZnCl$_2$)$_3$(1,3,5-tris(*p*-(2,2'-dipyridylamino)phenyl)benzene)] (**114**)	benzene (500 ppm) [209]
[Zn$_2$(3,3'-di-*tert*-butylsalen)$_2$] (**115**)	THF [210]
[[3,5-(CF$_3$)$_2$pz]Ag]$_3$ (**117**)	selective to: benzene, toluene, mesitylene [211]
[Re(CO)$_3$(bibzim)(4,4'-bpy)Re(CO)$_3$]$_2$ (**118**)	toluene, 4-fluorotoluene, benzene, fluorobenzene, hexafluorobenzene, THF [214]
[Ir(ppy)$_2$(qxn)]·0.25EtOH·0.5CHCl$_3$ (**119**·0.25EtOH·0.5CHCl$_3$)	CH$_3$CN [217]
[Cu(pz)$_2$] (**120**)	NH$_3$, CH$_3$OH, EtOH, CH$_3$CN, pyridine, MeNH$_2$ [218, 219]
[[Cu(bhnq)(H$_2$O)$_2$(H$_2$O)$_n$]$_n$ (**121**·(H$_2$O)$_n$)	MeOH, EtOH [220]
[Cu(bhnq)(THF)$_2$]$_n$ (**122**)	THF [221]
[Cu$_4$I$_4$(DABCO)$_2$] (**123**)	CH$_3$CN [222]
[(WS$_4$Cu$_4$)I$_2$(dptz)$_3$]$_n$ (**124**)	CH$_3$CN, H$_2$O, CH$_3$OH, DMF, Me$_2$CO, C$_2$H$_5$OH, CHCl$_3$ [223]
Ru(4,4'-^{t}Bubpy)$_2$(CN)$_2$ (**125**)	H$_2$O [230], MeOH, CH$_2$Cl$_2$, benzene, quinoline, pyridine with discrimination ability [231]
[Ru(5,6-Me$_2$phen)$_3$](tfpb) (**126**)	benzene, detection limit: 7600 ppm [233]

Challenges associated with the use of vapochromic substances in practical sensor device applications differ from material to material; details are found in sections 2 – 4. Some frequently occuring issues are the following: Long-term stability of the chemical sensors, interference by atmospheric oxygen or humidity, reversibility of the vapochromic response, selectivity to certain

VOCs, and sufficiently rapid response times. The targeted synthesis of vapochromic materials is very difficult because even the most basic structure / function relationships have remained elusive for many vapochromic substances. Even the optimization of known vapochromic materials is difficult since very minor structural changes may lead to complete disappearance of the vapochromic property. In many cases the application potential of newly discovered vapochromic materials was apparently considered low and therefore quantititative analytical measurements were only performed in rather few selected cases. [17, 84, 108, 130, 209, 233] It seems fair to state that with respect to quantified sensitivity data, the field is still much in its infancy. Changing this situation is certainly a challenge for the future in this field.

6. Concluding remarks

Vapochromism and vapoluminescence in coordination complexes is possible through a variety of different mechanisms. Changes in metal-metal interactions play an important role in many platinum(II) and gold(I) based substances, [13, 14, 17, 35, 37, 36, 50, 41, 66, 67, 68, 69, 70, 72, 73, 88, 91, 92, 93, 95, 97, 98, 99, 100, 102, 105, 106, 116, 117, 118, 121, 129, 128, 135, 144, 146, 148, 149, 156, 155, 158, 157, 160, 164, 212] and modifications in π-π stacking are relatively widespread as well. [59, 88, 91, 93, 95, 97, 99, 101, 105, 116, 117, 187, 209, 210, 217]. For transition metal ions other than platinum or gold (particularly the 3d elements vanadium, iron, cobalt nickel, and copper) changes in the coordination environment of the central metal ion are a frequent source of the vapochromism phenomenon. [14,17, 107-109, 112, 121, 129, 128, 156, 167, 169, 171, 174, 175, 176, 177, 178, 181, 182, 188, 189, 190, 191, 187, 188, 189, 190, 191, 195, 196, 199, 200].

Occasionally, vapochromsim is triggered through reaction of the analyte at a remote ligand site

in a complex.[156, 181, 182, 234] Host-guest interactions in materials with vapor-accessible channels are quite prominenently represented and in the future are likely to become increasingly important since much current effort appears to be devoted to the synthesis of new functional metal-organic frameworks.[69, 70, 220, 222, 190, 223, 234, 205, 214]

Until now the field of vapochromism and vapoluminescence was mostly driven by coordination chemists with a strong interest in understanding the vapor-induced phenomena at a fundamental (mechanistic) level. The application potential of many of the investigated substances was considered rather limited, and hence quantitative analytical data is available only for relatively few cases. However, it is clear that sensors based on vapochromic and vapoluminescent materials are potentially very sensitive towards VOCs, especially when a luminescence turn-on response can be induced. Provided a sufficiently rapid response time can be obtained, such sensing materials therefore hold great promise for real-time monitoring of VOCs in air. This might be a less cumbersome procedure than adsorbing VOCs on adsorbates for later extraction and chromatographic analysis. When compared to electrochemical gas sensors vapochromic or vapoluminescent sensors have the advantage that detection is not limited to redox-active analytes. However, selectivity for a certain specific analyte is very difficult to achieve with vapochromic or vapoluminescent materials. An important basic problem in this context is that the discovery of such substances frequently relies on serendipity because there is no other choice: In many cases even very minor modifications of the chemical structure of a known vapor-responsive substance leads to disappearance of the vapochromism / vapoluminescence phenomena.

For real-world analytical applications, the future of vapochromic and vapoluminescent substances probably lies in cross-reactive sensor arrays in which many different sensing

materials are combined, and in which characteristic fingerprint responses for individual analytes can potentially be obtained. On the other hand, the phenomena of vapor-induced color and luminescence changes are interesting in their own right and are likely to continue to fascinate chemists in academic research.

References

(1)　Nagel, C. C. U. S. Patent 4,834,909. 1989.

(2)　Albert, K. J.; Lewis, N. S.; Schauer, C. L.; Sotzing, G. A.; Stitzel, S. E.; Vaid, T. P.; Walt, D. R., *Chem. Rev.* **2000,** *100*, 2595.

(3)　Lewis, N. S., *Acc. Chem. Res.* **2004,** *37*, 663.

(4)　Jurs, P. C.; Bakken, G. A.; McClelland, H. E., *Chem. Rev.* **2000,** *100*, 2649.

(5)　Rock, F.; Barsan, N.; Weimar, U., *Chem. Rev.* **2008,** *108*, 705.

(6)　Grate, J. W.; Abraham, M. H., *Sens. Actuators B* **1991,** *3*, 85.

(7)　Balch, A. L., *Struct. Bonding* **2007,** *123*, 1.

(8)　He, X. M.; Yam, V. W. W., *Coord. Chem. Rev.* **2011,** *255*, 2111.

(9)　Keefe, M. H.; Benkstein, K. D.; Hupp, J. T., *Coord. Chem. Rev.* **2000,** *205*, 201.

(10)　Zhao, Q. A.; Li, F. Y.; Huang, C. H., *Chem. Soc. Rev.* **2010,** *39*, 3007.

(11)　Fiddler, M. N.; Begashaw, I.; Mickens, M. A.; Collingwood, M. S.; Assefa, Z.; Bililign, S., *Sensors* **2009,** *9*, 10447.

(12) Luquin, A.; Elosúa, C.; Vergara, E.; Estella, J.; Cerrada, E.; Bariáin, C.; Matías, I. R.; Garrido, J.; Laguna, M., *Gold Bull.* **2007,** *40*, 225.

(13) Kato, M., *Bull. Chem. Soc. Jpn.* **2007,** *80*, 287.

(14) Leznoff, D. B.; Lefebvre, J., *Gold Bull.* **2005,** *38*, 47.

(15) Fernández, E.; Laguna, A.; López-De-Luzuriaga, J. M., *Coord. Chem. Rev.* **2005,** *249*, 1423.

(16) Wong, K. M. C.; Yam, V. W. W., *Coord. Chem. Rev.* **2007,** *251*, 2477.

(17) Katz, M. J.; Sakai, K.; Leznoff, D. B., *Chem. Soc. Rev.* **2008,** *37*, 1884.

(18) Zhang, X.; Li, B.; Chen, Z. H.; Chen, Z. N., *J. Mater. Chem.* **2012,** *22*, 11427.

(19) Abdou, H. E.; Mohamed, A. A.; Fackler, J. P.; Burini, A.; Galassi, R.; López-de-Luzuriaga, J. M.; Olmos, M. E., *Coord. Chem. Rev.* **2009,** *253*, 1661.

(20) Ford, P. C.; Cariati, E.; Bourassa, J., *Chem. Rev.* **1999,** *99*, 3625.

(21) Houlding, V. H.; Miskowski, V. M., *Coord. Chem. Rev.* **1991,** *111*, 145.

(22) Gliemann, G.; Yersin, H., *Struct. Bonding* **1985,** *62*, 87.

(23) Balch, A. L., *Angew. Chem. Int. Ed.* **2009,** *48*, 2641.

(24) Omary, M. A.; Mohamed, A. A.; Rawashdeh-Omary, M. A.; Fackler, J. P., *Coord. Chem. Rev.* **2005,** *249*, 1372.

(25) Linert, W.; Fukuda, Y.; Camard, A., *Coord. Chem. Rev.* **2001,** *218*, 113.

(26) Day, J. H., *Chem. Rev.* **1968,** *68*, 649.

(27) Kaupp, G., *Crystengcomm* **2009,** *11*, 388.

(28) Schmidbaur, H.; Schier, A., *Chem. Soc. Rev.* **2008,** *37*, 1931.

(29) Schmidbaur, H.; Schier, A., *Chem. Soc. Rev.* **2012,** *41*, 370.

(30) Pyykkö, P., *Chem. Rev.* **1997,** *97*, 597.

(31) Roundhill, D. M., *Photochemistry and Photophysics of Metal Complexes*. Plenum Press: New York, 1994.

(32) Gray, H. B.; Maverick, A. W., *Science* **1981,** *214*, 1201.

(33) Miskowski, V. M.; Houlding, V. H., *Inorg. Chem.* **1989,** *28*, 1529.

(34) Miskowski, V. M.; Houlding, V. H., *Inorg. Chem.* **1991,** *30*, 4446.

(35) Bielli, E.; Gidney, P. M.; Gillard, R. D.; Heaton, B. T., *J. Chem. Soc., Dalton Trans.* **1974**, 2133.

(36) Morgan, G. T.; Burstall, F. H., *J. Chem. Soc.* **1934**, 965.

(37) Shih, K. C.; Herber, R. H., *Inorg. Chem.* **1992,** *31*, 5444.

(38) Kishi, S.; Kato, M., *Mol. Cryst. Liquid Cryst.* **2002,** *379*, 303.

(39) Kato, M.; Kishi, S.; Wakamatsu, Y.; Sugi, Y.; Osamura, Y.; Koshiyama, T.; Hasegawa, M., *Chem. Lett.* **2005,** *34*, 1368.

(40) Kobayashi, A.; Yonemura, T.; Kato, M., *Eur. J. Inorg. Chem.* **2010**, 2465.

(41) Kobayashi, A.; Hara, H.; Noro, S.; Kato, M., *Dalton Trans.* **2010,** *39,* 3400.

(42) Hara, H.; Kobayashi, A.; Noro, S.; Chang, H. C.; Kato, M., *Dalton Trans.* **2011,** *40,* 8012.

(43) Che, C. M.; Butler, L. G.; Gray, H. B.; Crooks, R. M.; Woodruff, W. H., *J. Am. Chem. Soc.* **1983,** *105,* 5492.

(44) Che, C. M.; Mak, T. C. W.; Miskowski, V. M.; Gray, H. B., *J. Am. Chem. Soc.* **1986,** *108,* 7840.

(45) Connick, W. B.; Miskowski, V. M.; Houlding, V. H.; Gray, H. B., *Inorg. Chem.* **2000,** *39,* 2585.

(46) Connick, W. B.; Henling, L. M.; Marsh, R. E.; Gray, H. B., *Inorg. Chem.* **1996,** *35,* 6261.

(47) Connick, W. B.; Marsh, R. E.; Schaefer, W. P.; Gray, H. B., *Inorg. Chem.* **1997,** *36,* 913.

(48) Bailey, J. A.; Hill, M. G.; Marsh, R. E.; Miskowski, V. M.; Schaefer, W. P.; Gray, H. B., *Inorg. Chem.* **1995,** *34,* 4591.

(49) Wenger, O. S.; Garcìa-Revilla, S.; Güdel, H. U.; Gray, H. B.; Valiente, R., *Chem. Phys. Lett.* **2004,** *384,* 190.

(50) Kobayashi, A.; Fukuzawa, Y.; Chang, H.-C.; Kato, M., *Inorg. Chem.* **2012,** *51,* 7508.

(51) Yam, V. W. W., *Acc. Chem. Res.* **2002,** *35,* 555.

(52) Williams, J. A. G., *Top. Curr. Chem.* **2007,** *281,* 205.

(53) Williams, J. A. G.; Develay, S.; Rochester, D. L.; Murphy, L., *Coord. Chem. Rev.* **2008,** *252*, 2596.

(54) Lu, W.; Mi, B. X.; Chan, M. C. W.; Hui, Z.; Che, C. M.; Zhu, N. Y.; Lee, S. T., *J. Am. Chem. Soc.* **2004,** *126*, 4958.

(55) Hijazi, A.; Walther, M. E.; Besnard, C.; Wenger, O. S., *Polyhedron* **2010,** *29*, 857.

(56) Hissler, M.; Connick, W. B.; Geiger, D. K.; McGarrah, J. E.; Lipa, D.; Lachicotte, R. J.; Eisenberg, R., *Inorg. Chem.* **2000,** *39*, 447.

(57) Hissler, M.; McGarrah, J. E.; Connick, W. B.; Geiger, D. K.; Cummings, S. D.; Eisenberg, R., *Coord. Chem. Rev.* **2000,** *208*, 115.

(58) Bronner, C.; Wenger, O. S., *Dalton Trans.* **2011,** *40*, 12409.

(59) Lu, W.; Chan, M. C. W.; Zhu, N. Y.; Che, C. M.; He, Z.; Wong, K. Y., *Chem. Eur. J.* **2003,** *9*, 6155.

(60) Hudson, Z. M.; Sun, C.; Harris, K. J.; Lucier, B. E. G.; Schurko, R. W.; Wang, S. N., *Inorg. Chem.* **2011,** *50*, 3447.

(61) Wade, C. R.; Broomsgrove, A. E. J.; Aldridge, S.; Gabbaï, F. P., *Chem. Rev.* **2010,** *110*, 3958.

(62) Yamaguchi, S.; Wakamiya, A., *Pure Appl. Chem.* **2006,** *78*, 1413.

(63) Entwistle, C. D.; Marder, T. B., *Angew. Chem. Int. Ed.* **2002,** *41*, 2927.

(64) Yam, V. W. W.; Wong, K. M. C.; Zhu, N. Y., *J. Am. Chem. Soc.* **2002,** *124*, 6506.

(65) Zuleta, J. A.; Bevilacqua, J. M.; Eisenberg, R., *Coord. Chem. Rev.* **1991,** *111*, 237.

(66) Ni, J.; Zhang, L. Y.; Wen, H. M.; Chen, Z. N., *Chem. Commun.* **2009**, 3801.

(67) Ni, J.; Wu, Y. H.; Zhang, X.; Li, B.; Zhang, L. Y.; Chen, Z. N., *Inorg. Chem.* **2009,** *48*, 10202.

(68) Ni, J.; Zhang, X.; Wu, Y. H.; Zhang, L. Y.; Chen, Z. N., *Chem. Eur. J.* **2011,** *17*, 1171.

(69) Zhang, X.; Wang, J. Y.; Ni, J.; Zhang, L. Y.; Chen, Z. N., *Inorg. Chem.* **2012,** *51*, 5569.

(70) Buss, C. E.; Mann, K. R., *J. Am. Chem. Soc.* **2002,** *124*, 1031.

(71) Dylla, A. G.; Janzen, D. E.; Pomije, M. K.; Mann, K. R., *Organometallics* **2007,** *26*, 6243.

(72) Drew, S. M.; Smith, L. I.; McGee, K. A.; Mann, K. R., *Chem. Mater.* **2009,** *21*, 3117.

(73) Zhang, Y.; Zhang, H. Y.; Mu, X. Y.; Lai, S. W.; Xu, B.; Tian, W. J.; Wang, Y.; Che, C. M., *Chem. Commun.* **2010,** *46*, 7727.

(74) Sun, Y.; Ye, K.; Zhang, H.; Zhang, J.; Zhao, L.; Li, B.; Yang, G.; Yang, B.; Wang, Y.; Lai, S. W.; Che, C. M., *Angew. Chem. Int. Ed.* **2006,** *45*, 5610.

(75) Buss, C. E.; Anderson, C. E.; Pomije, M. K.; Lutz, C. M.; Britton, D.; Mann, K. R., *J. Am. Chem. Soc.* **1998,** *120*, 7783.

(76) Exstrom, C. L.; Sowa, J. R.; Daws, C. A.; Janzen, D.; Mann, K. R.; Moore, G. A.; Stewart, F. F., *Chem. Mater.* **1995,** *7*, 15.

(77) Bailey, R. C.; Hupp, J. T., *J. Am. Chem. Soc.* **2002,** *124*, 6767.

(78) Daws, C. A.; Exstrom, C. L.; Sowa, J. R.; Mann, K. R., *Chem. Mater.* **1997,** *9*, 363.

(79) Exstrom, C. L.; Pomije, M. K.; Mann, K. R., *Chem. Mater.* **1998,** *10*, 942.

(80) Abraham, M. H., *Chem. Soc. Rev.* **1993,** *22*, 73.

(81) Kunugi, Y.; Mann, K. R.; Miller, L. L.; Exstrom, C. L., *J. Am. Chem. Soc.* **1998,** *120*, 589.

(82) Kunugi, Y.; Miller, L. L.; Mann, K. R.; Pomije, M. K., *Chem. Mater.* **1998,** *10*, 1487.

(83) Drew, S. M.; Janzen, D. E.; Buss, C. E.; MacEwan, D. I.; Dublin, K. M.; Mann, K. R., *J. Am. Chem. Soc.* **2001,** *123*, 8414.

(84) Drew, S. M.; Janzen, D. E.; Mann, K. R., *Anal. Chem.* **2002,** *74*, 2547.

(85) Gardner, J. W.; Bartlett, P. N., *Sens. Actuators B* **1994,** *18*, 211.

(86) Grate, J. W.; Moore, L. K.; Janzen, D. E.; Veltkamp, D. J.; Kaganove, S.; Drew, S. M.; Mann, K. R., *Chem. Mat.* **2002,** *14*, 1058.

(87) Cich, M. J.; Hill, I. M.; Lackner, A. D.; Martinez, R. J.; Ruthenburg, T. C.; Takeshita, Y.; Young, A. J.; Drew, S. M.; Buss, C. E.; Mann, K. R., *Sens. Actuators B* **2010,** *149*, 199.

(88) Muro, M. L.; Daws, C. A.; Castellano, F. N., *Chem. Commun.* **2008**, 6134.

(89) Field, J. S.; Haines, R. J.; McMillin, D. R.; Summerton, G. C., *J. Chem. Soc., Dalton Trans.* **2002**, 1369.

(90) Du, P. W., *Inorg. Chim. Acta* **2010,** *363*, 1355.

(91) Kobayashi, A.; Fukuzawa, Y.; Noro, S.; Nakamura, T.; Kato, M., *Chem. Lett.* **2009,** *38*, 998.

(92) Field, J. S.; Grimmer, C. D.; Munro, O. Q.; Waldron, B. P., *Dalton Trans.* **2010,** *39*, 1558.

(93) Wadas, T. J.; Wang, Q. M.; Kim, Y. J.; Flaschenreim, C.; Blanton, T. N.; Eisenberg, R., *J. Am. Chem. Soc.* **2004,** *126*, 16841.

(94) Du, P.; Schneider, J.; Brennessel, W. W.; Eisenberg, R., *Inorg. Chem.* **2008,** *47*, 69.

(95) Grove, L. J.; Rennekamp, J. M.; Jude, H.; Connick, W. B., *J. Am. Chem. Soc.* **2004,** *126*, 1594.

(96) Wang, K. H.; Haga, M. A.; Monjushiro, H.; Akiba, M.; Sasaki, Y., *Inorg. Chem.* **2000,** *39*, 4022.

(97) Grove, L. J.; Oliver, A. G.; Krause, J. A.; Connick, W. B., *Inorg. Chem.* **2008,** *47*, 1408.

(98) Rivera, E. J.; Barbosa, C.; Torres, R.; Grove, L.; Taylor, S.; Connick, W. B.; Clearfield, A.; Colon, J. L., *J. Mater. Chem.* **2011,** *21*, 15899.

(99) Mathew, I.; Sun, W. F., *Dalton Trans.* **2010,** *39*, 5885.

(100) Che, C. M.; Chow, C. F.; Yuen, M. Y.; Roy, V. A. L.; Lu, W.; Chen, Y.; Chui, S. S. Y.; Zhu, N. Y., *Chem. Sci.* **2011,** *2*, 216.

(101) Lu, W.; Chan, M. C. W.; Cheung, K. K.; Che, C. M., *Organometallics* **2001,** *20*, 2477.

(102) Choi, S. J.; Kuwabara, J.; Nishimura, Y.; Arai, T.; Kanbara, T., *Chem. Lett.* **2012,** *41*, 65.

(103) Che, C. M.; Fu, W. F.; Lai, S. W.; Hou, Y. J.; Liu, Y. L., *Chem. Commun.* **2003**, 118.

(104) Mathew, I.; Li, Y. J.; Li, Z. J.; Sun, W. F., *Dalton Trans.* **2010,** *39*, 11201.

(105) Kui, S. C. F.; Chui, S. S. Y.; Che, C. M.; Zhu, N. Y., *J. Am. Chem. Soc.* **2006,** *128*, 8297.

(106) Forniés, J.; Fuertes, S.; López, J. A.; Martin, A.; Sicilia, V., *Inorg. Chem.* **2008,** *47*, 7166.

(107) Albrecht, M.; Lutz, M.; Spek, A. L.; van Koten, G., *Nature* **2000,** *406*, 970.

(108) Albrecht, M.; van Koten, G., *Adv. Mater.* **1999,** *11*, 171.

(109) Albrecht, M.; Gossage, R. A.; Lutz, M.; Spek, A. L.; van Koten, G., *Chem. Eur. J.* **2000,** *6*, 1431.

(110) Muijsers, J. C.; Niemantsverdriet, J. W.; Wehmanooyevaar, I. C. M.; Grove, D. M.; van Koten, G., *Inorg. Chem.* **1992,** *31*, 2655.

(111) Shannon, R. D.; Prewitt, C. T., *Acta Crystallogr. B* **1969,** *B 25*, 925.

(112) Albrecht, M.; Gossage, R. A.; Frey, U.; Ehlers, A. W.; Baerends, E. J.; Merbach, A. E.; van Koten, G., *Inorg. Chem.* **2001,** *40*, 850.

(113) Lin, J. C. Y.; Huang, R. T. W.; Lee, C. S.; Bhattacharyya, A.; Hwang, W. S.; Lin, I. J. B., *Chem. Rev.* **2009,** *109*, 3561.

(114) Pugh, D.; Danopoulos, A. A., *Coord. Chem. Rev.* **2007,** *251*, 610.

(115) Diéz-González, S.; Marion, N.; Nolan, S. P., *Chem. Rev.* **2009,** *109*, 3612.

(116) Lee, C. S.; Sabiah, S.; Wang, J. C.; Hwang, W. S.; Lin, I. J. B., *Organometallics* **2010,** *29*, 286.

(117) Lee, C. S.; Zhuang, R. R.; Sabiah, S.; Wang, J. C.; Hwang, W. S.; Lin, I. J. B., *Organometallics* **2011,** *30*, 3897.

(118) Kato, M.; Omura, A.; Toshikawa, A.; Kishi, S.; Sugimoto, Y., *Angew. Chem. Int. Ed.* **2002,** *41*, 3183.

(119) Nastasi, F.; Puntoriero, F.; Palmeri, N.; Cavallaro, S.; Campagna, S.; Lanza, S., *Chem. Commun.* **2007**, 4740.

(120) Rosace, G.; Giuffrida, G.; Saitta, M.; Guglielmo, G.; Campagna, S.; Lanza, S., *Inorg. Chem.* **1996,** *35*, 6816.

(121) Forniés, J.; Sicilia, V.; Casas, J. M.; Martín, A.; López, J. A.; Larraz, C.; Borja, P.; Ovejero, C., *Dalton Trans.* **2011,** *40*, 2898.

(122) Pattacini, R.; Giansante, C.; Ceroni, P.; Maestri, M.; Braunstein, P., *Chem. Eur. J.* **2007,** *13*, 10117.

(123) Naka, K.; Kato, T.; Watase, S.; Matsukawa, K., *Inorg. Chem.* **2012,** *51*, 4420.

(124) Zipp, A. P., *Coord. Chem. Rev.* **1988,** *84*, 47.

(125) Roundhill, D. M.; Gray, H. B.; Che, C. M., *Acc. Chem. Res.* **1989,** *22*, 55.

(126) Mastuzaki, H.; Kishida, H.; Okamoto, H.; Takizawa, K.; Matsunaga, S.; Takaishi, S.; Hitoshi, M. A.; Sugiura, K.; Yamashita, M., *Angew. Chem. Int. Ed.* **2005,** *44*, 3240.

(127) Yamashita, M.; Takizawa, K.; Matsunaga, S.; Kawakami, D.; Iguchi, H.; Takaishi, S.; Kajiwara, T.; Iwahori, F.; Ishii, T.; Miyasaka, H.; Sugiura, K.; Matsuzaki, H.; Kishida, H.; Okamoto, H., *Bull. Chem. Soc. Jpn.* **2006,** *79*, 1404.

(128) Iguchi, H.; Takaishi, S.; Kajiwara, T.; Miyasaka, H.; Yamashita, M.; Matsuzaki, H.;

Okamoto, H., *J. Inorg. Organomet. Polym.* **2009,** *19*, 85.

(129) Lefebvre, J.; Batchelor, R. J.; Leznoff, D. B., *J. Am. Chem. Soc.* **2004,** *126*, 16117.

(130) Katz, M. J.; Ramnial, T.; Yu, H. Z.; Leznoff, D. B., *J. Am. Chem. Soc.* **2008,** *130*, 10662.

(131) Coker, N. L.; Bauer, J. A. K.; Elder, R. C., *J. Am. Chem. Soc.* **2004,** *126*, 12.

(132) Nagasundaram, N.; Roper, G.; Biscoe, J.; Chai, J. W.; Patterson, H. H.; Blom, N.; Ludi,

A., *Inorg. Chem.* **1986,** *25*, 2947.

(133) Timmer, B.; Olthuis, W.; van den Berg, A., *Sens. Actuators B* **2005,** *107*, 666.

(134) Mansour, M. A.; Connick, W. B.; Lachicotte, R. J.; Gysling, H. J.; Eisenberg, R., *J. Am.

Chem. Soc.* **1998,** *120*, 1329.

(135) King, C.; Wang, J. C.; Khan, M. N. I.; Fackler, J. P., *Inorg. Chem.* **1989,** *28*, 2145.

(136) Lee, Y. A.; Eisenberg, R., *J. Am. Chem. Soc.* **2003,** *125*, 7778.

(137) Bouas-Laurent, H.; Durr, H., *Pure Appl. Chem.* **2001,** *73*, 639.

(138) Vickery, J. C.; Olmstead, M. M.; Fung, E. Y.; Balch, A. L., *Angew. Chem. Int. Ed.* **1997,**
36, 1179.

(139) White-Morris, R. L.; Olmstead, M. M.; Attar, S.; Balch, A. L., *Inorg. Chem.* **2005,** *44*,

5021.

(140) Wenger, O. S., *Chem. Soc. Rev.* **2011,** *40*, 3538.

(141) Reynolds, G. T., *J. Lumin.* **1992,** *54*, 43.

(142) Fung, E. Y.; Olmstead, M. M.; Vickery, J. C.; Balch, A. L., *Coord. Chem. Rev.* **1998,** *171*, 151.

(143) Mu, X. Y.; Liu, D.; Cheng, X.; Li, L.; Zhang, H. Y.; Wang, Y., *Org. Electron.* **2012,** *13*, 457.

(144) Rawashdeh-Omary, M. A.; Omary, M. A.; Fackler, J. P.; Galassi, R.; Pietroni, B. R.; Burini, A., *J. Am. Chem. Soc.* **2001,** *123*, 9689.

(145) Tiripicchio, A.; Tiripicchiocamellini, M.; Minghetti, G., *J. Organomet. Chem.* **1979,** *171*, 399.

(146) Lim, S. H.; Olmstead, M. M.; Balch, A. L., *J. Am. Chem. Soc.* **2011,** *133*, 10229.

(147) Pathaneni, S. S.; Desiraju, G. R., *J. Chem. Soc., Dalton Trans.* **1993**, 319.

(148) Lim, S. H.; Olmstead, M. M.; Balch, A. L., *Chem. Sci.* **2012**, DOI: 10.1039/C2SC20820B.

(149) Ito, H.; Saito, T.; Oshima, N.; Kitamura, N.; Ishizaka, S.; Hinatsu, Y.; Wakeshima, M.; Kato, M.; Tsuge, K.; Sawamura, M., *J. Am. Chem. Soc.* **2008,** *130*, 10044.

(150) White-Morris, R. L.; Olmstead, M. M.; Balch, A. L., *J. Am. Chem. Soc.* **2003,** *125*, 1033.

(151) Bariáin, C.; Matías, I. R.; Romeo, I.; Garrido, J.; Laguna, M., *Appl. Phys. Lett.* **2000,** *77*, 2274.

(152) Bariáin, C.; Matías, I. R.; Romeo, I.; Garrido, J.; Laguna, M., *Sens. Actuators* **2001,** *B76*, 25.

(153) Fernández, E. J.; López-de-Luzuriaga, J. M.; Monge, M.; Olmos, M. E.; Pérez, J.; Laguna, A.; Mohamed, A. A.; Fackler, J. P., *J. Am. Chem. Soc.* **2003,** *125*, 2022.

(154) Fernández, E. J.; Laguna, A.; López-De-Luzuriaga, J. M.; Mendizabal, F.; Monge, M.; Olmos, M. E.; Pérez, J., *Chem. Eur. J.* **2003,** *9*, 456.

(155) Fernández, E. J.; López-De-Luzuriaga, J. M.; Monge, M.; Montiel, M.; Olmos, M. E.; Pérez, J.; Laguna, A.; Mendizabal, F.; Mohamed, A. A.; Fackler, J. P., *Inorg. Chem.* **2004,** *43*, 3573.

(156) Fernández, E. J.; Laguna, A.; López-de-Luzuriaga, J. M.; Montiel, M.; Olmos, M. E.; Pérez, J., *Organometallics* **2006,** *25*, 1689.

(157) Usón, R.; Laguna, A.; Laguna, M.; Manzano, B. R.; Jones, P. G.; Sheldrick, G. M., *J. Chem. Soc., Dalton Trans.* **1984**, 285.

(158) Fernández, E. J.; López-De-Luzuriaga, J. M.; Monge, M.; Olmos, M. E.; Puelles, R. C.; Laguna, A.; Mohamed, A. A.; Fackler, J. P., *Inorg. Chem.* **2008,** *47*, 8069.

(159) Fernández, E. J.; Gimeno, M. C.; Laguna, A.; López-de-Luzuriaga, J. M.; Monge, M.; Pyykkö, P.; Sundholm, D., *J. Am. Chem. Soc.* **2000,** *122*, 7287.

(160) Fernández, E. J.; Laguna, A.; López-de-Luzuriaga, J. M.; Monge, M.; Montiel, M.; Olmos, M. E.; Rodríguez-Castillo, M., *Organometallics* **2006,** *25*, 3639.

(161) Bariain, C.; Matias, I. R.; Fdez-Valdivielso, C.; Elosúa, C.; Luquín, A.; Garrido, J.; Laguna, M., *Sens. Actuators B* **2005,** *108*, 535.

(162) Luquin, A.; Bariain, C.; Vergara, E.; Cerrada, E.; Garrido, J.; Matias, I. R.; Laguna, M., *Appl. Organomet. Chem.* **2005,** *19*, 1232.

(163) Elosua, C.; Bariain, C.; Matias, I. R.; Arregui, F. J.; Vergara, E.; Laguna, M., *Sens. Actuators B* **2009,** *137*, 139.

(164) Laguna, A.; Lasanta, T.; López-de-Luzuriaga, J. M.; Monge, M.; Naumov, P.; Olmos, M. E., *J. Am. Chem. Soc.* **2010,** *132*, 456.

(165) Metrangolo, P.; Neukirch, H.; Pilati, T.; Resnati, G., *Acc. Chem. Res.* **2005,** *38*, 386.

(166) Fernández, E. J.; Laguna, A.; López-de-Luzuriaga, J. M.; Olmos, M. E.; Puelles, R. C., *Z. Naturforsch. B* **2009,** *64*, 1500.

(167) Lasanta, T.; Olmos, M. E.; Laguna, A.; López-de-Luzuriaga, J. M.; Naumov, P., *J. Am. Chem. Soc.* **2011,** *133*, 16358.

(168) White-Morris, R. L.; Olmstead, M. M.; Jiang, F. L.; Tinti, D. S.; Balch, A. L., *J. Am. Chem. Soc.* **2002,** *124*, 2327.

(169) Strasser, C. E.; Catalano, V. J., *J. Am. Chem. Soc.* **2010,** *132*, 10009.

(170) Osawa, M.; Kawata, I.; Igawa, S.; Hoshino, M.; Fukunaga, T.; Hashizume, D., *Chem. Eur. J.* **2010,** *16*, 12114.

(171) Kojima, M.; Taguchi, H.; Tsuchimoto, M.; Nakajima, K., *Coord. Chem. Rev.* **2003,** *237*, 183.

(172) Nakajima, K.; Kojima, M.; Azuma, S.; Kasahara, R.; Tsuchimoto, M.; Kubozono, Y.; Maeda, H.; Kashino, S.; Ohba, S.; Yoshikawa, Y.; Fujita, J., *Bull. Chem. Soc. Jpn.* **1996,** *69*, 3207.

(173) Kojima, M.; Nakajima, K.; Tsuchimoto, M.; Treichel, P. M.; Kashino, S.; Yoshikawa, Y., *Proc. Jpn. Acad. Ser. B* **1995,** *71*, 175.

(174) Kasahara, R.; Tsuchimoto, M.; Ohba, S.; Nakajima, K.; Ishida, H.; Kojima, M., *Inorg. Chem.* **1996,** *35*, 7661.

(175) Helm, L.; Merbach, A. E., *Chem. Rev.* **2005,** *105*, 1923.

(176) Beauvais, L. G.; Shores, M. P.; Long, J. R., *J. Am. Chem. Soc.* **2000,** *122*, 2763.

(177) Boonmak, J.; Nakano, M.; Chaichit, N.; Pakawatchai, C.; Youngme, S., *Dalton Trans.* **2010,** *39*, 8161.

(178) Baho, N.; Zargarian, D., *Inorg. Chem.* **2007,** *46*, 299.

(179) Flamini, A.; Mattei, G.; Panusa, A., *J. Incl. Phenom. Macrocycl. Chem.* **1999,** *33*, 377.

(180) Lee, E. Y.; Suh, M. P., *Angew. Chem. Int. Ed.* **2004,** *43*, 2798.

(181) Cariati, E.; Bourassa, J.; Ford, P. C., *J. Chem. Soc., Chem. Commun.* **1998**, 1623.

(182) Cariati, E.; Bu, X. H.; Ford, P. C., *Chem. Mater.* **2000,** *12*, 3385.

(183) Mínguez Espallargas, G.; Brammer, L.; van de Streek, J.; Shankland, K.; Florence, A. J.; Adams, H., *J. Am. Chem. Soc.* **2006,** *128*, 9584.

(184) Mínguez Espallargas, G.; Hippler, M.; Florence, A. J.; Fernandes, P.; van de Streek, J.; Brunelli, M.; David, W. I. F.; Shankland, K.; Brammer, L., *J. Am. Chem. Soc.* **2007,** *129*, 15606.

(185) Mínguez Espallargas, G.; van de Streek, J.; Fernandes, P.; Florence, A. J.; Brunelli, M.; Shankland, K.; Brammer, L., *Angew. Chem. Int. Ed.* **2010,** *49*, 8892.

(186) Mínguez Espallargas, G.; Florence, A. J.; van de Streek, J.; Brammer, L., *Crystengcomm* **2011,** *13*, 4400.

(187) Li, Y. J.; Deng, Z. Y.; Xu, X. F.; Wu, H. B.; Cao, Z. X.; Wang, Q. M., *Chem. Commun.* **2011,** *47*, 9179.

(188) Mobin, S. M.; Srivastava, A. K.; Mathur, P.; Lahiri, G. K., *Dalton Trans.* **2010,** *39*, 1447.

(189) Lee, J. Y.; Kim, H. J.; Jung, J. H.; Sim, W.; Lee, S. S., *J. Am. Chem. Soc.* **2008,** *130*, 13838.

(190) Maini, L.; Braga, D.; Mazzeo, P. P.; Ventura, B., *Dalton Trans.* **2012,** *41*, 531.

(191) Ley, A. N.; Dunaway, L. E.; Brewster, T. P.; Dembo, M. D.; Harris, T. D.; Baril-Robert, F.; Li, X. B.; Patterson, H. H.; Pike, R. D., *Chem. Commun.* **2010,** *46*, 4565.

(192) Lim, M. J.; Murray, C. A.; Tronic, T. A.; DeKrafft, K. E.; Ley, A. N.; Debutts, J. C.; Pike, R. D.; Lu, H. Y.; Patterson, H. H., *Inorg. Chem.* **2008,** *47*, 6931.

(193) Tronic, T. A.; DeKrafft, K. E.; Lim, M. J.; Ley, A. N.; Pike, R. D., *Inorg. Chem.* **2007,** *46*, 8897.

(194) Bayse, C. A.; Brewster, T. P.; Pike, R. D., *Inorg. Chem.* **2009,** *48*, 174.

(195) Safko, J. P.; Kuperstock, J. E.; McCullough, S. M.; Noviello, A. M.; Li, X.; Killarney, J. P.; Murphy, C.; Patterson, H. H.; Bayse, C.; Pike, R. D., *Dalton Trans.* **2012,** *41*, 11663.

(196) Baldauff, E. A.; Buriak, J. M., *Chem. Commun.* **2004**, 2028.

(197) Molloy, K. C.; Bigwood, M. P.; Herber, R. H.; Zuckerman, J. J., *Inorg. Chem.* **1982,** *21*, 3709.

(198) Donaldson, J. D.; Nicholson, D. G.; Senior, B. J., *J. Chem. Soc. A* **1968**, 2928.

(199) Rakow, N. A.; Suslick, K. S., *Nature* **2000,** *406*, 710.

(200) Vaughan, A. A.; Baron, M. G.; Narayanaswamy, R., *Anal. Commun.* **1996,** *33*, 393.

(201) Li, B.; Wei, R. J.; Tao, J.; Huang, R. B.; Zheng, L. S.; Zheng, Z. P., *J. Am. Chem. Soc.* **2010,** *132*, 1558.

(202) Wei, R. J.; Tao, J.; Huang, R. B.; Zheng, L. S., *Inorg. Chem.* **2011,** *50*, 8553.

(203) Gütlich, P.; Hauser, A.; Spiering, H., *Angew. Chem. Int. Ed.* **1994,** *33*, 2024.

(204) Chang, M.; Kobayashi, A.; Nakajima, K.; Chang, H. C.; Kato, M., *Inorg. Chem.* **2011,** *50*, 8308.

(205) Kobayashi, A.; Dosen, M.; Chang, M.; Nakajima, K.; Noro, S.; Kato, M., *J. Am. Chem. Soc.* **2010,** *132*, 15286.

(206) Ishida, H.; Kashino, S., *Acta Crystallogr. C* **1999,** *55*, 1714.

(207) Suzuki, H.; Mori, H.; Yamaura, J. I.; Matsuda, M.; Tajima, H.; Mochida, T., *Chem. Lett.* **2007,** *36*, 402.

(208) Gutmann, V., *The Donor-Acceptor Approach to Molecular Interaction*. Plenum Press: 1978.

(209) Pang, J.; Marcotte, E. J. P.; Seward, C.; Brown, R. S.; Wang, S. N., *Angew. Chem. Int. Ed.* **2001,** *40*, 4042.

(210) Mizukami, S.; Houjou, H.; Sugaya, K.; Koyama, E.; Tokuhisa, H.; Sasaki, T.; Kanesato, M., *Chem. Mater.* **2005,** *17*, 50.

(211) Rawashdeh-Omary, M. A.; Rashdan, M. D.; Dharanipathi, S.; Elbjeirami, O.; Ramesh, P.; Dias, H. V. R., *Chem. Commun.* **2011,** *47*, 1160.

(212) Omary, M. A.; Patterson, H. H., *J. Am. Chem. Soc.* **1998,** *120*, 7696.

(213) Benkstein, K. D.; Hupp, J. T.; Stern, C. L., *J. Am. Chem. Soc.* **1998,** *120*, 12982.

(214) Benkstein, K. D.; Hupp, J. T.; Stern, C. L., *Angew. Chem. Int. Ed.* **2000,** *39*, 2891.

(215) Baldo, M. A.; O'Brien, D. F.; You, Y.; Shoustikov, A.; Sibley, S.; Thompson, M. E.; Forrest, S. R., *Nature* **1998,** *395*, 151.

(216) Yersin, H., *Transition Metal and Rare Earth Compounds III* **2004,** *241*, 1.

(217) Liu, Z. W.; Bian, Z. Q.; Bian, J.; Li, Z. D.; Nie, D. B.; Huang, C. H., *Inorg. Chem.* **2008,** *47*, 8025.

(218) Bencini, A.; Casarin, M.; Forrer, D.; Franco, L.; Garau, F.; Masciocchi, N.; Pandolfo, L.; Pettinari, C.; Ruzzi, M.; Vittadini, A., *Inorg. Chem.* **2009,** *48*, 4044.

(219) Cingolani, A.; Galli, S.; Masciocchi, N.; Pandolfo, L.; Pettinari, C.; Sironi, A., *J. Am. Chem. Soc.* **2005,** *127*, 6144.

(220) Yamada, K.; Yagishita, S.; Tanaka, H.; Tohyama, K.; Adachi, K.; Kaizaki, S.; Kumagai, H.; Inoue, K.; Kitaura, R.; Chang, H. C.; Kitagawa, S.; Kawata, S., *Chem.-Eur. J.* **2004,** *10*, 2648.

(221) Yamada, K.; Tanaka, H.; Yagishita, S.; Adachi, K.; Uemura, T.; Kitagawa, S.; Kawata, S., *Inorg. Chem.* **2006,** *45*, 4322.

(222) Braga, D.; Maini, L.; Mazzeo, P. P.; Ventura, B., *Chem.-Eur. J.* **2010,** *16*, 1553.

(223) Lu, Z. Z.; Zhang, R.; Li, Y. Z.; Guo, Z. J.; Zheng, H. G., *J. Am. Chem. Soc.* **2011,** *133*, 4172.

(224) Reichardt, C., *Chem. Rev.* **1994,** *94*, 2319.

(225) Chang, Q.; Murtaza, Z.; Lakowicz, J. R.; Rao, G., *Anal. Chim. Acta* **1997,** *350*, 97.

(226) Bignozzi, C. A.; Chiorboli, C.; Indelli, M. T.; Scandola, M. A. R.; Varani, G.; Scandola, F., *J. Am. Chem. Soc.* **1986,** *108*, 7872.

(227) Winkler, J. R.; Creutz, C.; Sutin, N., *J. Am. Chem. Soc.* **1987,** *109*, 3470.

(228) Kato, M.; Yamauchi, S.; Hirota, N., *J. Phys. Chem.* **1989,** *93*, 3422.

(229) Timpson, C. J.; Bignozzi, C. A.; Sullivan, B. P.; Kober, E. M.; Meyer, T. J., *J. Phys. Chem.* **1996,** *100*, 2915.

(230) Abe, T.; Shinozaki, K., *Inorg. Chem.* **2005,** *44*, 849.

(231) Abe, T.; Suzuki, T.; Shinozaki, K., *Inorg. Chem.* **2010,** *49*, 1794.

(232) Gutmann, V., *Coord. Chem. Rev.* **1976,** *18*, 225.

(233) McGee, K. A.; Marquardt, B. J.; Mann, K. R., *Inorg. Chem.* **2008,** *47*, 9143.
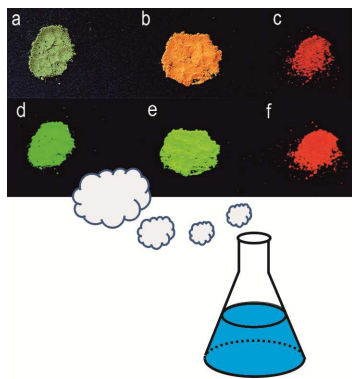
(234) Evju, J. K.; Mann, K. R., *Chem. Mat.* **1999,** *11*, 1425.

AUTHOR BIOGRAPHY

Oliver S. Wenger received a Ph. D. degree from the University of Berne (Switzerland) in 2002 after work with Hans U. Güdel. From 2002 to 2004 he was a postdoctoral researcher in the group of Harry B. Gray at Caltech and from 2004 to 2006 in the group of Jean-Pierre Sauvage at Université Louis Pasteur in Strasbourg (France). From 2006 to 2009 he performed independent research as an assistant professor at the University of Geneva, endowed with a "Förderungsprofessur" from the Swiss National Science Foundation. From 2009 to 2012 he held an associate professor position (W2) at Georg-August-Universität Göttingen (Germany). In 2012 he moved back to Switzerland to the University of Basel where he currently has a tenured professorship.

ACKNOWLEDGMENT

SYNOPSIS TOC / COVER ART